Instantaneous Power Spectrum

de Oliveira, Paulo M.D. Monica

Monterey, California. Naval Postgraduate School

NAVAL POSTGRADUATE SCHOOL
Monterey, California

THESIS

INSTANTANEOUS POWER SPECTRUM

by

Paulo M. D. Mónica de Oliveira

March 1989

Thesis Advisor Ralph D. Hippenstiel

Approved for public release; distribution is unlimited.

nclassified

curity classification of this page

REPORT DOCUMENTATION PAGE

a Report Security Classification Unclassified		1b Restrictive Markings	
a Security Classification Authority		3 Distribution Availability of Report	
b Declassification Downgrading Schedule		Approved for public release; distribution is unlimited	
Performing Organization Report Number(s)		5 Monitoring Organization Report Number(s)	
a Name of Performing Organization Naval Postgraduate School	6b Office Symbol *(If applicable)* 32	7a Name of Monitoring Organization Naval Postgraduate School	
c Address *(city, state, and ZIP code)* Monterey, CA 93943-5000		7b Address *(city, state, and ZIP code)* Monterey, CA 93943-5000	
a Name of Funding Sponsoring Organization	8b Office Symbol *(If applicable)*	9 Procurement Instrument Identification Number	
c Address *(city, state, and ZIP code)*		10 Source of Funding Numbers	
		Program Element No	Project No / Task No / Work Unit Accession No

1 Title *(Include security classification)* INSTANTANEOUS POWER SPECTRUM

2 Personal Author(s) Paulo M. D. Mónica de Oliveira

3a Type of Report	13b Time Covered	14 Date of Report *(year, month, day)*	15 Page Count
Master's Thesis	From To	March 1989	98

6 Supplementary Notation The views expressed in this thesis are those of the author and do not reflect the official policy or position of the Department of Defense or the U.S. Government.

7 Cosati Codes			18 Subject Terms *(continue on reverse if necessary and identify by block number)*
ield	Group	Subgroup	Instantaneous Power Spectrum, non-stationary, Spectral estimation

9 Abstract *(continue on reverse if necessary and identify by block number)*

The need for tools capable of handling non-stationarities in the spectral content of the data has been recognized as early as 1946. The Wigner-Ville Distribution (WD) has been extensively used since its introduction in 1948, but suffers from some associated problems (e.g., spectral cross-terms and requiring the use of analytic signals). An alternative Distribution is proposed, which has its origin in the definition proposed by Page of "Instantaneous Power Spectrum" (IPS). Its characteristics are examined and, when pertinent, compared to the WD. It is shown to be less sensitive to the problems affecting the WD, but provides less frequency resolution. The usefulness of a parametric (AR) version is investigated. Some typical test signals are examined, to demonstrate the performance and trade-offs of IPS and its parametric version.

20 Distribution Availability of Abstract	21 Abstract Security Classification	
☒ unclassified unlimited ☐ same as report ☐ DTIC users	Unclassified	
22a Name of Responsible Individual Ralph D. Hippenstiel	22b Telephone *(Include Area code)* (408) 646-2768	22c Office Symbol 62Hi

D FORM 1473,84 MAR 83 APR edition may be used until exhausted
All other editions are obsolete

security classification of this page

Unclassified

Approved for public release; distribution is unlimited.

Instantaneous Power Spectrum

by

Paulo M. D. Mónica de Oliveira
Lieutenant, Portuguese Navy
B.S., Portuguese Naval Academy, 1982

Submitted in partial fulfillment of the
requirements for the degrees of

MASTER OF SCIENCE IN ELECTRICAL ENGINEERING
and
ELECTRICAL ENGINEER

from the

NAVAL POSTGRADUATE SCHOOL
March 1989

Gordon E. Schacher,
Dean of Science and Engineering

ABSTRACT

The need for tools capable of handling non-stationarities in the spectral content of the data has been recognized as early as 1946. The Wigner-Ville Distribution (WD) has been extensively used since its introduction in 1948, but suffers from some associated problems (e.g., spectral cross-terms and requiring the use of analytic signals). An alternative Distribution is proposed, which has its origin in the definition proposed by Page of "Instantaneous Power Spectrum" (IPS). Its characteristics are examined and, when pertinent, compared to the WD. It is shown to be less sensitive to the problems aflicting the WD, but provides less frequency resolution. The usefulness of a parametric (AR) version is investigated. Some typical test signals are examined, to demonstrate the performance and trade-offs of IPS and its parametric version.

TABLE OF CONTENTS

ACKNOWLEDGEMENTS

To my wife and children for always being there.

To my thesis advisor, Professor Ralph Hippenstiel, for his constant availability.

I. INTRODUCTION

A. THE PROBLEM

The use of the Fourier Transform as a spectral description of signals is a concept whose usefulness is restricted to the class of stationary signals. Though mathematically elegant and convenient, Fourier decomposition of a signal can often mask the true spectrum, since the assumed basis-functions implicitly oppose any notion of time-dependency.

When the spectral content of the signal changes with time, as is often the case in fields such as Communications, Seismology or Speech Processing, more powerful tools are needed. The time-dependency of the spectral content should be apparent and measurable through the use of a more general type of representation of the signal. Gabor [Ref. 1] proposed such a representation by introducing the concept of a spectral description in a joint time-frequency plane.

Since then, several attempts have been made [Refs. 2, 3, 4, 5] to derive a, or the, function capable of correctly describing the distribution of the signal's energy in this plane. Short Time Fourier Analysis (STFA) has been widely used and is regarded as a very convenient approximation to the "true" distribution.

However, obtaining this distribution is an under-determined problem, since an infinity of valid solutions is introduced by allowing non-stationary descriptions. For example, any time signal can be represented as a time-varying DC component. To illustrate, consider the following discrete time signal:

$$x(n) = \cos\left(\frac{2\pi}{10} n\right). \tag{1}$$

Two equally valid representations, in the sense that each one is capable of generating the observed signal, are shown in Figures 1 and 2.

Each one of these descriptions explains the existence of a sinusoidal time-series. Though there is no conceptual distinction between them, the algorithm of analysis must have the ability to decide which one will be taken as the "true" one, based on an explicitly or implicitly built-in set of rules. The situation thus arises, where "one will see what one wants to see".

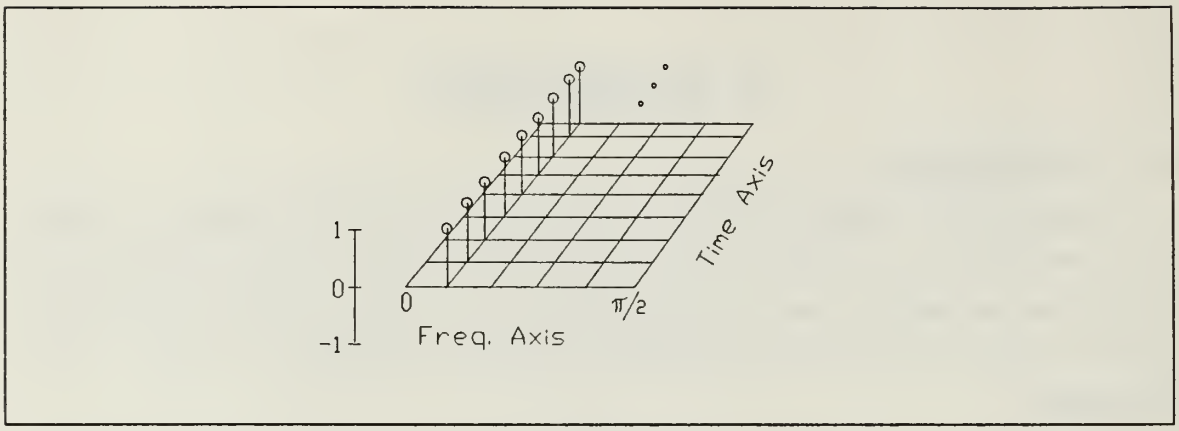

Figure 1. $x(n)$ represented as a constant sinusoid

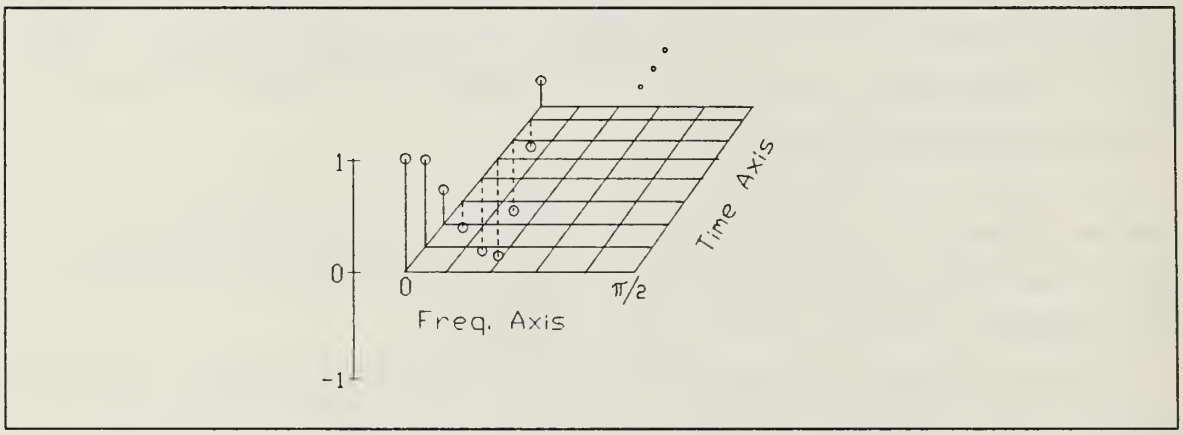

Figure 2. $x(n)$ represented as a time-varying DC component

Further complications appear when we consider the fact that, given a time-series, we cannot determine if the underlying process is or is not stationary, without using arbitrary and often inappropriate assumptions about what is the *local behavior*. When the algorithm of analysis produces a time-varying spectrum, the fact remains that there is at least one equally valid time-invariant spectral description (the Fourier Transform based), which is arbitrarily ruled out.

B. APPROACHES

If the signal is to be represented in the joint time-frequency plane in a sensible manner, the distribution must have some key properties. For example, a shift in the time-series should always imply a corresponding shift of the spectral representation along the time-axis. Also, a multiplication of the time-series by a complex exponential

should result into a shift of the spectral representation along the frequency axis. Without these properties, physical interpretation of the representation can be an impossible goal. This is one of the reasons why Ambiguity functions are not used in spectral estimation.

This technique of imposing constraints that are felt needed in a distribution can be carried further, and the distribution (or one of the distributions) formed in this refinement process *defined* as the true distribution. One of the most successful representations obtained by this approach is the Wigner-Ville Distribution (WD), which has extensively been used since its introduction in 1948 [Ref. 2].

A different approach to solve the indeterminacy is to define, a priori and unambiguously, what the considered true distribution is. Though this approach lacks control of the properties of the resulting distribution, it has the advantage of more closely preserving physical meaning in whatever results it produces. A typical example is the definition of "Instantaneous Power Spectrum" proposed by Page [Ref. 5], uniquely determining a resulting distribution which is amenable to physical interpretation.

C. OBJECTIVES

The Wigner-Ville Distribution has been extensively studied [Refs. 6, 7, 8, 9], and its characteristics are fairly well understood. However, its use is still hampered by some problems. First, it has uneven performance for different classes of signals. It performs optimally for single-component linear FM (linear chirp), but has worse performance for less regular spectral dynamics. Also, when multi-component signals are present, the WD creates artifacts in the spectrum, lying mid-way between true components. These artifacts are, up to some degree, recognizable and treatable due to an alternating sign [Ref. 6], but can severely mask results when analyzing more complex signals. The use of analytic signals is usually required, not only to avoid the need for sampling at twice the Nyquist rate, but also to prevent the appearance of undesirable artifacts that would otherwise be created by the interference between positive and negative frequencies [Refs. 6, 7, 10].

Though it has not received proper attention in the literature, Page's Instantaneous Power Spectrum is, once properly understood and treated, a practical alternative to estimate the time-varying spectrum.

The study and development of such an alternative is the main goal of this thesis.

II. INSTANTANEOUS POWER SPECTRUM (IPS)

A. DEFINITION

In an attempt to accommodate the notion of *instantaneous frequency content*, Page defined the Instantaneous Power Spectrum as the derivative of a running energy spectrum [Ref. 5]:

$$\rho^{-}(t, f) = \frac{\partial}{\partial t} | S_t^{-}(f) |^2 \tag{2}$$

where

$$S_t^{-}(f) = \int_{-\infty}^{t} s(\tau) e^{-j2\pi f\tau} d\tau \,. \tag{3}$$

That is, the Instantaneous Power Spectrum was defined as being, at each frequency, the rate of change of the energy collected by a Fourier transform taken from $-\infty$, up to the time of analysis. This concept was later extended by Levin [Ref. 3], who introduced a complementary backward run, similarly defined as:

$$\rho^{+}(t, f) = \frac{-\partial}{\partial t} | S_t^{+}(f) |^2 \tag{4}$$

where

$$S_t^{+}(f) = \int_{t}^{\infty} s(\tau) e^{-j2\pi f\tau} d\tau \,, \tag{5}$$

and defining the Instantaneous Power Spectrum as the average of these two runs:

$$IPS(t, f) = \frac{1}{2} [\rho^{-}(t, f) + \rho^{+}(t, f)] \,. \tag{6}$$

This expression can be put in the form [Refs. 3, 11]

$$IPS(t, f) = \text{Real}\,[s^*(t)S(f)e^{j2\pi ft}] \tag{7}$$

where $S(f)$ is the Fourier Transform of $s(t)$.

IPS can thus be seen to be the real part of Rihaczek's distribution [Ref. 4], which allows one to think of $IPS(t,f)$ as being the energy density entering, at time t, an infinitely narrow filter centered at frequency f. An enlightening treatment of this point can be found in Ackroyd [Ref. 12].

1. Time Domain

Let us now consider the following: we want a function of t, τ whose Fourier Transform is $IPS(t,f)$. That is, we want $G(t, \tau)$ such that

$$IPS(t,f) = \int_{-\infty}^{\infty} G(t, \tau)e^{-j2\pi f\tau}d\tau\,. \tag{8}$$

Then, using (7)

$$G(t, \tau) = \frac{1}{2}\int_{-\infty}^{\infty} [s(t)S^*(f)e^{-j2\pi ft} + s(t)^*S(f)e^{j2\pi ft}]\, e^{j2\pi f\tau}df \tag{9}$$

from where, with the appropriate variable substitutions we obtain

$$G(t, \tau) = \frac{1}{2}\int_{-\infty}^{\infty}\left[s(t)\int_{-\infty}^{\infty} s^*(t-\eta)e^{-j2\pi f\eta}d\eta + s^*(t)\int_{-\infty}^{\infty} s(t+\eta)e^{-j2\pi f\eta}d\eta\right]e^{j2\pi f\tau}df\,. \tag{10}$$

Interchanging the order of integration, we get

$$G(t, \tau) = \frac{1}{2}\,[s(t)s^*(t-\tau) + s^*(t)s(t+\tau)]\,. \tag{11}$$

IPS can now be restated as:

$$IPS(t,f) = \frac{1}{2}\int_{-\infty}^{\infty} [s(t)s^*(t-\tau) + s^*(t)s(t+\tau)]\, e^{-j2\pi f\tau} d\tau \,. \tag{12}$$

2. Frequency domain

Alternatively, a dual expression can be derived, expressing IPS in terms of the Fourier Transform of the signal.

$$\begin{aligned}
IPS(t,f) &= \frac{1}{2}\int_{-\infty}^{\infty} s(t)s^*(t-\tau)e^{-j2\pi f\tau} d\tau + \frac{1}{2}\int_{-\infty}^{\infty} s^*(t)s(t+\tau)e^{-j2\pi f\tau} d\tau \\
&= \frac{1}{2}\int_{-\infty}^{\infty}\int_{-\infty}^{\infty} S(\mu)e^{j2\pi\mu t} d\mu \int_{-\infty}^{\infty} S^*(\gamma)e^{-j2\pi\gamma(t-\tau)} d\gamma\, e^{-j2\pi f\tau} d\tau + \\
&\quad + \frac{1}{2}\int_{-\infty}^{\infty}\int_{-\infty}^{\infty} S^*(\mu)e^{-j2\pi\mu t} d\mu \int_{-\infty}^{\infty} S(\gamma)e^{j2\pi\gamma(t+\tau)} d\gamma\, e^{-j2\pi f\tau} d\tau \\
&= \frac{1}{2}\int_{-\infty}^{\infty}\int_{-\infty}^{\infty} S(\mu)S^*(\gamma)e^{j2\pi\mu t}\, e^{-j2\pi\gamma t}\delta(\gamma - f) d\gamma d\mu + \\
&\quad + \frac{1}{2}\int_{-\infty}^{\infty}\int_{-\infty}^{\infty} S^*(\mu)S(\gamma)e^{-j2\pi\mu t}\, e^{j2\pi\gamma t}\delta(\gamma - f) d\gamma d\mu \\
&= \frac{1}{2}\int_{-\infty}^{\infty} S(\mu)S^*(f)e^{-j2\pi(f-\mu)t} d\mu + \frac{1}{2}\int_{-\infty}^{\infty} S^*(\mu)S(f)e^{-j2\pi(\mu-f)t} d\mu \,.
\end{aligned} \tag{13}$$

With the appropriate variable substitutions, we get

$$IPS(t, f) = \frac{1}{2}\int_{-\infty}^{\infty} S(f+\gamma)S^*(f)e^{j2\pi\gamma t}d\gamma + \frac{1}{2}\int_{-\infty}^{\infty} S^*(f-\gamma)S(f)e^{j2\pi\gamma t}d\gamma \qquad (14)$$

and, finally

$$IPS(t,f) = \frac{1}{2}\int_{-\infty}^{\infty} [S(f)S^*(f-\gamma) + S^*(f)S(f+\gamma)]\, e^{j2\pi\gamma t}d\gamma\,. \qquad (15)$$

3. IPS for discrete signals

The discrete version of IPS follows directly from (12) as

$$IPS(n, \theta) = \frac{\Delta T}{2}\sum_{k=-\infty}^{\infty} [s(n)s^*(n-k) + s^*(n)s(n+k)]e^{-j\theta k}. \qquad (16)$$

A formal derivation of (16) can be found in Appendix A.

B. RELATIONS WITH OTHER TIME-FREQUENCY DISTRIBUTIONS

1. Rihaczek's Distribution

The Rihaczek Distribution was proposed in 1968 as the true energy[1] distribution in an attempt to unify existing results.

Formally, the distribution is [Ref. 4]

$$\varepsilon(t, f) = s(t)S^*(f)e^{-j2\pi ft} \qquad (17)$$

where $s(t)$ is the analytic signal being analyzed, and $S(f)$ is its Fourier Transform.

As was derived, $\varepsilon(t_0, f_0)$ is the complex energy density at the point (t_0, f_0) in the time-frequency plane. A similar expression had been considered by Levin, who defined the *Complex Instantaneous Power Spectrum* as the complex conjugate of (17).

---

[1] Rihaczek used the concept of "complex energy", whose real part is the real energy, while the imaginary part is the reactive energy.

Using Levin's notation, the *Complex Instantaneous Power Spectrum* is

$$\hat{X}(t, f) = \hat{s}^*(t)\hat{S}(f)e^{j2\pi ft}, \tag{18}$$

where $\hat{s}(t)$ is the complex envelope of the real signal under analysis.

We thus see from (7) that, though addressing a broader class of signals, IPS is both the real part of Rihaczek's Distribution and the real part of Levin's Complex Instantaneous Power Spectrum. Formally,

$$IPS(t,f) = \text{Real}[\varepsilon(t, f)] . \tag{19}$$

2. Cohen's Generalized Phase-Space Distribution Functions

In 1966, Cohen introduced a generalized class of time-frequency signal representations, given by

$$c(t, f) = \int_{-\infty}^{\infty}\int_{-\infty}^{\infty}\int_{-\infty}^{\infty} \Phi(\upsilon, \tau)\, s(t_1 + \frac{\tau}{2})s^*(t_1 - \frac{\tau}{2})\; e^{j2\pi(\upsilon t_1 - \upsilon t - \tau f)} d\upsilon dt_1 d\tau \tag{20}$$

where the choice of $\Phi(\upsilon, \tau)$ will determine the resulting distribution [Ref. 13].

If we slightly rearrange (20) to read

$$c(t, f) = \int_{-\infty}^{\infty}\int_{-\infty}^{\infty} \Phi(\upsilon, \tau)\left[\int_{-\infty}^{\infty} s(t_1 + \frac{\tau}{2})s^*(t_1 - \frac{\tau}{2})e^{j2\pi\upsilon t_1} dt_1\right] e^{-j2\pi(\upsilon t + \tau f)} d\upsilon d\tau , \tag{21}$$

we can interpret it as the double Fourier Transform of $\Psi(\upsilon, \tau)$ [Ref. 14], where

$$\Psi(\upsilon, \tau) = \Phi(\upsilon, \tau)\int_{-\infty}^{\infty} s(t_1 + \frac{\tau}{2})s^*(t_1 - \frac{\tau}{2})e^{j2\pi\upsilon t_1} dt_1 . \tag{22}$$

We can now recognize (22) as a general expression for the well known Ambiguity function, which can serve as a general definition of the time/frequency autocorrelation function [Refs. 3, 4].

Each choice of weighting function $\Phi(\upsilon, \tau)$ in (20) provides a different distribution, because each one defines the combined autocorrelation (22) in a somewhat different way.

Let us see which distributions result from three different realizations of $\Phi(\upsilon, \tau)$ (complex exponential, constant, and real sinusoid) [Refs. 4, 13, 14].

a. Complex exponential

$$\Phi(\upsilon, \tau) = e^{\frac{j2\pi\upsilon\tau}{2}} \tag{23}$$

The combined autocorrelation becomes

$$\begin{aligned}\Psi(\upsilon, \tau) &= e^{j\pi\upsilon\tau}\int_{-\infty}^{\infty} s(t_1 + \tfrac{\tau}{2})s^*(t_1 - \tfrac{\tau}{2})\, e^{j2\pi\upsilon t_1}dt_1 \\ &= \int_{-\infty}^{\infty} s(t_1 + \tfrac{\tau}{2})s^*(t_1 - \tfrac{\tau}{2})e^{j2\pi\upsilon(t_1 + \frac{\tau}{2})}dt_1\end{aligned} \tag{24}$$

and, defining a new variable $t = t_1 + \frac{\tau}{2}$, we obtain

$$\Psi(\upsilon, \tau) = \int_{-\infty}^{\infty} s(t_1)s^*(t_1 - \tau)e^{j2\pi\upsilon t_1}dt_1 \,. \tag{25}$$

The resulting distribution is

$$c(t, f) = \int_{-\infty}^{\infty}\int_{-\infty}^{\infty}\int_{-\infty}^{\infty} s(t_1)s^*(t_1 - \tau)e^{j2\pi\upsilon t_1}\, e^{-j2\pi(\upsilon t + \tau f)}dt_1 d\tau d\upsilon \,, \tag{26}$$

$$
\begin{aligned}
c(t, f) &= \int_{-\infty}^{\infty} \int_{-\infty}^{\infty} s(t_1) s^*(t_1 - \tau)\, e^{-j2\pi\tau f} \delta(t_1 - t) dt_1 d\tau \\
&= \int_{-\infty}^{\infty} s(t) s^*(t - \tau) e^{-j2\pi\tau f} d\tau \\
&= s(t) S^*(f) e^{-j2\pi f t}
\end{aligned}
\tag{27}
$$

which is the well-known Rihaczek Distribution.

Though this definition of the combined autocorrelation is probably the most intuitive one, its lack of mathematical symmetry has the undesirable effect of making the distribution complex. It has extensively been used in radar theory, since (25) is exactly Woodward's definition of the Ambiguity function [Ref. 3].

b. Constant

$$
\Phi(\upsilon, \tau) = 1 \tag{28}
$$

The combined autocorrelation becomes

$$
\Psi(\upsilon, \tau) = \int_{-\infty}^{\infty} s(t_1 + \frac{\tau}{2}) s^*(t_1 - \frac{\tau}{2})\, e^{j2\pi\upsilon t_1} dt_1 \,. \tag{29}
$$

The resulting distribution is

$$
c(t, f) = \int_{-\infty}^{\infty} \int_{-\infty}^{\infty} \int_{-\infty}^{\infty} s(t_1 + \frac{\tau}{2}) s^*(t_1 - \frac{\tau}{2}) e^{j2\pi\upsilon t_1}\, e^{-j2\pi(\upsilon t + \tau f)} dt_1 d\tau d\upsilon \,, \tag{30}
$$

$$
\begin{aligned}
c(t, f) &= \int_{-\infty}^{\infty} \int_{-\infty}^{\infty} s(t_1 + \tfrac{\tau}{2}) s^*(t_1 - \tfrac{\tau}{2}) e^{-j2\pi\tau f} \delta(t_1 - t) dt_1 d\tau \\
&= \int_{-\infty}^{\infty} s(t + \tfrac{\tau}{2}) s^*(t - \tfrac{\tau}{2}) e^{-j2\pi\tau f} d\tau
\end{aligned} \tag{31}
$$

which is the Wigner-Ville Distribution. This definition of the combined autocorrelation, though only slightly different from the one in (25), has the needed symmetry to make this distribution real, and mathematically very convenient (when dealing with analytic signals).

c. Cosine function

$$
\Phi(\upsilon, \tau) = \cos(\pi\upsilon\tau) \tag{32}
$$

The combined autocorrelation becomes

$$
\begin{aligned}
\Psi(\upsilon, \tau) &= \cos(\pi\upsilon\tau) \int_{-\infty}^{\infty} s(t_1 + \tfrac{\tau}{2}) s^*(t_1 - \tfrac{\tau}{2}) e^{j2\pi\upsilon t_1} dt_1 \\
&= \frac{(e^{j\pi t\tau} + e^{-j\pi t\tau})}{2} \int_{-\infty}^{\infty} s(t_1 + \tfrac{\tau}{2}) s^*(t_1 - \tfrac{\tau}{2}) e^{j2\pi\upsilon t_1} dt_1 \\
&= \frac{1}{2} \left[\int_{-\infty}^{\infty} s(t_1 + \tfrac{\tau}{2}) s^*(t_1 - \tfrac{\tau}{2}) e^{j2\pi\upsilon(t_1 + \frac{\tau}{2})} dt_1 \right. \\
&\quad \left. + \int_{-\infty}^{\infty} s(t_1 + \tfrac{\tau}{2}) s^*(t_1 - \tfrac{\tau}{2}) e^{j2\pi\upsilon(t_1 - \frac{\tau}{2})} dt_1 \right].
\end{aligned} \tag{33}
$$

Substituting t for $t_1 + \frac{\tau}{2}$ in the first integral, and t for $t_1 - \frac{\tau}{2}$ in the second, we get

$$\begin{aligned}\Psi(\upsilon, \tau) &= \frac{1}{2}\left[\int_{-\infty}^{\infty} s(t)s^*(t-\tau)e^{j2\pi\upsilon t}dt + \int_{-\infty}^{\infty} s^*(t)s(t+\tau)e^{j2\pi\upsilon t}dt\right] \\ &= \frac{1}{2}\int_{-\infty}^{\infty}\left[s(t)s^*(t-\tau) + s^*(t)s(t+\tau)\right]e^{j2\pi\upsilon t}dt\,.\end{aligned} \tag{34}$$

The resulting distribution is

$$\begin{aligned}c(t,\, f) &= \int_{-\infty}^{\infty}\int_{-\infty}^{\infty}\int_{-\infty}^{\infty}\frac{1}{2}\left[s(t_1)s^*(t_1-\tau) + s^*(t_1)s(t_1+\tau)\right]e^{j2\pi\upsilon t_1}e^{-j2\pi(\upsilon t+\tau f)}dt_1 d\upsilon d\tau \\ &= \int_{-\infty}^{\infty}\int_{-\infty}^{\infty}\frac{1}{2}\left[s(t_1)s^*(t_1-\tau) + s^*(t_1)s(t_1+\tau)\right]e^{-j2\pi\tau f}\delta(t_1-t)dt_1 d\tau \\ &= \frac{1}{2}\int_{-\infty}^{\infty}\left[s(t)s^*(t-\tau) + s^*(t)s(t+\tau)\right]e^{-j2\pi\tau f}d\tau\end{aligned} \tag{35}$$

which is the expression we had found earlier for IPS. In this case, the definition of the combined autocorrelation also possesses the symmetry needed for a real distribution. The kernel that generates IPS ($\Phi(\upsilon, \tau) = \cos(\pi\upsilon\tau)$) has been considered by Cohen [Ref. 13], and shown to generate the Margeneau-Hill distribution [Ref. 15], well known in quantum mechanics theory.

3. Wigner-Ville Distribution

Since the Wigner-Ville Distribution (WD) has enjoyed wide acceptance, we will define more closely the relations between IPS and WD. As an indirect connection, we can relate both to the Rihaczek Distribution. From (29) the WD implicitly defines the combined autocorrelation as [Ref. 4]

$$\Psi(\upsilon, \tau) = \int_{-\infty}^{\infty} s(t_1 + \frac{\tau}{2}) s^*(t_1 - \frac{\tau}{2}) e^{j2\pi\upsilon t_1} dt_1$$
$$= e^{-j\pi\upsilon\tau} \int_{-\infty}^{\infty} s(t_1) s^*(t_1 - \tau) e^{j2\pi\upsilon t_1} dt_1 . \tag{36}$$

Hence, the Wigner-Ville Distribution is given by [Ref. 4]

$$WD(t, f) = F_{\upsilon, \tau}\left[e^{-j\pi\upsilon\tau} \int_{-\infty}^{\infty} s(t_1) s^*(t_1 - \tau) e^{j2\pi\upsilon t_1} dt_1 \right] , \tag{37}$$

where $F_{\upsilon, \tau}[\,.\,]$ denotes the 2-D Fourier transform. From the convolution property of this operator, and using (25),

$$\begin{aligned} WD(t, f) &= F_{\upsilon, \tau}\left[e^{-j\pi\upsilon\tau}\right] ** F_{t, \tau}\left[\int_{-\infty}^{\infty} s(t_1) s^*(t_1 - \tau) e^{j2\pi\upsilon t_1} dt_1 \right] \\ &= F_{\upsilon, \tau}\left[e^{-j\pi t\tau}\right] ** \varepsilon(t, f) \\ &= e^{j4\pi ft} ** \varepsilon(t, f) \end{aligned} \tag{38}$$

where ** stands for 2-D convolution, and $\varepsilon(t, f)$ is the Rihaczek Distribution. From (38), using (19) and the realness property of WD (see Section II-C), we obtain

$$\begin{aligned} WD(t, f) &= \text{Real}\left[e^{j4\pi ft} ** \varepsilon(t, f)\right] \\ IPS(t, f) &= \text{Real}[\, \delta(t, f) ** \varepsilon(t, f)] . \end{aligned} \tag{39}$$

We thus see how the two distributions can be obtained from the Rihaczek Distribution by an appropriate choice of the function convolved with $\varepsilon(t, f)$.

We found earlier that each choice of $\Psi(\upsilon, \tau)$ in Cohen's class of Distributions (20) yields a particular definition of the combined autocorrelation function

$$\Psi(\upsilon, \tau) = \Phi(\upsilon, \tau) \int_{-\infty}^{\infty} s(t_1 + \frac{\tau}{2}) s^*(t_1 - \frac{\tau}{2}) e^{j2\pi\upsilon t_1} dt_1 \tag{40}$$

and that the 2-D Fourier transform of (40) resulted in a particular distribution, depending on $\Phi(\upsilon, \tau)$.

We see now that (40) is the product of two functions, $\Phi(\upsilon, \tau)$ and the integral. Its double Fourier Transform is thus a double convolution in the transform domain.[Ref. 14]

That is:

$$\begin{aligned} c(t, f) &= F_{\upsilon, \tau}[\Psi(\upsilon, \tau)] \\ &= F_{\upsilon, \tau}\left[\Phi(\upsilon, \tau) \int_{-\infty}^{\infty} s(t_1 + \frac{\tau}{2}) s^*(t_1 - \frac{\tau}{2}) e^{j2\pi\upsilon t_1} dt_1 \right] \\ &= F_{\upsilon, \tau}[\Phi(\upsilon, \tau)] \;**\; F_{\upsilon, \tau}\left[\int_{-\infty}^{\infty} s(t_1 + \frac{\tau}{2}) s^*(t_1 - \frac{\tau}{2}) e^{j2\pi\upsilon t_1} dt_1 \right] \\ &= F_{\upsilon, \tau}[\Phi(\upsilon, \tau)] \;**\; WD(t, f) \,. \end{aligned} \tag{41}$$

In the particular case of IPS,

$$IPS(t, f) = F_{\upsilon, \tau}[\cos(\pi\upsilon\tau)] \;**\; WD(t, f) \,. \tag{42}$$

Therefore,

$$IPS(t, f) = \cos(4\pi f t) \;**\; WD(t, f) \,, \tag{43}$$

which we could have deduced directly from (39) and the fact that the WD is always real, as follows:

$$\begin{aligned} IPS(t, f) &= \text{Real}[\varepsilon(t, f)] \\ &= \frac{1}{2}[\varepsilon(t, f) + \varepsilon^*(t, f)] \,. \end{aligned} \tag{44}$$

Using (38),

$$\begin{aligned} IPS(t, f) &= \frac{1}{2}\left[e^{-j4\pi ft} ** WD(t, f) + e^{j4\pi ft} ** WD(t, f)\right] \\ &= \frac{1}{2}\left[e^{-j4\pi ft} + e^{j4\pi ft}\right] ** WD(t, f) \\ &= \cos(4\pi ft) ** WD(t, f) . \end{aligned} \tag{45}$$

At this point, we would like to be able to express the WD in terms of IPS, with a relation of the form:

$$WD(t, f) = O[IPS(t, f)] , \tag{46}$$

where $O[\,.\,]$ is an arbitrary operator. Unfortunately, the inverse filter does not exist, since

$$F_{\upsilon, \tau}\left[\frac{1}{\cos(\pi\upsilon\tau)}\right] \tag{47}$$

is not defined over the required range of υ and τ .

4. Short-Time Fourier Transform

Though the Short-Time Fourier Transform (STFT) can not be considered a true Time-Frequency Distribution [Ref. 14], its widespread use fully justifies the study of how it relates to IPS. This hs been addressed in [Ref. 11], and will be done here, after which some indirect results will emerge. Let us thus consider the STFT as defined in (48):

$$\begin{aligned} STFT(t, \omega) &= |F(t, \omega)|^2 \\ &= \left| \int_{-\infty}^{\infty} s(t+\tau) w^*(\tau) e^{j\omega\tau} d\tau \right|^2 \\ &= \int_{-\infty}^{\infty} \int_{-\infty}^{\infty} s(t+\tau) s^*(t+\upsilon) w^*(\tau) w(\upsilon) e^{-j\omega\tau} e^{j\omega\upsilon} d\tau d\upsilon \end{aligned} \tag{48}$$

Substituting $s(t+\tau)$ and $w^*(\tau)$ by their Fourier definitions, we have that

$$
\begin{aligned}
STFT(t,\omega) &= \int_{-\infty}^{\infty}\int_{-\infty}^{\infty} s^*(t+\upsilon)w(\upsilon)\int_{-\infty}^{\infty} S(\xi)e^{j\xi(t+\tau)}d\xi\int_{-\infty}^{\infty} W^*(\rho)e^{-j\rho\tau}d\rho e^{-j\omega\tau}e^{j\omega\upsilon}d\tau d\upsilon \\
&= \int_{-\infty}^{\infty}\int_{-\infty}^{\infty} s^*(t+\upsilon)w(\upsilon)S(\rho+\omega)W^*(\rho)e^{j(\omega+\rho)t}e^{j\omega\upsilon}d\upsilon d\rho \qquad (49) \\
&= \int_{-\infty}^{\infty}\int_{-\infty}^{\infty} s^*(t+\upsilon)S(\rho+\omega)e^{j(\rho+\omega)(t+\upsilon)}w(\upsilon)W^*(\rho)e^{-j\rho\upsilon}d\upsilon d\rho\,.
\end{aligned}
$$

We thus see that the STFT is a time-frequency smoothed version of the Rihaczek distribution of the signal. The smoothing function is the Rihaczek distribution of the window used to compute the STFT. Since the right-hand side of (49) is always real and positive, and the previous relations are valid for arbitrary signals and windows, we conclude that windowing a Rihaczek distribution with a Rihaczek distribution guarantees a real and everywhere positive distribution. This result will be important when addressing the issue of positivity.

C. BASIC PROPERTIES OF IPS

As was already mentioned, and is easily seen from (20), it is the choice of a particular $\Phi(\upsilon,\tau)$ that determines the particular distribution and, hence, its properties. It is thus desirable to establish direct connections between the properties of $\Phi(\upsilon,\tau)$ and the properties of the resulting distribution. This issue has been addressed [Ref. 14], and we will in the most part only state results, as applicable to IPS. The basic properties of IPS are:

1. *Time shift*

If $\omega(t) = s(t-t_0)$, then

$$IPS_\omega(t,f) = IPS_s(t-t_0,f)\,. \qquad (50)$$

2. *Modulation*

If $\omega(t) = s(t)e^{j2\pi f_0 t}$, then

$$IPS_\omega(t,f) = IPS_s(t,f-f_0)\,. \qquad (51)$$

3. *Marginal in Time*

$$\int_{-\infty}^{\infty} IPS(t, f)\, df = |\, s(t)\,|^2 . \tag{52}$$

4. *Marginal in Frequency*

$$\int_{-\infty}^{\infty} IPS(t, f)\, dt = |\, S(f)\,|^2 . \tag{53}$$

where $S(f) = F[s(t)]$.

5. *Realness*

$$IPS(t, f) \text{ is real for all } t, f. \tag{54}$$

6. *Instantaneous Frequency*[2]

$$\frac{\int_{-\infty}^{\infty} f \cdot IPS(t, f) df}{|\, s(t)\,|^2} = f_i(t) \quad (\textit{instantaneous frequency}) \tag{55}$$

7. *Group Delay*

$$\frac{\int_{-\infty}^{\infty} t \cdot IPS(t, f) dt}{|\, S(f)\,|^2} = T_g(f) \quad (\textit{group delay}) \tag{56}$$

8. *Zero Power*

$$\begin{aligned} s(t_0) = 0 &\Rightarrow IPS(t_0, f) = 0 \\ S(f_0) = 0 &\Rightarrow IPS(t, f_0) = 0 \end{aligned} \tag{57}$$

The Wigner-Ville Distribution also respects properties 1-7 [Ref. 6], but only a weaker version of property 8.

D. FURTHER PROPERTIES

Though the properties presented in Section II-C constitute the basic set of rules to which IPS is bound, some further analysis must be made. The effects of linear operators should be investigated, to fully understand the behavior of IPS.

---

[2] This property is valid for analytic signals only (see Appendix B).

1. **Windowing in the time-domain**

The issue here is to determine how IPS is affected by windowing the original time signal.

We will at this point introduce the notation:

$$IPS_d(t, f) = \frac{1}{2} IPS_d^-(t, f) + \frac{1}{2} IPS_d^+(t, f) \tag{58}$$

where

$$IPS_d^-(t, f) = \int_{-\infty}^{\infty} d(t)d^*(t-\tau)e^{-j2\pi f\tau}d\tau \tag{59}$$

and

$$IPS_d^+(t, f) = \int_{-\infty}^{\infty} d^*(t)d(t+\tau)e^{-j2\pi f\tau}d\tau\,. \tag{60}$$

If the signal is windowed, that is:

$$d(t) = s(t)w(t)\,, \tag{61}$$

then the IPS of the windowed signal will be

$$\begin{aligned} IPS_d(t\,f) &= \frac{1}{2}\int_{-\infty}^{\infty} [d(t)d^*(t-\tau) + d^*(t)d(t-\tau)]e^{-j2\pi f\tau}d\tau \\ &= \frac{1}{2}\int_{-\infty}^{\infty} [s(t)w(t)s^*(t-\tau)w^*(t-\tau) + \\ &\qquad + s^*(t)w^*(t)s(t+\tau)w(t+\tau)]e^{-j2\pi f\tau}d\tau\,. \end{aligned} \tag{62}$$

Separating the two terms,

$$IPS_d(t, f) = \frac{1}{2}\int_{-\infty}^{\infty} [s(t)s^*(t-\tau)][w(t)w^*(t-\tau)]e^{-j2\pi f\tau}d\tau$$

$$+\frac{1}{2}\int_{-\infty}^{\infty} [s^*(t)s(t+\tau)][w^*(t)w(t+\tau)]e^{-j2\pi f\tau}d\tau$$

$$=\frac{1}{2}\int_{-\infty}^{\infty} F^{-1}[IPS_s^-]\,F^{-1}[IPS_w^-]e^{-j2\pi f\tau}d\tau \qquad (63)$$

$$+\frac{1}{2}\int_{-\infty}^{\infty} F^{-1}[IPS_s^+]\,F^{-1}[IPS_w^+]e^{-j2\pi f\tau}d\tau$$

$$=\frac{1}{2}\int_{-\infty}^{\infty} IPS_s^-(t,\upsilon)IPS_w^-(t,f-\upsilon)d\upsilon + \frac{1}{2}\int_{-\infty}^{\infty} IPS_s^+(t,\upsilon)IPS_w^+(t,f-\upsilon)d\upsilon\,,$$

where $F^{-1}[.]$ is the inverse Fourier Transform operator. Hence

$$IPS_d(t, f) = \frac{1}{2}\left[IPS_s^-(t, f) \underset{f}{*} IPS_w^-(t, f)\right] + \frac{1}{2}\left[IPS_s^+(t, f) \underset{f}{*} IPS_w^+(t, f)\right], \qquad (64)$$

where $\underset{f}{*}$ denotes convolution in the f variable.

That is, while for the Wigner-Ville, windowing the time signal implies the convolution along the frequency axis of the signal's WD with the window's WD [Ref. 6], for IPS we have a sum of two convolutions: the first term of the signal's IPS (IPS_s^-) is convolved with the first term of the window's IPS (IPS_w^-), and a similar convolution is applied to (IPS_s^-) and (IPS_w^-) .

A special case occurs when the window, the signal, or both, possess conjugate symmetry about t, the time at which we are computing IPS (i.e., $s(t+\tau) = s^*(t-\tau)$, $w(t+\tau) = w^*(t-\tau)$, or both). If $w(t)$ possesses that symmetry, then

$$IPS_w^-(t, f) = IPS_w^+(t, f) = IPS_w(t, f) \qquad (65)$$

and, by linearity of the convolution operator, (64) becomes

$$IPS_d(t, f) = \int_{-\infty}^{\infty} IPS_s(t, \upsilon) IPS_w(t, f-\upsilon) d\upsilon \,. \tag{66}$$

We thus see that in this case IPS and WD respond similarly to the windowing of the data: the IPS of the windowed signal is the convolution (in frequency) of the IPS of the signal with the IPS of the window.

In summary, the IPS of a windowed signal is a frequency-smoothed version of the IPS of the unwindowed signal. The time-resolution is not affected.

2. Convolution in the Time-domain

The question now is: how is the IPS of a signal affected if the signal is pre-processed with a filtering operation? So, let

$$d(t) = s(t) * h(t) \,. \tag{67}$$

Then,

$$\begin{aligned} IPS_d(t, f) &= \text{Real}\left[[s^*(t) * h^*(t)]\, F\,[s(t) * h(t)]\, e^{j2\pi ft}\right] \\ &= \text{Real}\left[[s^*(t) * h^*(t)] S(f) H(f) e^{j2\pi ft}\right] \\ &= \text{Real}\left[\left[s^*(t) S(f) e^{j2\pi ft}\right] \underset{t}{*} \left[h^*(t) H(f) e^{j2\pi ft}\right]\right], \end{aligned} \tag{68}$$

where we used the fact that

$$\begin{aligned} e^{j2\pi ft}[a(t) * b(t)] &= e^{j2\pi ft} \int_{-\infty}^{\infty} a(\tau) b(t-\tau) d\tau \\ &= \int_{-\infty}^{\infty} a(\tau) e^{j2\pi f\tau} b(t-\tau) e^{j2\pi f(t-\tau)} d\tau \\ &= [a(t) e^{j2\pi ft}] * [b(t) e^{j2\pi ft}] \,. \end{aligned} \tag{69}$$

We thus see that (contrary to what happens in the WD[3]) filtering the signal does not, in general, correspond to the convolution in time of the signal's IPS with the IPS of the impulse response of the filter. What is observable from (68) is that the IPS of the filtered signal is now the real part of the convolution, along the time axis, of the two Rihaczek Distributions. The net effect produced on IPS is, thus, still a smoothing operation along the time axis. The frequency resolution is not affected.

3. IPS and Moyal's Formula

As is often stated in the literature, IPS does not, in general, respect Moyal's formula [Ref. 16]. When applied to the WD, Moyal's formula states [Ref. 17]:

$$\int_{-\infty}^{\infty}\int_{-\infty}^{\infty} WD_s(t,f)WD_g(t,f)dtdf = < s,g > < s,g >^{*} \tag{70}$$

where $< s,g >$ is the inner product of s and g . Let us now see what happens in the IPS case:

$$\begin{aligned}
&\int_{-\infty}^{\infty}\int_{-\infty}^{\infty} IPS_s(t,f)IPS_g(t,f)dtdf = \\
&= \frac{1}{4}\int_{-\infty}^{\infty}\int_{-\infty}^{\infty}\left[\int_{-\infty}^{\infty}[s(t)s^{*}(t-\tau)+s^{*}(t)s(t+\tau)]e^{-j2\pi f\tau}d\tau\right. \\
&\qquad\left.\cdot\int_{-\infty}^{\infty}[g(t)g^{*}(t-\upsilon)+g^{*}(t)g(t+\upsilon)]e^{-j2\pi f\upsilon}d\upsilon\right]dtdf .
\end{aligned} \tag{71}$$

---

[3] The WD of a filtered signal is the convolution along the time-axis of the original signal's WD with the WD of the impulse response of the filter [Ref. 6].

$$\int_{-\infty}^{\infty}\int_{-\infty}^{\infty} IPS_s(t,\, f)IPS_g(t,\, f)dtdf =$$

$$= \frac{1}{4}\int_{-\infty}^{\infty}\int_{-\infty}^{\infty}\int_{-\infty}^{\infty} [s(t)s^*(t-\tau) + s^*(t)s(t+\tau)][g(t)g^*(t-\upsilon) + g^*(t)g(t+\upsilon)]$$

$$\cdot\left[\int_{-\infty}^{\infty} e^{-j2\pi f(\tau+\upsilon)}df\right]d\tau dt d\upsilon \tag{72}$$

$$= \frac{1}{4}\int_{-\infty}^{\infty}\int_{-\infty}^{\infty} [s(t)s^*(t-\tau) + s^*(t)s(t+\tau)][g(t)g^*(t+\tau) + g^*(t)g(t-\tau)]\, dt\, d\tau$$

$$= \frac{1}{4} <s, g>^* <s,g> + \frac{1}{4} <s, g> <s,g>^*$$

$$+ \frac{1}{2}\,\text{Real}\left[\int_{-\infty}^{\infty} s(t)g(t)\left[\int_{-\infty}^{\infty} s^*(t-\tau)g^*(t+\tau)d\tau\right]dt\right],$$

and, finally

$$\int_{-\infty}^{\infty}\int_{-\infty}^{\infty} IPS_s(t,\, f)IPS_g(t,\, f)dtdf =$$

$$= \frac{1}{2} <s, g> <s,g>^* + \frac{1}{2}\,\text{Real}\left[\int_{-\infty}^{\infty} s(t)g(t)\left[\int_{-\infty}^{\infty} s^*(t-\tau)g^*(t+\tau)d\tau\right]dt\right]. \tag{73}$$

The result confirms that Moyal's formula is not, in general, valid for IPS. Only in the trivial case of one of the functions being a real constant would the second term in the right hand-side of (73) reduce to $\frac{1}{2} <s,g> <s,g>^*$, and hence would IPS obey Moyal's formula.

4. Recovery of time-signals

To address the problem of recovering a signal from its IPS, we will find it convenient to consider two separate cases.

a. Infinite duration signals

For real signals with $S(0) \neq 0$, recovery of the signal is always possible except for a sign indeterminacy, by considering

$$\begin{aligned} IPS(t,\ 0) &= \text{Real}[s(t)S(0)] \\ &= S(0)s(t) \end{aligned} \tag{74}$$

and, since $|\ S(0)\ |$ can be found by using Property 4 (53), only the sign of $S(0)$ remains undetermined. No similar results are available for complex signals of infinite duration. However, if $s(t)$ possesses conjugate symmetry around some t_0, then we can also recover complex signals of infinite duration up to a phase term, by considering $F^{-1}\ [\ IPS(t_0, f)\ ]$. Similarly, if $S(f)$ possesses conjugate symmetry around some f_0 and $S(0) \neq 0$, we can again recover complex signals of infinite duration up to a phase term, by considering $F\ [\ IPS(t, f_0)\ ]$.

b. Finite duration signals

For finite duration signals, recovery of real or complex signals is always possible except for a constant phase term (or a sign, in the case of real signals).

Let us denote the starting time by $t = 0$. From (12)

$$F^{-1}\ [IPS(0,\ f)] = \frac{1}{2}\ [\ s(0)s^*(-\tau) + s^*(0)s(\tau)\ ] \tag{75}$$

and, since $s(-\tau) = 0$ for $\tau > 0$,

$$F^{-1}\ [IPS(0,\ f)]\ |_{\tau>0} = \frac{1}{2}\ s^*(0)s(\tau) \tag{76}$$

which, by property 3 (52), leaves an unknown phase term.

E. IPS - A GENERALIZATION OF THE WIENER-KHINCHIN THEOREM

By redefining auto-correlation, IPS offers a very straightforward extension of the Wiener-Khinchin theorem to the non-stationary case, as we shall see.

Let us define the auto-correlation function of a signal as

$$R(t, \tau) = \frac{1}{2}\ E\{s(t)s^*(t-\tau) + s^*(t)s(t+\tau)\}\ . \tag{77}$$

We have, then, using (12) and by linearity of the convolution operator the following pair of relations:

- $E\{IPS(t, f)\} = \int_{-\infty}^{\infty} R(t, \tau)\, e^{-j2\pi f\tau} d\tau$
- $R(t, \tau) = \int_{-\infty}^{\infty} E\{IPS(t, f)\}\, e^{j2\pi f\tau} df$

These relations can be read as a generalization of the Wiener-Khinchin theorem to non-stationary signals, since for stationary signals they promptly reduce to that theorem. If $s(t)$ is a stationary signal, then

$$\begin{aligned} R(t, \tau) &= \frac{1}{2} E\left\{s(t)s^*(t-\tau) + s^*(t)s(t+\tau)\right\} \\ &= \frac{1}{2} E\left\{s(t)s^*(t-\tau)\right\} + \frac{1}{2} E\left\{s^*(t)s(t+\tau)\right\} \\ &= \frac{1}{2} R(\tau) + \frac{1}{2} R^*(-\tau) \\ &= R(\tau) \end{aligned} \tag{78}$$

$$E\{IPS(t, f)\} = \int_{-\infty}^{\infty} R(\tau) e^{-j2\pi f\tau} d\tau = |\, S(f)\,|^2 \tag{79}$$

The expected value of IPS is, thus, for stationary signals, the usual Power Spectral Density (PSD).

Since in the non-stationary case we cannot try to infer ensemble averages from time averages, the IPS of a signal is *one realization* of the generalized Wiener-Khinchin relations of the underlying stochastic process.

A different view of IPS when applied to stochastic processes can be found in Grace [Ref. 11], where $E\{IPS(t, f)\}$ is shown to be the Fourier Transform of Loeve's Generalized Power Spectral Density.

III. RETHINKING IPS

A. ON THE USE OF WINDOWS

IPS, as given in (12), suffers from intense ringing at all frequencies "touched" by the signal. This same effect is one of the reasons why Rihaczek's Distribution did not find much acceptance. An example can be seen in Figure 3, where a linear chirp was used as the test signal.

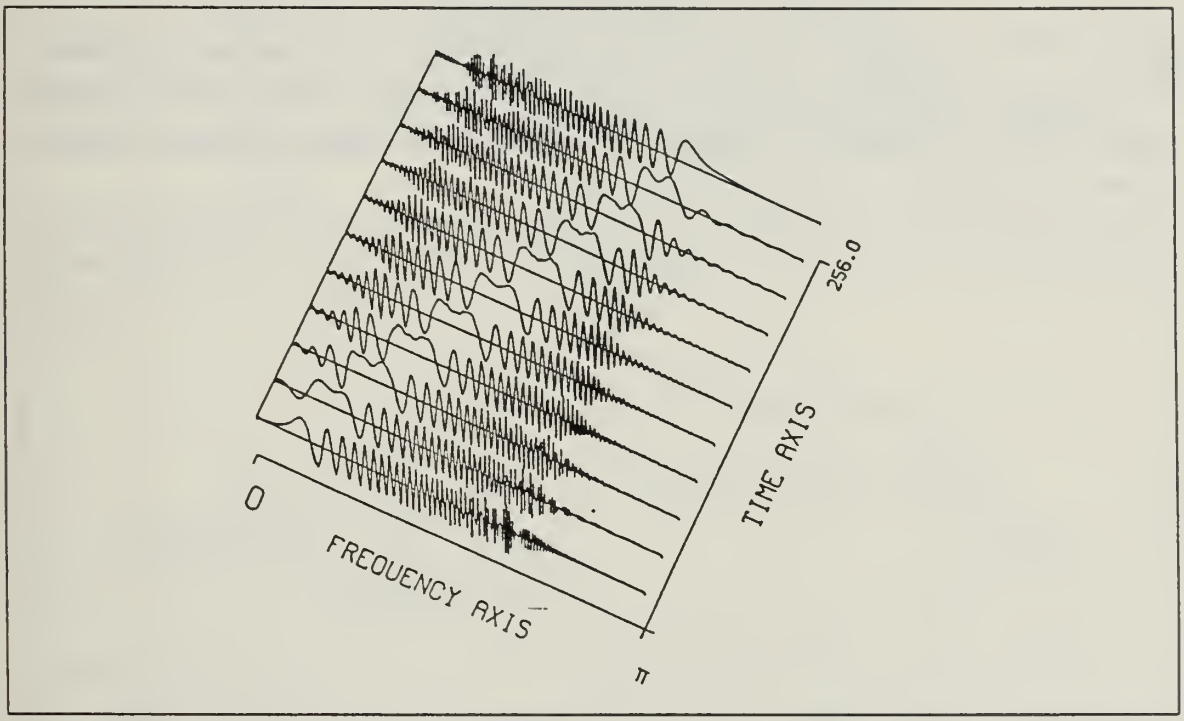

Figure 3. IPS for a linear chirp

This ringing effect can easily be understood by slightly rearranging (12) to :

$$IPS(t, f) = \frac{1}{2}\left[s(t)\int_{-\infty}^{\infty} s^{*}(t-\tau)e^{-j2\pi f\tau}d\tau + s^{*}(t)\int_{-\infty}^{\infty} s(t+\tau)e^{-j2\pi f\tau}d\tau \right]. \qquad (80)$$

With the appropriate changes of variable, we get

$$
\begin{aligned}
IPS(t, f) &= \frac{1}{2}\left[s(t)\int_{-\infty}^{\infty} s^*(t_1)e^{-j2\pi f(t-t_1)}dt_1 + s^*(t)\int_{-\infty}^{\infty} s(t_2)e^{j2\pi f(t-t_2)}dt_2 \right] \\
&= \frac{1}{2}\left[s(t)\left[s(t) * e^{j2\pi ft}\right]^* + s^*(t)\left[s(t) * e^{j2\pi ft}\right]\right] \\
&= \text{Real}\left[s^*(t)\left[s(t) * e^{j2\pi ft}\right]\right].
\end{aligned}
\tag{81}
$$

But $s(t) * e^{j2\pi ft}$ is the output of a filter whose impulse response is a complex exponential. IPS is, thus, for each frequency, the real part of the product of the signal's complex conjugate and the output of an infinitely narrow non-causal filter (non-causal oscillator) (Figure 4). [Ref. 12]

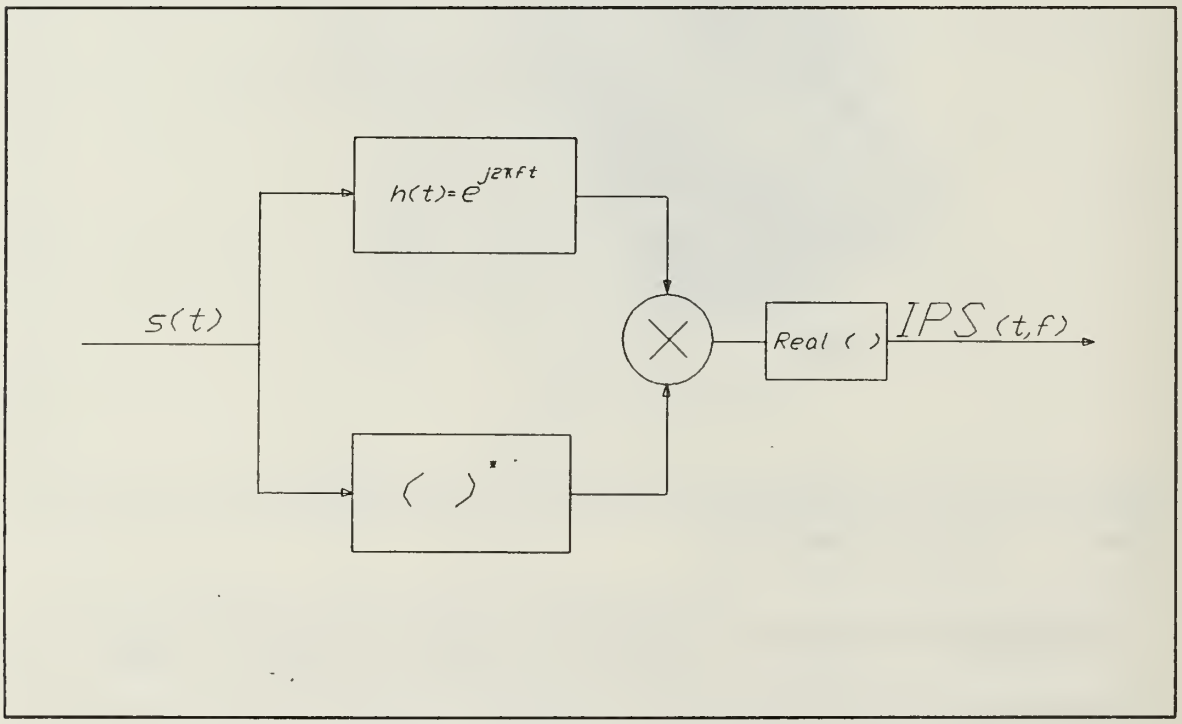

Figure 4. Model of IPS

The ringing is hence unavoidable, and will persist until the filter's impulse response becomes negligible. We should consider stable filters, with decaying impulse responses, if we want to diminish this effect. This reasoning leaves us very close to the work of Fano [Ref. 18], which was later extended by Schroeder and Atal [Ref. 19].

If we replace the oscillators in the IPS definition by stable filters with impulse responses of the form

$$h(t) = w(t)e^{j2\pi ft}, \tag{82}$$

where $w(t)$ is any real and symmetric function of t with general lowpass characteristics and $w(0) = 1$, then the resulting distribution $D(t, f)$ is given by

$$\begin{aligned} D_s(t, f) &= \text{Real}\left[s^*(t)[s(t) * w(t)e^{j2\pi ft}]\right] \\ &= \frac{1}{2}\left[s(t)[s(t) * w(t)e^{j2\pi ft}]^* + s^*(t)[s(t) * w(t)e^{j2\pi ft}]\right] \\ &= \frac{1}{2}\int_{-\infty}^{\infty} s(t)s^*(\tau)w(t-\tau)e^{-j2\pi f(t-\tau)}d\tau + \frac{1}{2}\int_{-\infty}^{\infty} s^*(t)s(\upsilon)w(t-\upsilon)e^{j2\pi f(t-\upsilon)}d\upsilon. \end{aligned} \tag{83}$$

Substituting t_1 for $(t-\tau)$ in the first integral, and $-t_2$ for $(t-\upsilon)$ in the second integral, we get

$$\begin{aligned} D_s(t, f) &= \frac{1}{2}\int_{-\infty}^{\infty} \left[s(t)s^*(t-t_1) + s^*(t)s(t+t_1)\right] w(t_1)\, e^{-j2\pi ft_1}dt_1 \\ &= IPS_{(s,\chi)}(t, f) \end{aligned} \tag{84}$$

where $\chi(\tau) = w(\tau - t)$.

That is, the resulting distribution is the IPS of the windowed signal, where the window is the envelope of the filter impulse response, centered at the time of analysis. Since $w(t-\tau)$ is real and symmetric around t, we see from (66) that a smoothing of the IPS in the frequency direction will result.

IPS in general can hence be written as

$$IPS(t, f) = \frac{1}{2}\int_{-\infty}^{\infty} \left[s(t)s^*(t-\tau) + s^*(t)s(t+\tau)\right] w(0)w(\tau)e^{-j2\pi f\tau}d\tau, \tag{85}$$

where $w(\tau)$ is the chosen window.

To illustrate the effectiveness of the windowing operation, we computed the IPS of the test signal used in Figure 3. A Hamming window was used in (85), and the results are shown in Figure 5. As is observable, the ringing is avoided.

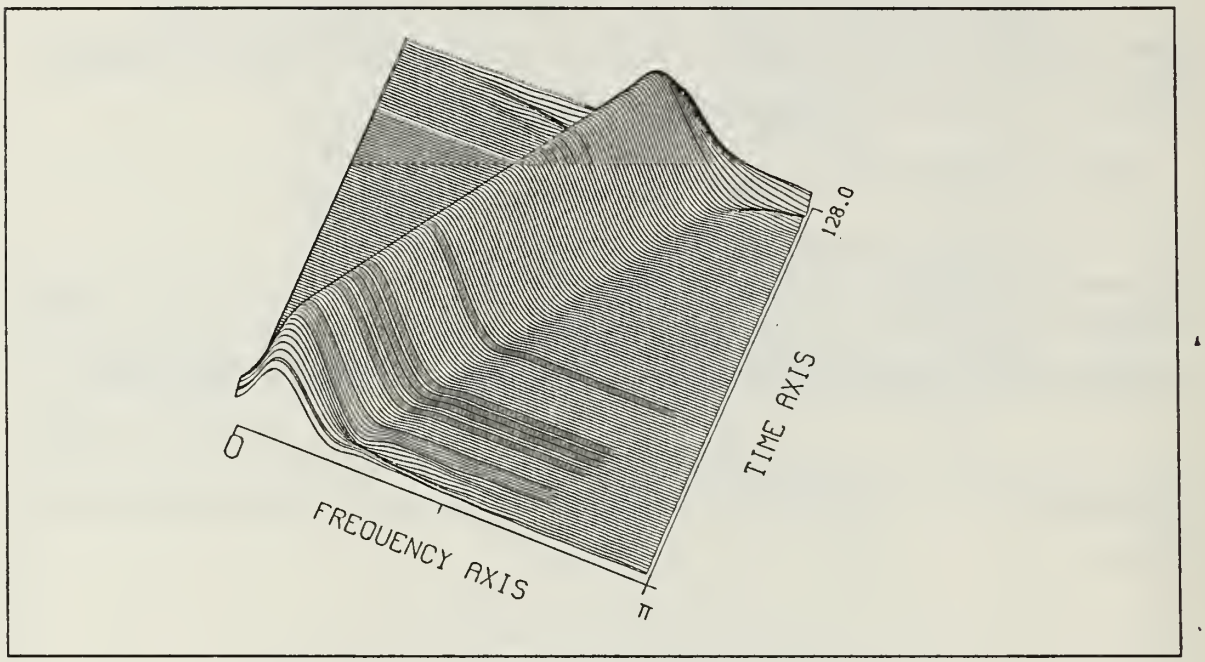

Figure 5. IPS for a linear chirp - Hamming window

B. PROPERTIES AFTER WINDOWING

Some of the properties of IPS will be affected by the windowing operation. It will thus be necessary to determine which properties are modified and establish the connections between the characteristics of the used window, and the effects it generates.

Tracing back the windowing operation to the kernel function ($\Phi(\upsilon, \tau)$) in (20) that it implies, we will be able to use well established results [Ref. 14] about these functions.

The resulting kernel function will be

$$\Phi(\upsilon, \tau) = w(0)w(\tau)\cos(\pi\upsilon\tau)\,, \tag{86}$$

which can be proved using (19) as follows :

$$IPS(t, f) = \int_{-\infty}^{\infty}\int_{-\infty}^{\infty}\int_{-\infty}^{\infty} w(0)w(\tau)\cos(\pi\upsilon\tau)s(t_1+\frac{\tau}{2})s^*(t_1-\frac{\tau}{2})e^{j2\pi\upsilon t_1}e^{-j2\pi(\upsilon t+\tau f)}d\upsilon d\tau dt_1\,. \tag{87}$$

Replacing the cosine by complex exponentials, we have

$$IPS(t, f) = \int_{-\infty}^{\infty}\int_{-\infty}^{\infty} \frac{w(0)w(\tau)}{2} \int_{-\infty}^{\infty} s(t_1 + \tfrac{\tau}{2})s^*(t_1 - \tfrac{\tau}{2})e^{j2\pi\upsilon(t_1 + \frac{\tau}{2})}dt_1 e^{-j2\pi(\upsilon t + \tau f)}d\upsilon d\tau$$
$$+ \int_{-\infty}^{\infty}\int_{-\infty}^{\infty} \frac{w(0)w(\tau)}{2} \int_{-\infty}^{\infty} s(t_1 + \tfrac{\tau}{2})s^*(t_1 - \tfrac{\tau}{2})e^{j2\pi\upsilon(t_1 - \frac{\tau}{2})}dt_1 e^{-j2\pi(\upsilon t + \tau f)}d\upsilon d\tau \tag{88}$$

and, by convenient change of variables,

$$IPS(t, f) = \int_{-\infty}^{\infty}\int_{-\infty}^{\infty} \frac{w(0)w(\tau)}{2} \int_{-\infty}^{\infty} s(\mu)s^*(\mu - \tau)e^{j2\pi\upsilon\mu}d\mu e^{-j2\pi(\upsilon t + \tau f)}d\upsilon d\tau$$
$$+ \int_{-\infty}^{\infty}\int_{-\infty}^{\infty} \frac{w(0)w(\tau)}{2} \int_{-\infty}^{\infty} s^*(\mu)s(\mu + \tau)e^{j2\pi\upsilon\mu}d\mu e^{-j2\pi(\upsilon t + \tau f)}d\upsilon d\tau\,. \tag{89}$$

Interchanging the order of integration, we obtain

$$IPS(t, f) = \frac{1}{2}\int_{-\infty}^{\infty} [s(t)s^*(t - \tau) + s^*(t)s(t + \tau)]w(0)w(\tau)e^{-j2\pi f\tau}d\tau\,,$$

completing the proof.

We can now easily determine which properties are maintained after the windowing operation, by direct application of the results in [Ref. 14], mapping the characteristics of the kernel function to the properties of the distribution. The conditions on $\Phi(\upsilon, \tau)$ necessary for the preservation of each of the properties will also be given.

1. *Time shift*

If $\omega(t) = s(t - t_0)$, then

$$IPS_{\omega}(t, f) = IPS_s(t - t_0, f) . \tag{91}$$

The requirement on $\Phi(\upsilon, \tau)$ is:

$$\Phi(\upsilon, \tau) \text{ constant for all } t . \tag{92}$$

This property will thus be maintained for every used window.

2. *Modulation*

If $\omega(t) = s(t)e^{j2\pi f_0 t}$, then

$$IPS_{\omega}(t, f) = IPS_s(t, f - f_0) . \tag{93}$$

The requirement on $\Phi(\upsilon, \tau)$ is:

$$\Phi(\upsilon, \tau) \text{ constant for all } f . \tag{94}$$

This property will thus be maintained for every used window.

3. *Marginal in Time*

$$\int_{-\infty}^{\infty} IPS(t, f)\, df = |\, s(t)\,|^2 . \tag{95}$$

The requirement on $\Phi(\upsilon, \tau)$ is:

$$\Phi(\upsilon, 0) = 1 \quad \text{for all } \upsilon . \tag{96}$$

Maintained iff $w(0) = 1$.

4. *Marginal in Frequency*

$$\int_{-\infty}^{\infty} IPS(t, f)\, dt = |\, S(f)\,|^2 . \tag{97}$$

The requirement on $\Phi(\upsilon, \tau)$ is:

$$\Phi(0, \tau) = 1 \quad \text{for all } \tau . \tag{98}$$

Not maintained for practical windows.

5. *Realness*

$$IPS(t, f) \text{ is real for all } t, f. \tag{99}$$

The requirement on $\Phi(\upsilon, \tau)$ is:

$$\Phi(\upsilon, \tau) = \Phi^*(-\upsilon, -\tau). \tag{100}$$

Maintained if the window is real and even, or at least possesses conjugate symmetry around the origin.

6. *Instantaneous Frequency*

$$\frac{\int_{-\infty}^{\infty} f \cdot IPS(t, f) df}{|s(t)|^2} = f_i(t) \quad (\textit{instantaneous frequency}) \tag{101}$$

The requirement on $\Phi(\upsilon, \tau)$ is:

$$\Phi(\upsilon, 0) = 1 \quad \text{and} \quad \frac{\partial}{\partial \tau} \Phi(\upsilon, \tau)\,|_{\tau=0} = 0 \quad \text{for all } \upsilon. \tag{102}$$

Maintained if

- $w(0) = 1$.
- $w'(\tau)\,|_{\tau=0} = 0$.

7. *Group Delay*

$$\frac{\int_{-\infty}^{\infty} t \cdot IPS(t, f) dt}{|S(f)|^2} = T_g(f) \quad (\textit{group delay}) \tag{103}$$

The requirement on $\Phi(\upsilon, \tau)$ is:

$$\Phi(0, \tau) = 1 \quad \text{and} \quad \frac{\partial}{\partial \upsilon} \Phi(\upsilon, \tau)\,|_{\upsilon=0} = 0 \quad \text{for all } \tau. \tag{104}$$

Not maintained for practical windows.

8. *Zero Power*

$$s(t_0) = 0 \Rightarrow IPS(t_0, f) = 0 \tag{105}$$

This property is clearly maintained, due to the multiplicative nature of the windowing operation.

$$S(f_0) = 0 \Rightarrow IPS(t, f_0) = 0 \tag{106}$$

This property will not be maintained since, from (64), a convolution along the frequency axis will be performed.

C. SPECTRAL RESOLUTION

1. Time-invariant Components

Though IPS is a tool directed towards the analysis of signals with time-varying spectral contents, some insight into its inner workings will be gained by considering its resolution capabilities for time-invariant spectral components. A comparison of resolution capabilities for IPS and WD will be made, and contrasted with the standard Fourier Transform.

As seen in (6), IPS is a coherent average of two terms, one of which uses only past data, while the other uses only future information.[4] When analyzing finite duration signals, the "past term" will have its maximum resolution capability at the end of the data segment, since it is at this point that the most past data is available. Similarly, the "future term" will resolve better at the beginning of the data segment. This can be seen in Figure 6 and Figure 7, for the past and future terms, respectively.

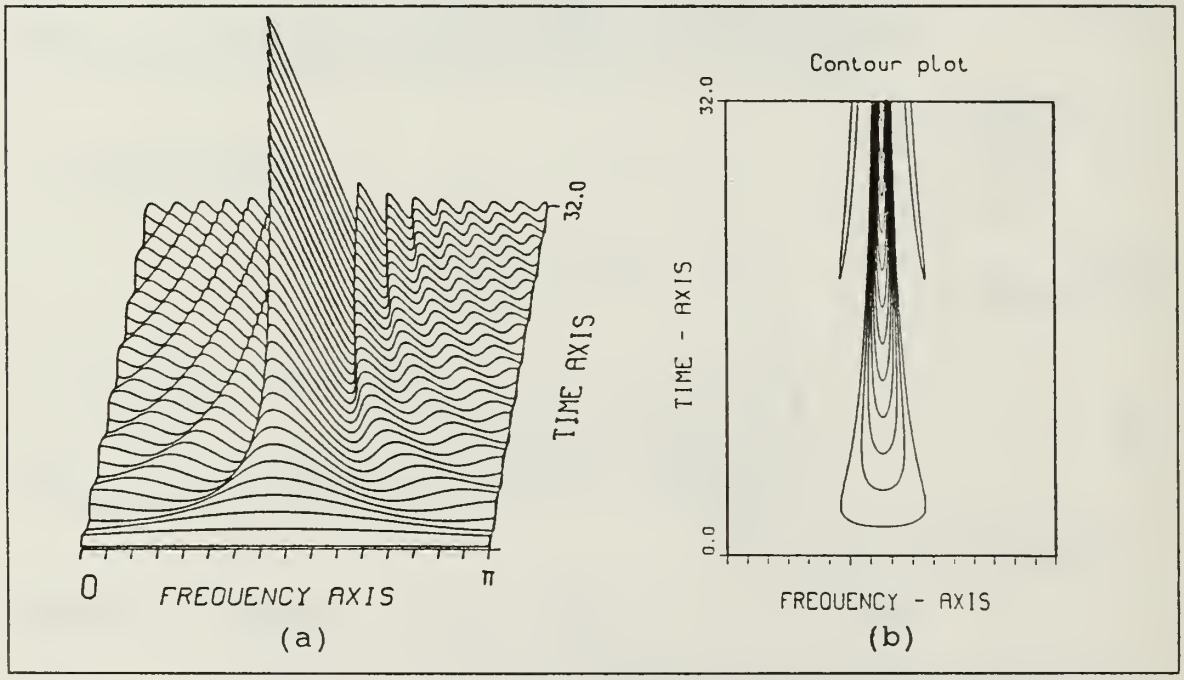

Figure 6. Sinusoidal component. Past term. 3-D (a) and Contour (b) plots

If the two terms are averaged as in (6), the resulting expression (IPS) will keep the good resolution at end-points that each component provides, degrading its resolution

[4] A note of caution should be made here. These "past" and "future" terms should not be identified with the two terms in (12), since each one of the terms in this formula spans all the data, from $-\infty$ to ∞.

capabilities towards the center of the time segment. This effect can be observed in the contour plot of Figure 8.

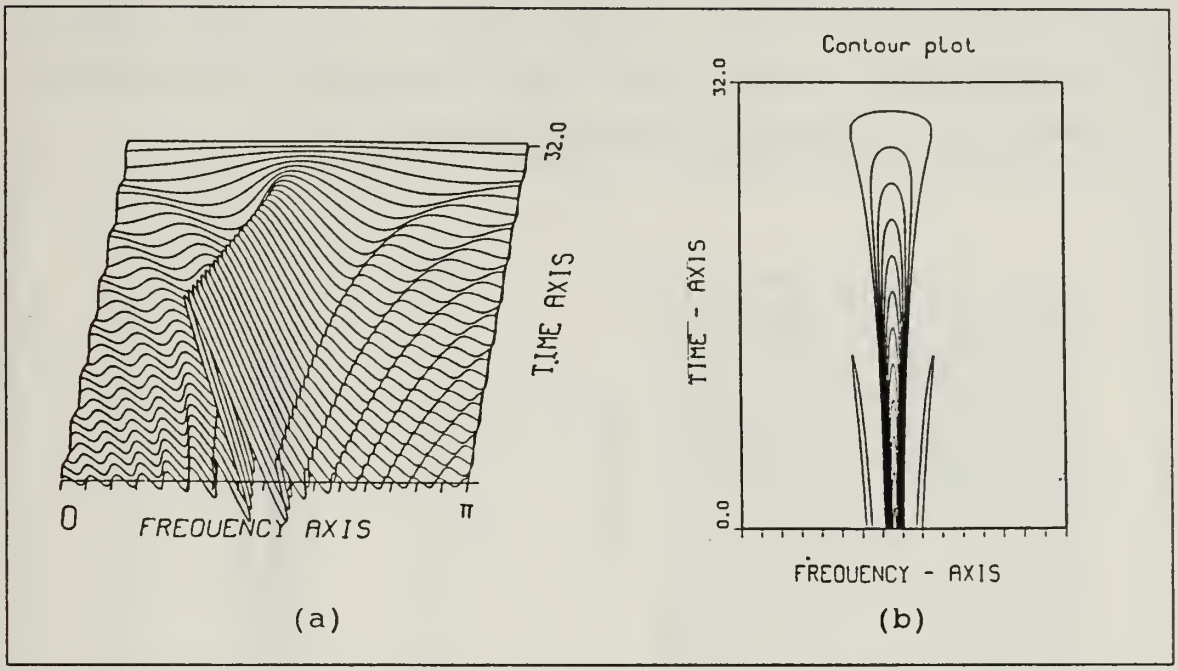

Figure 7. Sinusoidal component. Future term. 3-D (a) and Contour (b) plots

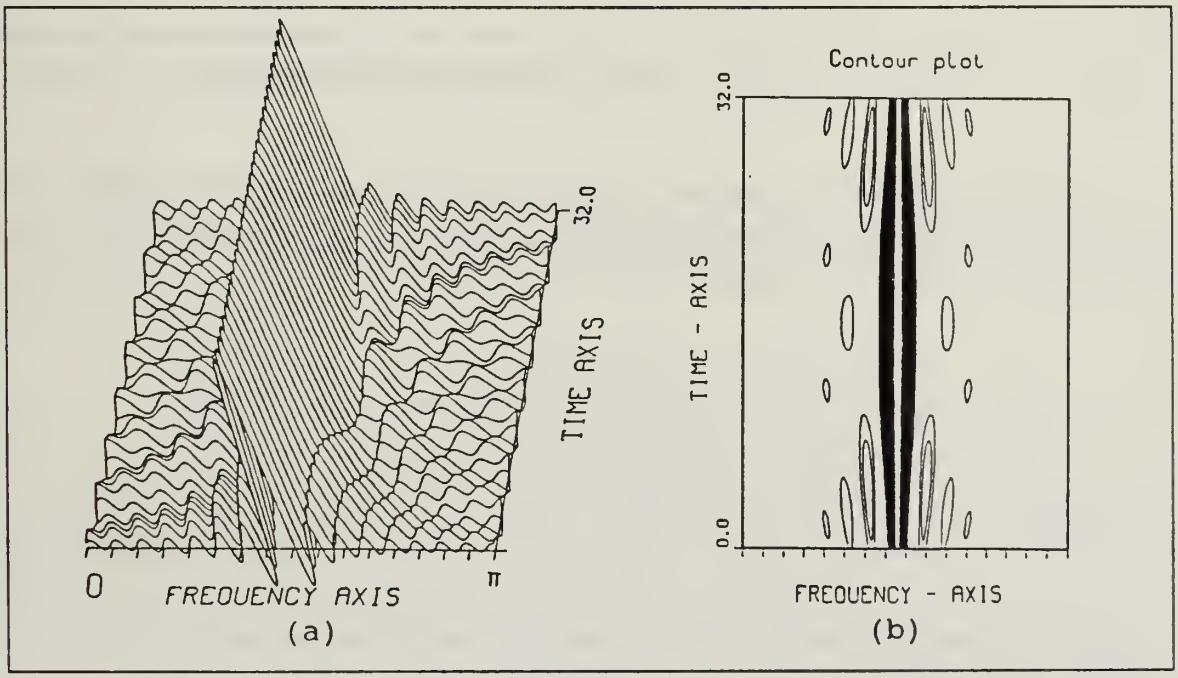

Figure 8. IPS for a sinusoidal component. 3-D (a) and Contour (b) plots

This is one of the characteristics of the unwindowed IPS. It has better resolution at end-points than it does in the middle of the data segment. We should point out that the WD does the opposite, presenting a thinner main-lobe at the center of the time interval, and loosing resolution capabilities towards the end-points (Figure 9).

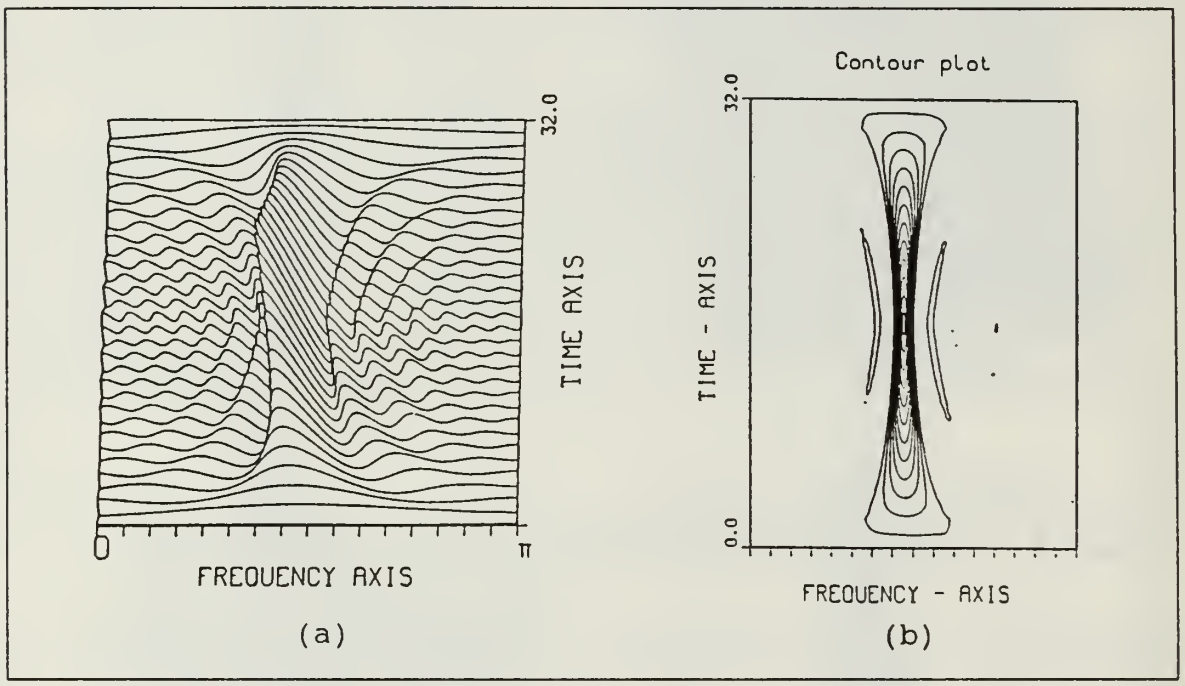

Figure 9. WD for a sinusoidal component. 3-D (a) and Contour (b) plots

A more formal discussion can be made as follows: Let us denote by $CW_{t_0}(\tau)$ the function of τ whose Fourier Transform is $WD(t_0, f)$ and, similarly, denote by $CI_{t_0}(\tau)$ the function of τ whose Fourier Transform is $IPS(t_0, f)$. Hence,

$$\begin{aligned} CW_{t_0}(\tau) &= s^*(t_0 - \frac{\tau}{2})s(t_0 + \frac{\tau}{2}) \\ CI_{t_0}(\tau) &= \frac{1}{2}[s(t_0)s^*(t_0 - \tau) + s^*(t_0)s(t_0 + \tau)] \end{aligned} \tag{107}$$

where $s(t)$ is the stationary signal of interest. That is, both IPS and WD create, from the data, a new "signal", whose Fourier Transform is the wanted spectrum (Figure 10). It is thus the effective duration of this new signal that determines the resolution obtainable in the frequency domain.

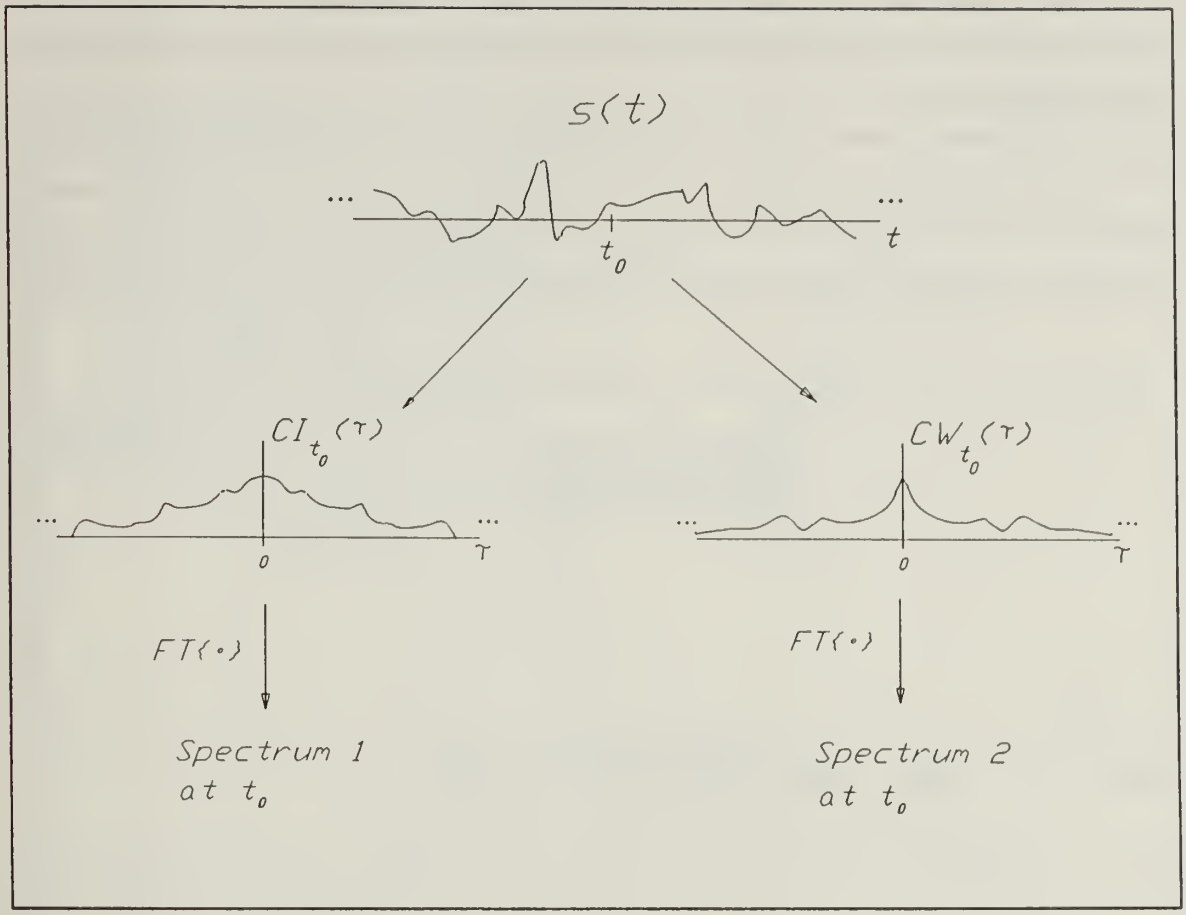

Figure 10. IPS and WD : conceptual diagram

Let us now assume that s(t) is only known within a finite segment of length L, and compare the theoretical resolution of IPS and WD at both the end-points and the middle of the segment.

a. End-points

Since both end-points are treated similarly, we will only consider the starting point of the known signal, which we will denote by t_0. Let us consider that a rectangular window of length L was applied to the signal (Figure 11). It is easily seen from (107) that

$$CW_{t_0} = \begin{cases} 0 & \tau \neq 0 \\ |s(t_0)|^2 & \tau = 0 \end{cases} \tag{108}$$

and thus, $WD_{t_0}(f)$ (Fourier transform of a delta function) is a constant. On the other hand, the windowing of the data implies that a window ($w_1(t)$) of length 2L is applied to $CI_{t_0}(\tau)$ (Figure 12).

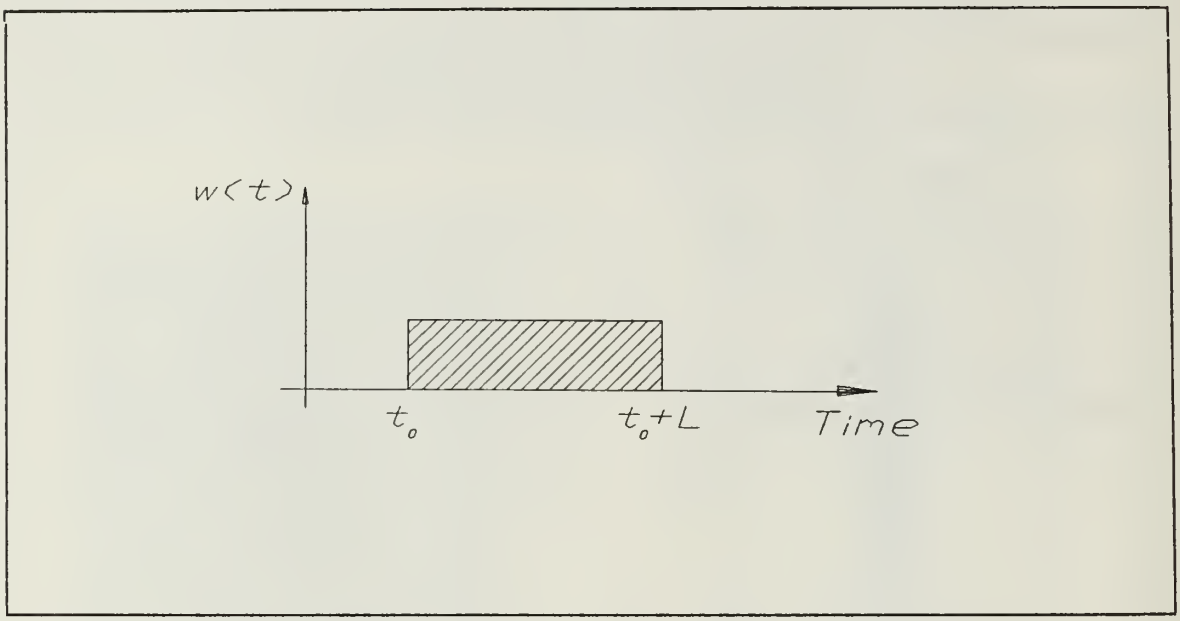

Figure 11. Window applied to the signal

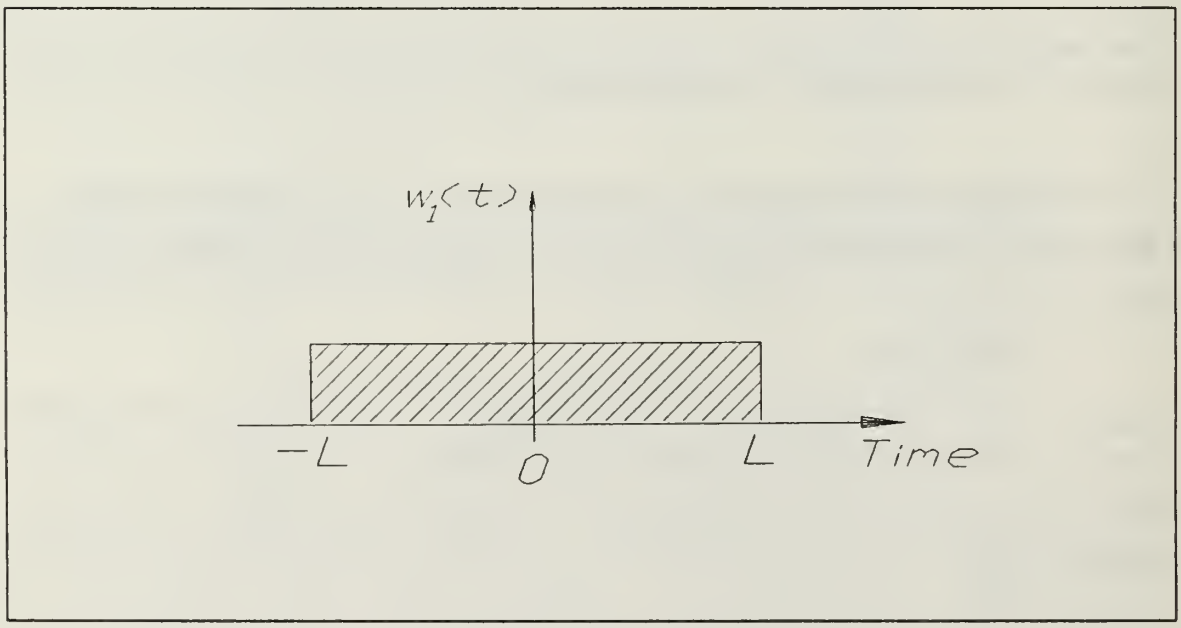

Figure 12. Window applied to $CI_{t_0}(\tau)$

When we now take the Fourier transform of $CI_{t_0}(\tau)$, we will be taking the transform of a signal twice as long as the original data. This creates a main-lobe twice as narrow as the main-lobe that would be obtained if we were to Fourier transform the data. However, we know from (107) that $CI_{t_0}(\tau) = CI^{*}_{t_0}(-\tau)$. This then implies that, from the obtained segment of length 2L, only half contains information. As a result, at end-points, IPS presents a main-lobe twice as narrow as the one obtainable by Fourier transforming the data, but without an equivalent improvement in effective resolution.

b. Middle-point

We now consider that the window is symmetrically placed around t_0, as in Figure 13.

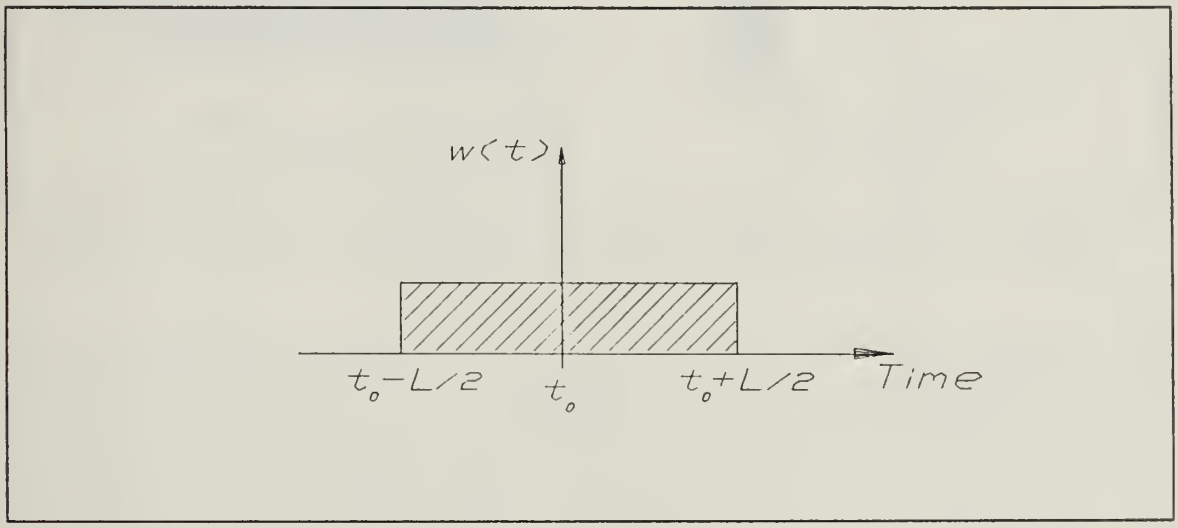

Figure 13. Symmetric window applied to the signal

Again, it is readily seen from (107) that windowing the data with a window of length L centered at t_0 implies the windowing of $CW_{t_0}(\tau)$ with a window of length 2L. The effect on $CI_{t_0}(\tau)$, however, is to window it with a window of length L. This discrepancy implies that, in the middle of the interval, the WD has twice the effective resolution of IPS. Let us note that, as discussed before, for both $CW_{t_0}(\tau)$ and $CI_{t_0}(\tau)$, only half of the length carries information. Hence, their Fourier-transform will have its main-lobe artificially narrowed by a factor of two, without improvement in effective resolution. In summary, the WD has at the middle of the time interval the same effective resolution that IPS has at end-points, and hence the same effective resolution obtainable by Fourier-transforming the data.

This fact of IPS having twice as poor resolution in the middle of the time interval than at end-points will be important, since the windowed implementation normally uses the window centered at the time of interest. This then means that these implementations are using, at each time, the worst estimate (in terms of resolution) that IPS will provide. The model of a typical windowed implementation of IPS can be seen in Figure 14.

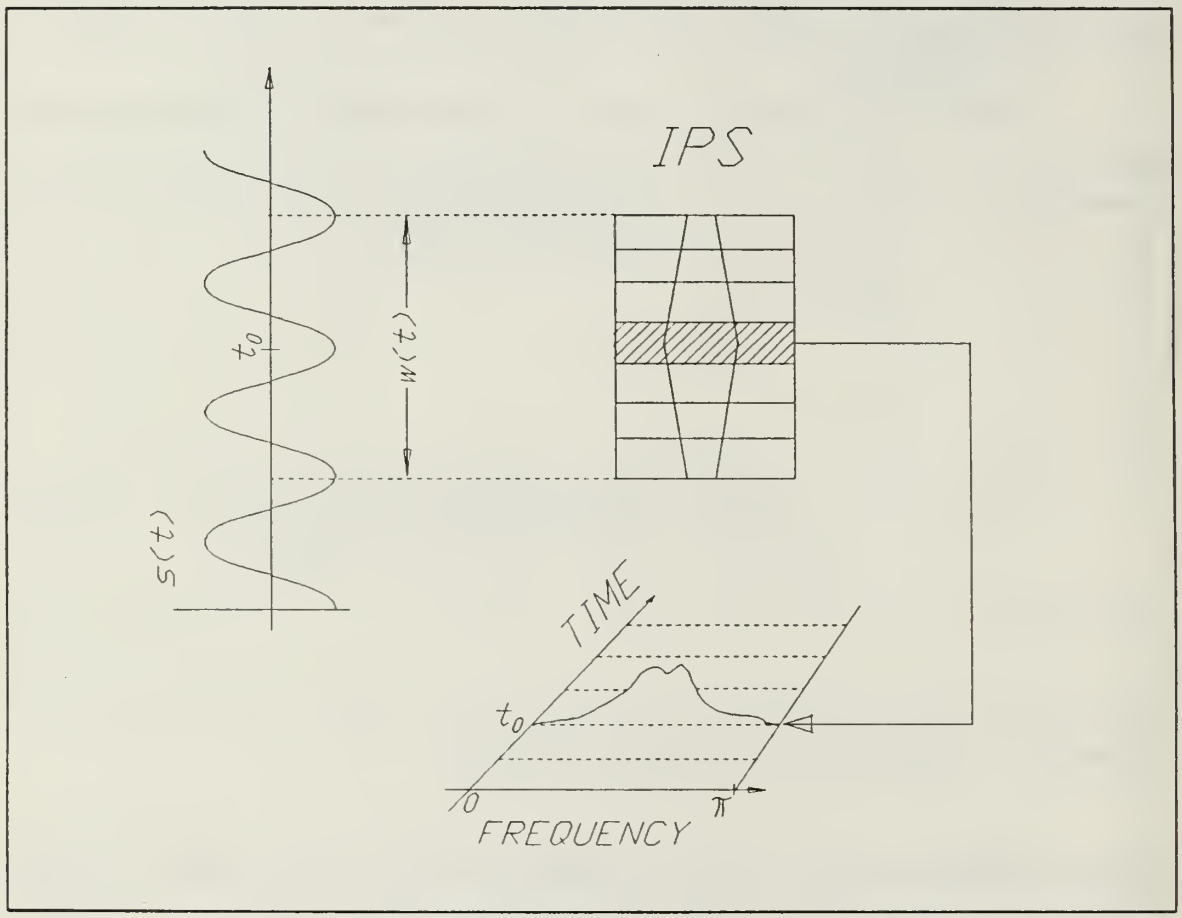

Figure 14. Typical implementation of IPS

The overall result is that, for these implementations, IPS has, by a factor of two, lower effective resolution for stationary components when compared with the WD.

2. Time-varying Components

One of the most noticeable characteristics of IPS is the fact that the width of its main-lobe depends on the dynamics of the signal. A typical example can be seen in Figure 15, where a quadratically chirped FM signal is used.

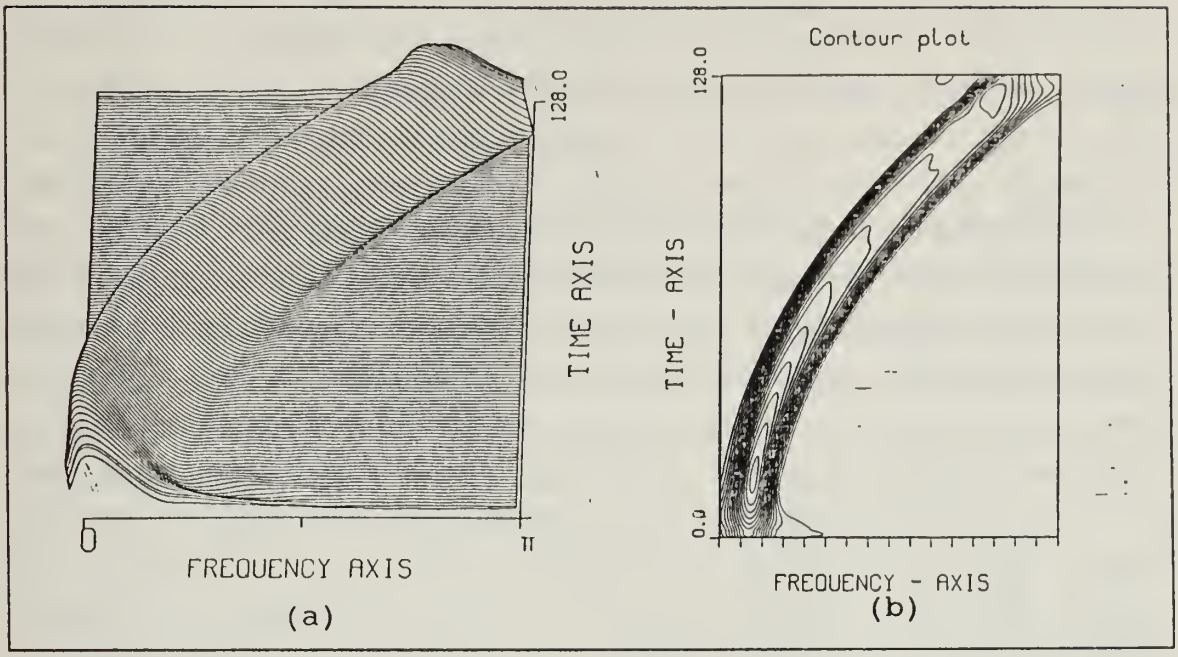

Figure 15. IPS for FM signal - Quadratic chirp. 3-D (a) and Contour (b) plots

This test signal has its instantaneous frequency increasing quadratically with time. The width of the main-lobe is directly proportional to the slew rate. In Figure 16, a cross section along the frequency axis of IPS for the same test signal is presented. The past and future terms are also indicated.

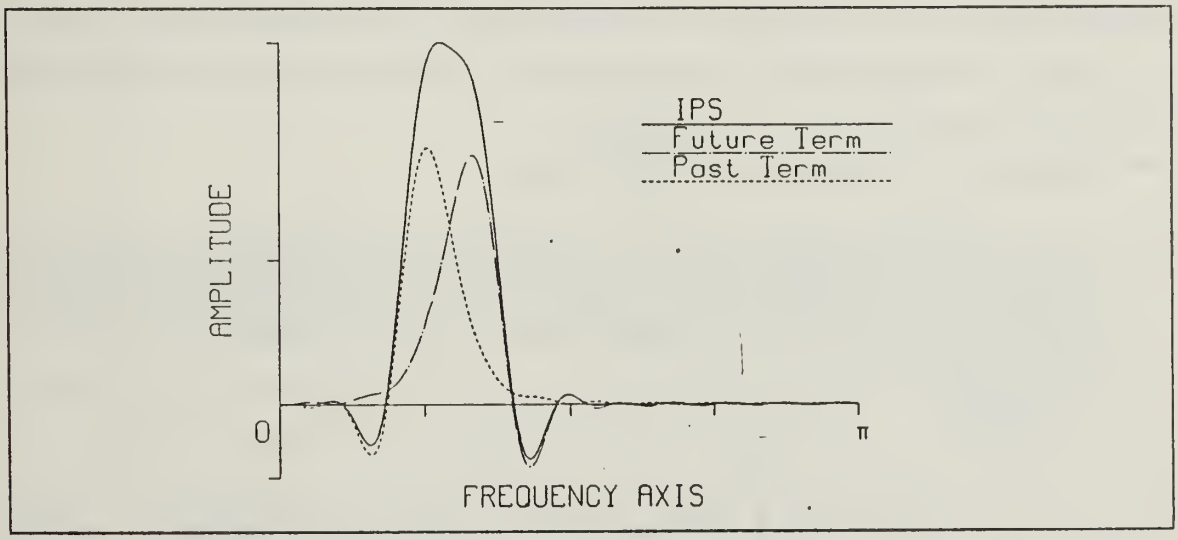

Figure 16. IPS for FM signal - Quadratic chirp. Cross-section

As is seen, the width of the main-lobe of IPS results from the imperfect alignment of the two terms: the past term seems to lag the true position of the instantaneous frequency, showing a tendency to be positioned in locations previously occupied by the signal, while the future term leads the true location of the instantaneous frequency. This lag and lead effect become more severe for faster dynamics, hence broadening the main-lobe of IPS.

In an attempt to explain this feature, one might be tempted to argue that IPS lacks symmetry in its definition. Despite being clearly insufficient, as we will see, it will be instructive to pursue this type of reasoning a little further, since some additional results will emerge. When computing $CI_{t_0}(\tau)$, we are, for each τ (without loss of generality assume $\tau > 0$), coherently averaging two terms. One results from the present and past signal history $(x^*(t)x(t+\tau))$, and the other results from present and future signal history $(x(t)x^*(t+\tau))$. To obtain IPS, we will extract the frequency contents of the sequence so obtained. However, if the signal has frequency dynamics, each one of the terms will contribute differently to the frequency contents of $CI_{t_0}(\tau)$. For example, if the instantaneous frequency of the signal is increasing in time, the contribution of the present-future term $(x^*(t)x(t+\tau))$ will have higher frequencies than the present-past term, since it is centered in a region with higher average instantaneous frequency. The temptation thus arises to compensate for the difference in the centers of the two regions. This effectively corresponds to forcing the two terms in Figure 16 to align "correctly", thus eliminating the broadening of the main-lobe. To do so, it suffices to introduce compensating phase terms in the process of computing IPS (see . *Alternate way of computing the Wigner-Ville* below). When these compensating terms are introduced, the distribution that results is the Wigner-Ville distribution. We can now interpret WD as: the WD is the distribution that results by aligning the two terms of IPS.

- *Alternate way of computing the Wigner-Ville*

  From the previous discussion, an alternate way of computing the WD can be derived, which allows us to directly apply the WD to real signals sampled at the conventional Nyquist rate, thus avoiding the need for oversampling that would be required if the WD was to be computed in the usual way [Refs. 7, 10]. The two step procedure is:

  1. Compute

$$F(\tau, \upsilon) = \frac{1}{2} \int_{-\infty}^{\infty} [s(t)s^*(t-\tau)e^{-j\pi\upsilon\tau} + s^*(t)s(t+\tau)e^{j\pi\upsilon\tau}]e^{j2\pi\upsilon t}dt \qquad (109)$$

2. Compute

$$WD(t, f) = \int_{-\infty}^{\infty} \int_{-\infty}^{\infty} F(\tau, \upsilon) e^{-j2\pi(\upsilon t + \tau f)} d\upsilon d\tau \tag{110}$$

As can easily be recognized, the need for a 2-D Fourier transform places the cost of this procedure well above the one needed if an interpolation scheme is used. This consideration may disappear in emerging fields such as optical signal processing.

All our previous discussion has been based on a loosely defined lack of symmetry, intimately related with the concepts of past and future. As pointed out earlier, this explanation is clearly insufficient. To illustrate why, a different definition of "Instantaneous Power Spectrum" is made in Appendix E, thus creating a new distribution. The important point to be made is: not only are the concepts of past and future inexistent in this new definition, but it also possesses perfect symmetry. However, the resulting distribution is very similar to IPS, with the characteristic data-dependent width. Since lack of symmetry cannot be argued for this definition, the explanation for the broadening of the main-lobe must be found somewhere else.

In Appendix C, the issue of uncertainty is addressed. One important result to extract from there is: the maximum obtainable frequency resolution when analyzing signals with unknown frequency dynamics is $\sqrt{df_i/dt}$. This result is in agreement with the fact, proven by Rihaczek [Ref. 4], that signals with strong phase modulation have, at each time, their energy concentrated within a frequency band B_d of size

$$B_d = \sqrt{\frac{1}{2\pi} \frac{d^2\Phi(t)}{dt^2}} \ , \tag{111}$$

where $\Phi(t)$ is the signal's phase. It thus explains the broadening of the main-lobe of IPS in terms of the expression of uncertainty. Since the uncertainty region grows for increasingly faster dynamics, so does the width of the main-lobe. Put in simpler terms, "the faster it moves, the harder it is to locate". According to the results of Appendix C, any algorithm should behave in this manner, unless it has, or assumes (directly or indirectly), information concerning the dynamics of the signal. However, *not assuming* is the key rule for a robust algorithm, one whose performance does not depend on the class of signals being analyzed.

D. THE CHOICE OF A WINDOW

We know from (66) that, if we pre-window the signal with a window real and symmetric around the time at which we are evaluating IPS, the resulting IPS will be:

$$IPS_{(s\cdot w)}(t, f) = \int_{-\infty}^{\infty} IPS_s(t, v)\cdot IPS_w(t, f - v)dv \,. \tag{112}$$

But

$$IPS_w(t, f) = \frac{1}{2}\int_{-\infty}^{\infty} [w(t)w(t-\tau) + w(t)w(t+\tau)]e^{-j2\pi f\tau}d\tau \tag{113}$$

and, since $w(t-\tau) = w(t+\tau)$,

$$\begin{aligned} IPS_w(t, f) &= \int_{-\infty}^{\infty} w(t)w(t+\tau)e^{-j2\pi f\tau}d\tau \\ &= w(t)W(f)e^{j2\pi ft} \\ &= w_o(0)W_o(f) \,, \end{aligned} \tag{114}$$

where $w_o(\tau) = w(t+\tau)$, that is, w_o is the used window shifted to the origin.

Hence, if a real and even sliding window is used, the smoothing function in (112) is the Fourier Transform of the window $w_o(\tau)$. It is interesting to compare this result with the Pseudo-Wigner Ville (frequency smoothed Wigner-Ville), where the smoothing function is not the Fourier Transform of the window itself, but the Fourier Transform of the square of the window (in a rescaled frequency axis) [Ref. 6]. We thus see that all the knowledge on window functions for the Fourier Transform can be directly applied to the choice of a window to be used with IPS.

Though the smoothing function in (112) is always real (we are considering only real and even windows), it may be negative. This can contribute to the presence of strongly negative values in the resulting IPS, especially if the side-lobe structure of the window is not controlled. This thus suggests that windows with good side-lobe suppression

should be preferred. Spectral resolution is another important issue to be considered when choosing a window.

As discussed in the previous section (Section III-C), IPS has a main lobe whose width is proportional to $\sqrt{df_i/dt}$, in accordance with the uncertainty principles of Appendix C. Hence, degrading the apparent frequency resolution of the unwindowed IPS does not become a relevant issue, if working with windows whose effective duration is well above the reciprocal of the uncertainty region. The width of this region should thus be the criteria for the choice of window size, but would require a-priori knowledge of the dynamics of the signal. In the absence of this knowledge, optimality will not be achieved. However, as we will see, IPS is a very forgiving tool, in the sense that its performance is not seriously affected even for large deviations from the optimal window size.

IV. EXPERIMENTAL RESULTS

To illustrate the types of behavior predicted in the previous sections, some test cases will be presented. For all the cases the test signals are 128 point sequences, with one spectrum for each sample. All plots are on a linear scale. Some considerations relating to the Pseudo Wigner-Ville (PWD) were made: all test signals are analytic, thus freeing the PWD from the somewhat annoying interferences between positive and negative frequencies. The exception to this rule will be Figure 19, since its sole purpose is to illustrate the effects of the use of real signals. Also, when noise is present (Figure 24), analytic noise is used. Unless otherwise stated, all Figures use a 41-point Hamming window, and present the distributions after smoothing along the time direction. Hence, most of the spectral cross-terms of the PWD due to multi-component signals do not appear in the plots. To illustrate the effectiveness of time-smoothing, Figure 17 was provided, differing from Figure 21 only in the fact that the time-smoothing technique was not used.

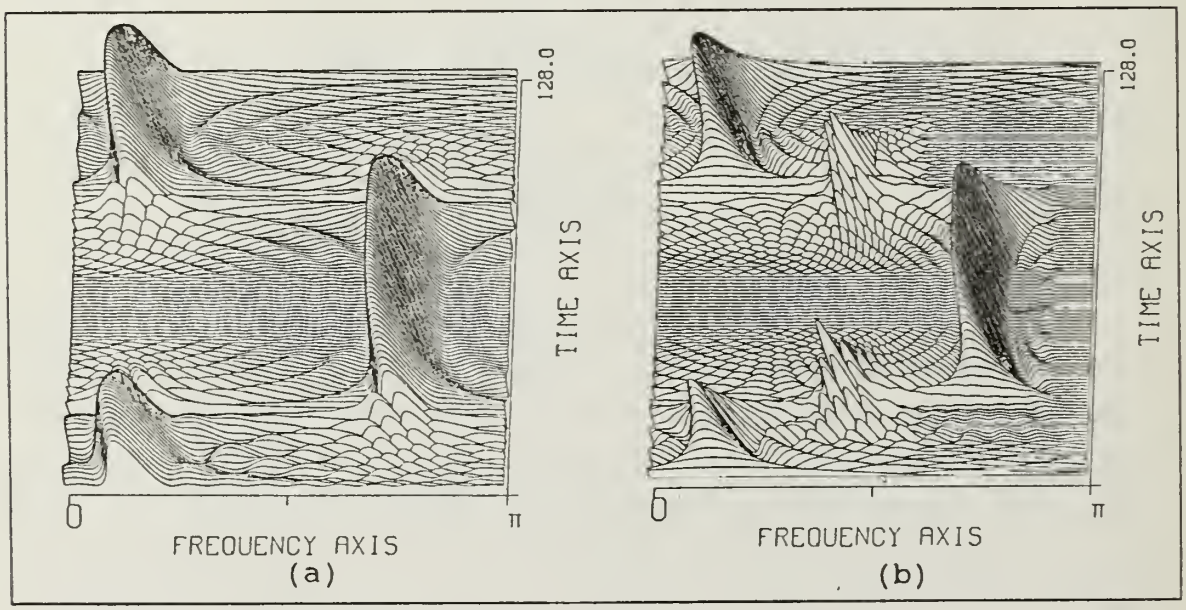

Figure 17. FSK. IPS (a) and PWD (b). No time-smoothing.

A. REAL SIGNALS

In Figure 18, IPS and PWD for a linear analytic FM chirp are presented. Comparing Figure 18 with Figure 19, where the test signal is a linearly chirped cosine

function, we can appreciate how insensitive IPS is to the fact of the signal being real. The artifacts present in the PWD when analyzing real signals are, for all practical purposes, absent in IPS.

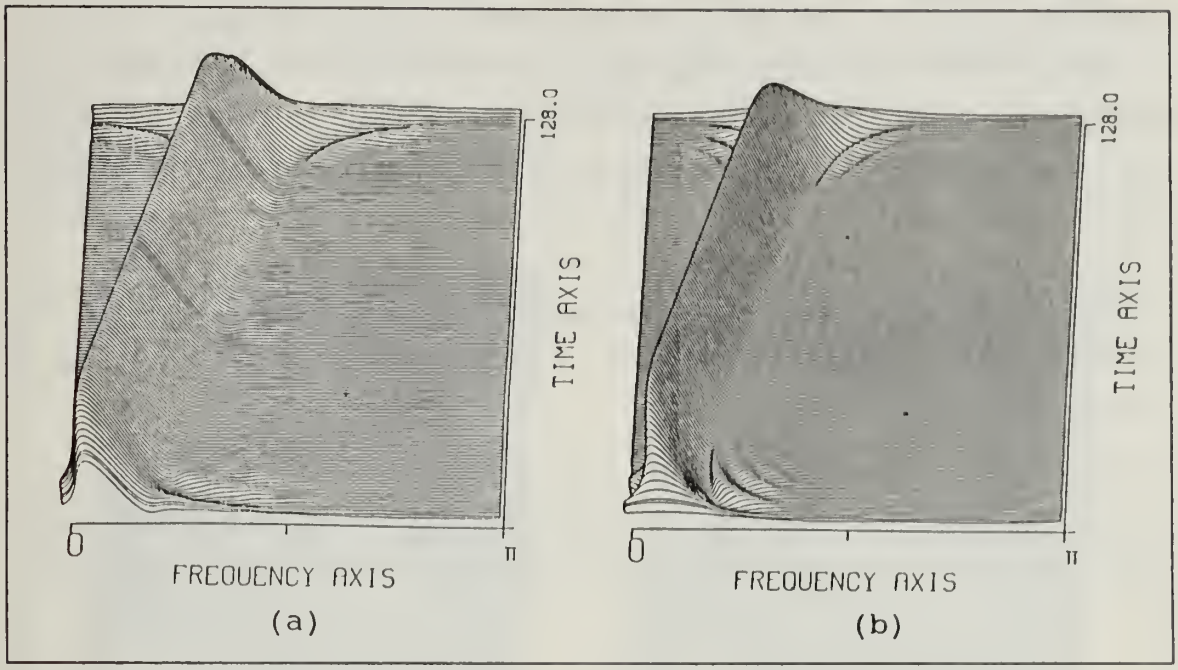

Figure 18. Analytic linear FM chirp. IPS (a) and PWD (b).

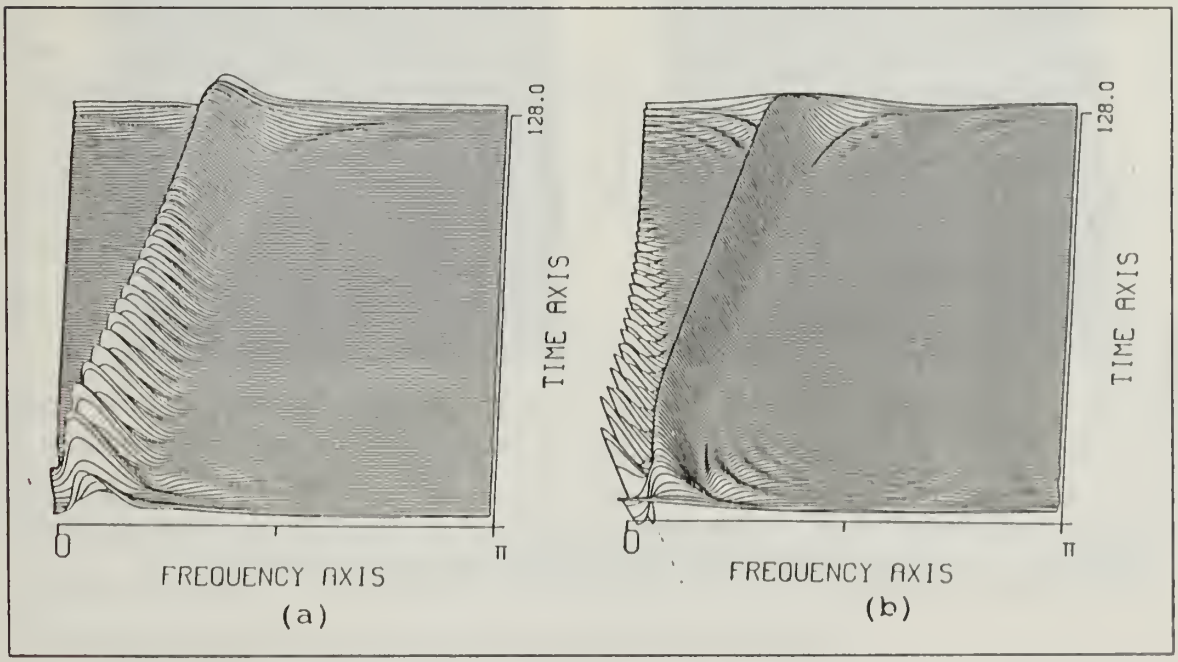

Figure 19. Linearly chirped cosine. IPS (a) and PWD (b).

B. INSTANTANEOUS POWER

Another visible effect in Figure 19 is the "amplitude modulation" of the main-lobe of IPS. IPS gives us the distribution in frequency of the instantaneous power of the signal. It then follows that, when computing the spectrum at a low power sample, the amplitudes of the frequency components will have to be small, since their total power must add up to the low power of the sample. This is a direct consequence of (95) and is a requirement that has be fulfilled by any positive distribution. It is not observable in Figure 18, since the used analytic signal has the same power at all samples.

The WD, though also obeying the Marginal in Time property, tends to absorb the fluctuations of the instantaneous power in its cross-terms, and, in order to do so, is forced to assume strongly negative values.

C. END-POINT RESOLUTION

Though the better resolution at end-points provided by IPS is in general well visible in all the plots that are presented, Figure 20 is probably one of the most representatives.

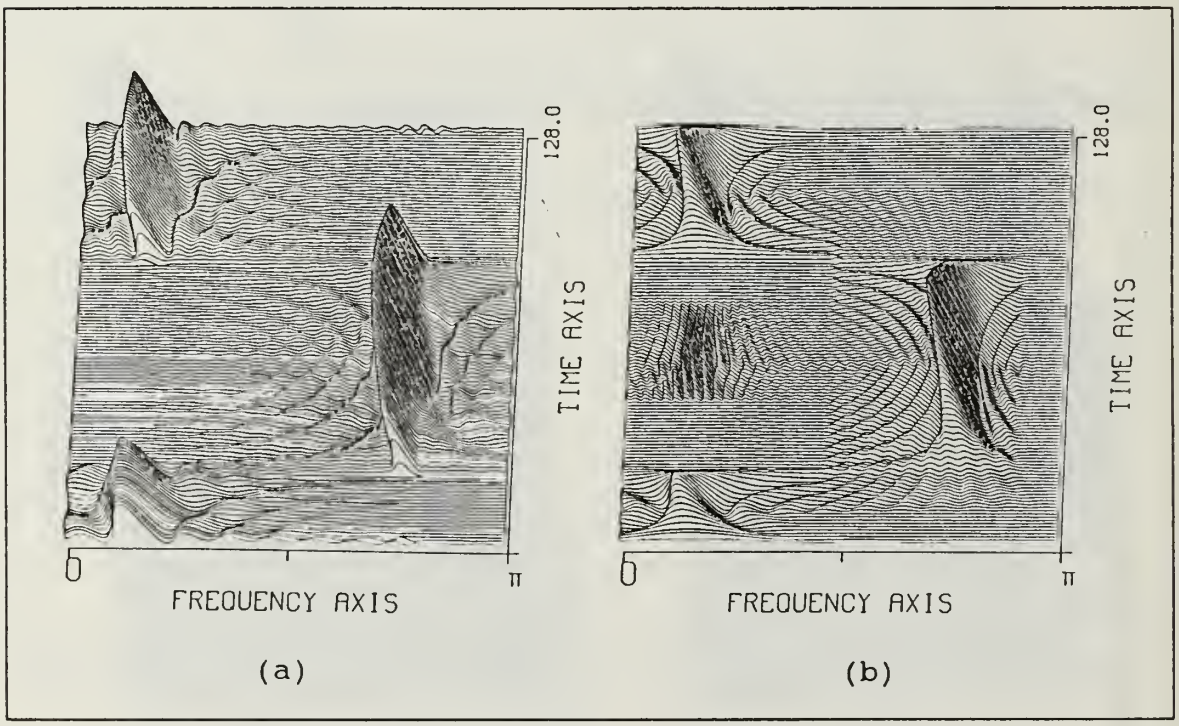

Figure 20. FSK (127-point Hamming window). IPS (a) and PWD (b).

Considering it, we see that not only is the end-point resolution of IPS better, but also the transition times are shorter, allowing a more accurate definition of the time of spectral jumps.

As stated in Section III-D, IPS is a forgiving tool, in the sense that we can deviate from the optimal length of window without severely degrading its performance. To illustrate, Figure 21 is presented, which differs from Figure 20 only in that it uses a window with different effective duration.

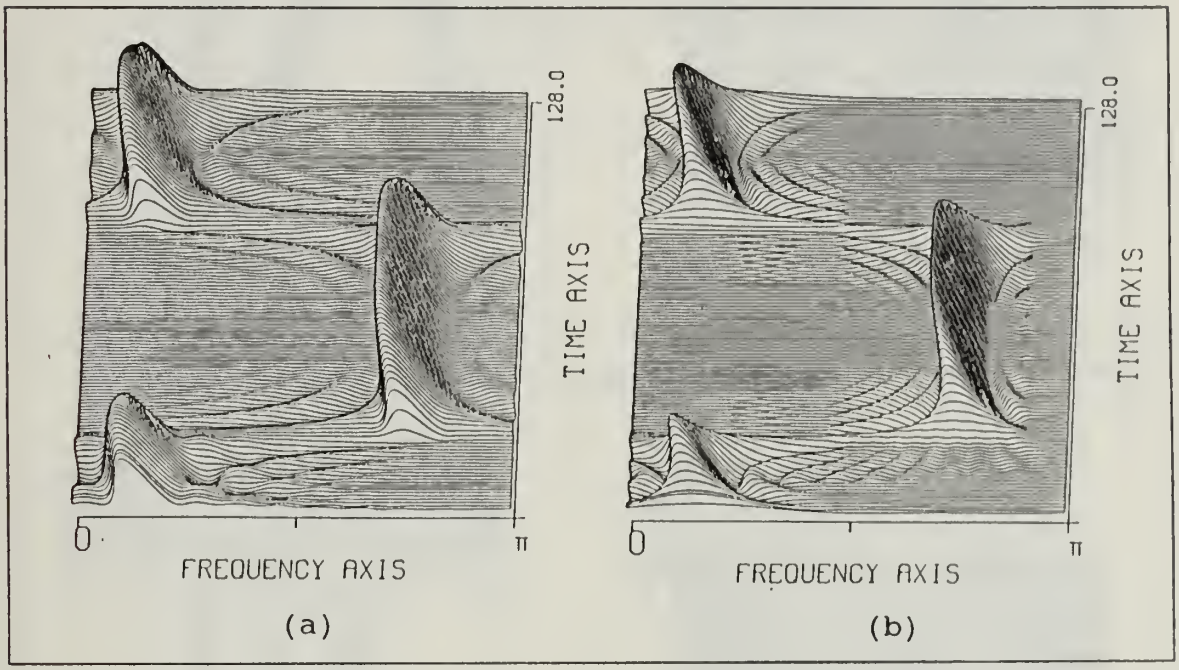

Figure 21. FSK (51-point Hamming window). IPS (a) and PWD (b)

As is seen, the time resolution is basically kept the same, the only noticeable difference being the width of the window's main-lobe.

D. MULTI-COMPONENT SIGNALS

Performance for multi-component signals is addressed in Figure 22 and Figure 23, where the test signal has three components: a linearly chirped FM signal, a quadratically chirped FM signal, and a stationary component. As seen, IPS is free of the cross-terms appearing in the PWD. However, for IPS, each one of the spectral components has its width affected by the associated uncertainty region and is, hence, wider than the corresponding one in the PWD. Again, the instantaneous power modulation is visible in IPS. These effects are also apparent in the provided contour plots.

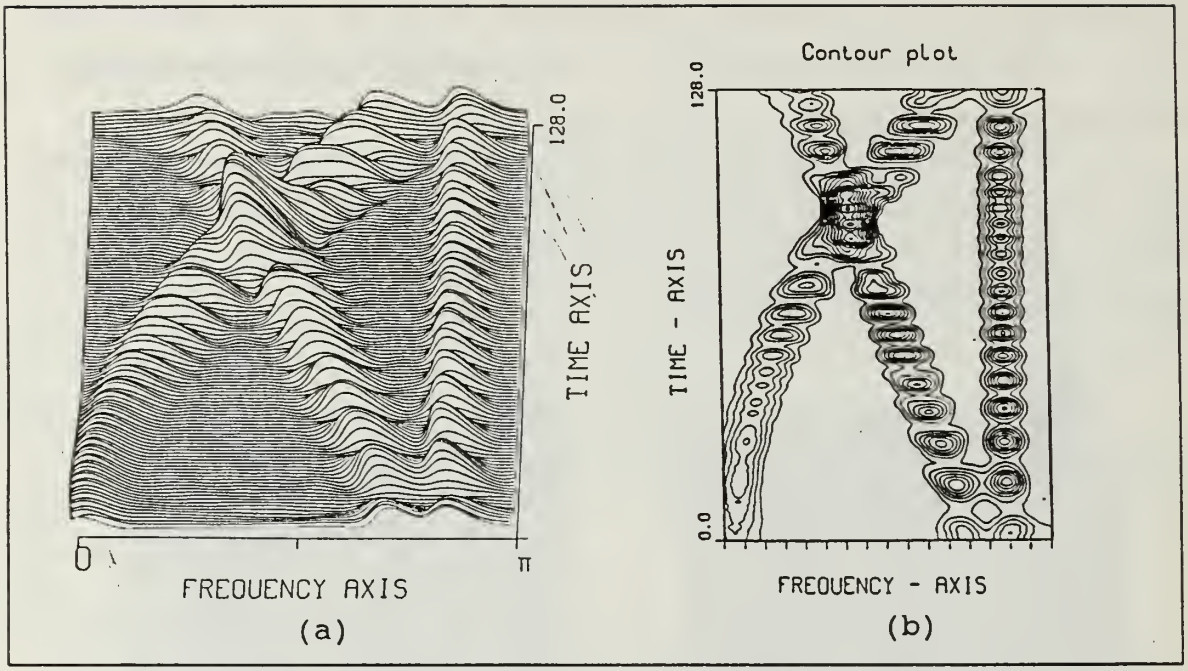

Figure 22. IPS for Multi-component signal. 3-D (a) and Contour (b) plots

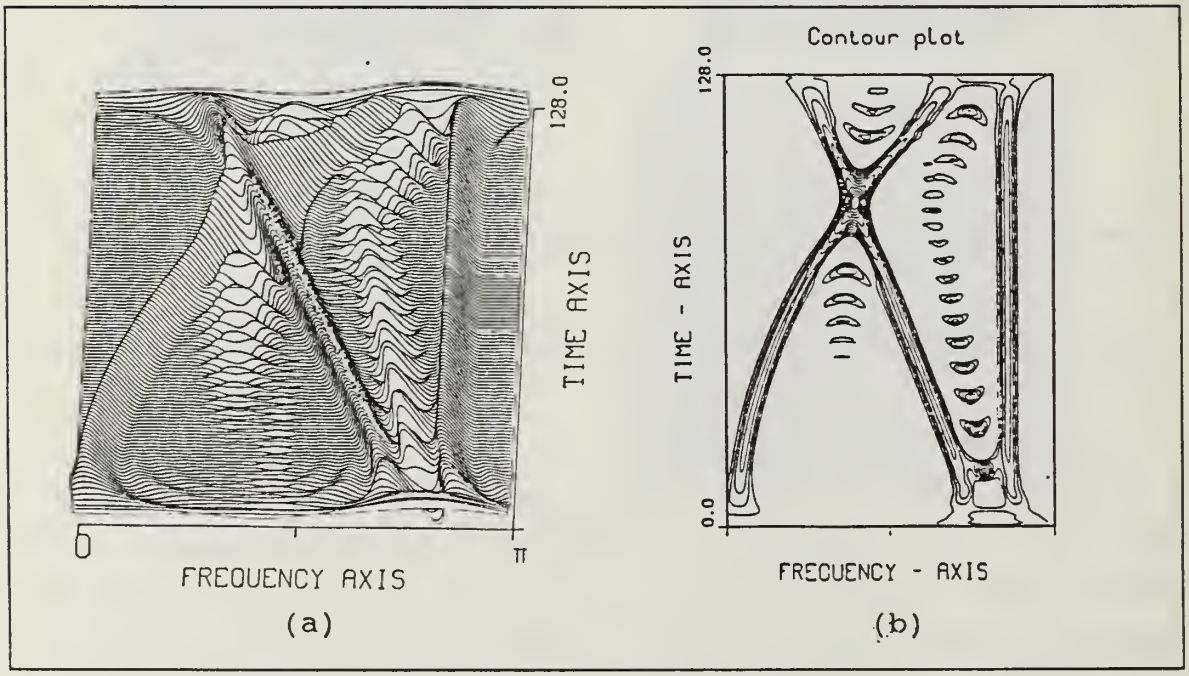

Figure 23. PWD for Multi-component signal. 3-D (a) and Contour (b) plots

E. PERFORMANCE IN NOISE

One issue still not addressed is the performance in noise. In Appendix D, a proof is given that, for a signal embedded in additive bandlimited white Gaussian noise, the variance of IPS is, on the average,[5] smaller than the variance of WD. Also, from the same Appendix, we have that, when the bandwidth of the noise approaches infinity, the improvement in the variance given by IPS approaches the limiting value of 3 dB. Figure 24 is provided to illustrate this theoretical result. The SNR for this picture is 5 dB, and it is seen that IPS does, indeed, present a smoother estimate of the instantaneous spectrum.

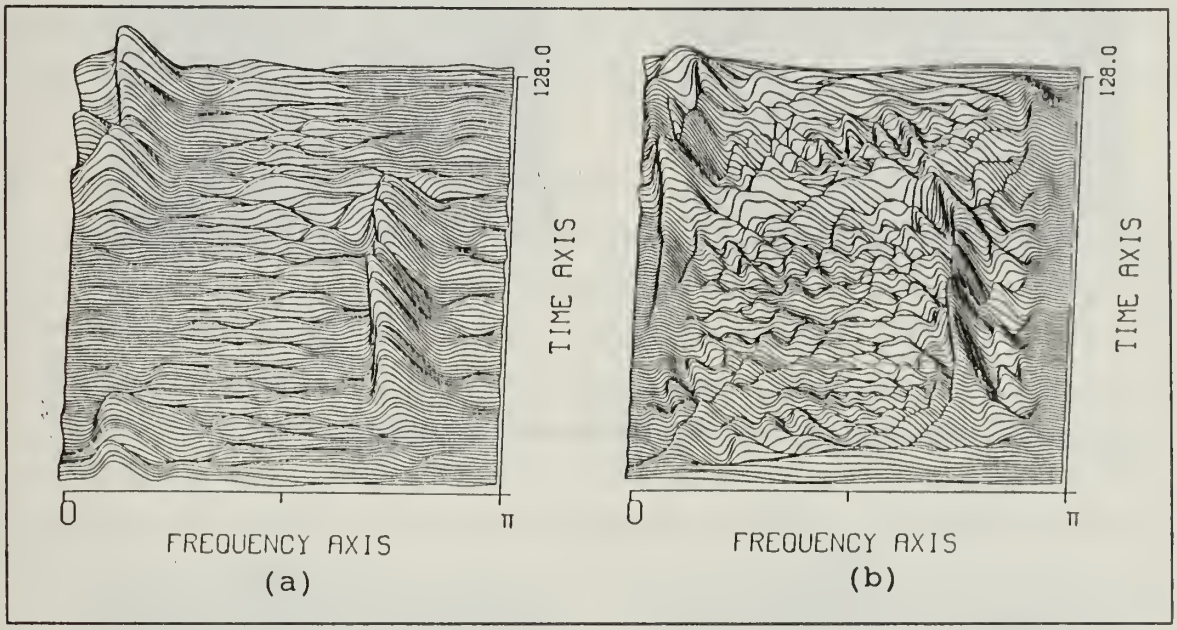

Figure 24. FSK (SNR = 5 dB). IPS (a) and PWD (a)

F. THE CAPTURE EFFECT

Having borrowed the term from communication theory (FM demodulation), our goal is to compare the behaviors of IPS and PWD when analyzing multi-component signals, when the components have different amplitudes. In Figure 25, the two components have amplitudes differing by a factor a four (12 dB). As is observable, both IPS and PWD detect the weaker component, despite the fact of the cross-terms in the PWD being already more energetic than the weak signal itself. In Figure 26, the same two

[5] The variance of IPS is time dependent. When we say that "...the variance is...on the average....", we are referring to the time average of the variance.

component signal is presented, now with a factor of 8 between amplitudes (18 dB). It is obvious that the PWD lost the weak component. The cross-terms, however, still remain. In this case, the position of the weaker term could be inferred from the cross-terms, but such a technique would be impossible to apply to more complex signals.

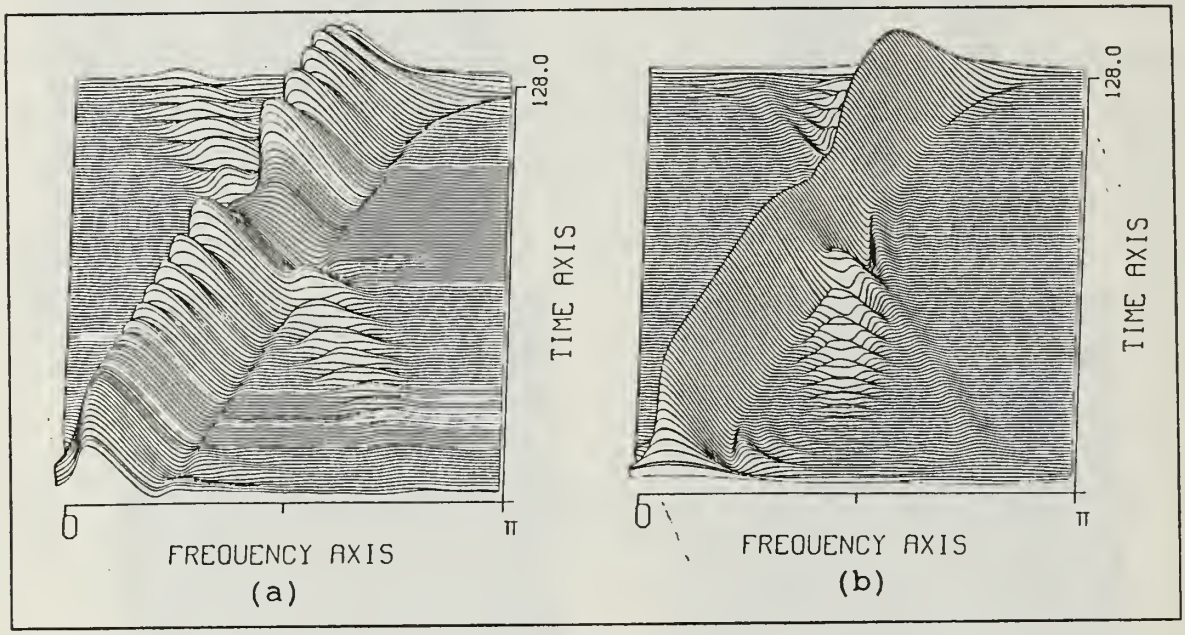

Figure 25. Power ratio = 12 dB. IPS (a) and PWD (b)

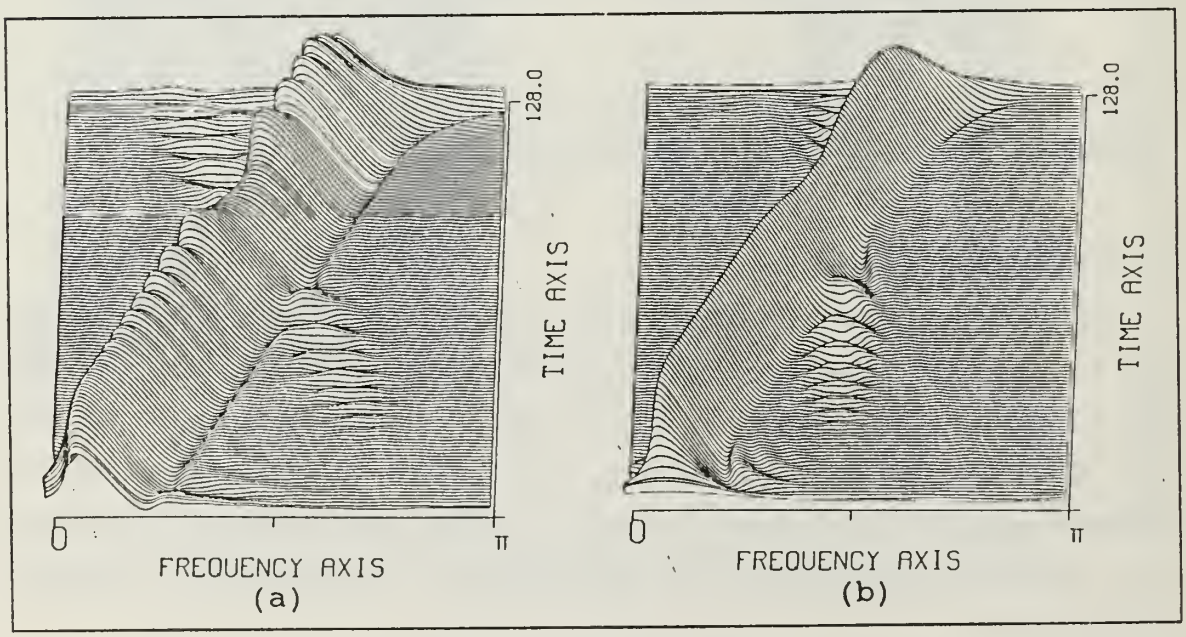

Figure 26. Power ratio = 18 dB. IPS (a) and PWD (b)

V. PARAMETRIC IPS

A. INTRODUCTION

We have, from (12), that the IPS of a signal is, at each time, the Fourier transform of a function of the signal. This implies that the wanted information lies in the spectral content of this function. The process of obtaining the IPS can therefore be reduced to the problem of performing conventional spectral estimation on a function $G(t, \tau)$ which is derived from the signal as in (11). The use of parametric methods should thus be considered, in an attempt to improve the resolution capabilities of IPS. These considerations are also applicable to the WD, and a parametric version of this distribution has been considered [Ref. 20].

B. AR MODELING - CONSIDERATIONS

Though obtained as a bilinear transformation of the data, the function in (11) can not be considered a true autocorrelation function, since it is not constrained in any way other than possessing conjugate symmetry around the origin. It can not be guaranteed to give rise to a positive definite autocorrelation matrix, and hence can not be used to directly solve the normal equations. We can however estimate its autocorrelation function and fit the model to this autocorrelation. In a sense,[6] we will be fitting the model in the fourth moment of the data. In all the results presented, the AR parameters are obtained using the Modified Covariance Method. This method has been found to possess good resolution properties, while alleviating some of the problems associated with the Maximum Entropy Method (MEM) [Ref. 21]. All plots are on a logarithmic scale.

C. EXPERIMENTAL RESULTS

Choosing the order of the model is a sensitive issue. From Figure 16, we know that the main lobe of IPS consists of two terms, which do not align exactly. We might thus expect that, if the correct order is exceeded, the extra poles will tend to resolve these two terms, and each spectral component will have two associated peaks in the spectrum. In Figure 27, where the test signal is again a single component quadratically chirped FM signal, this effect is well visible. In the left, a one-pole model was used (analytic test signal). With the addition of one extra pole, we can see that the two terms were resolved

---

[6] Lacking both temporal and statistical averaging, (11) can not be considered to represent the second moment of the data.

(with some bias), and the undesired effect is now present. In Figure 28, a fourth order model was used to fit a three component signal.

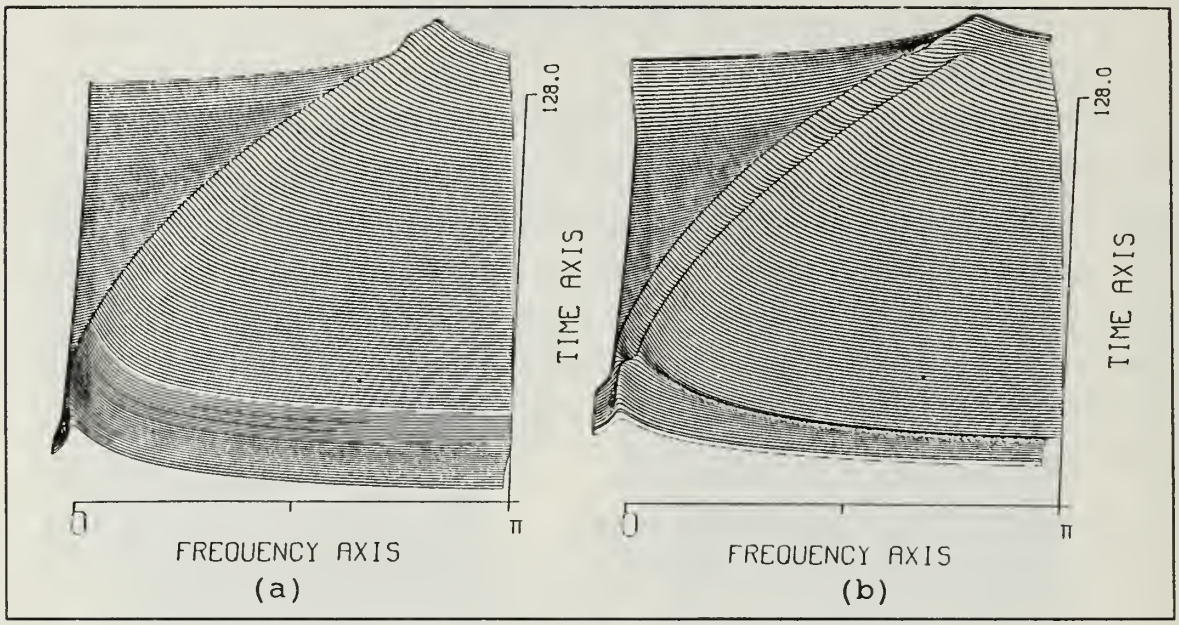

Figure 27. Parametric IPS. First (a) and second (b) order models

We can observe that, since the main lobes were not over-resolved, the signal components are well defined, and can be located with greater precision than what would have been possible with the non-parametric IPS.

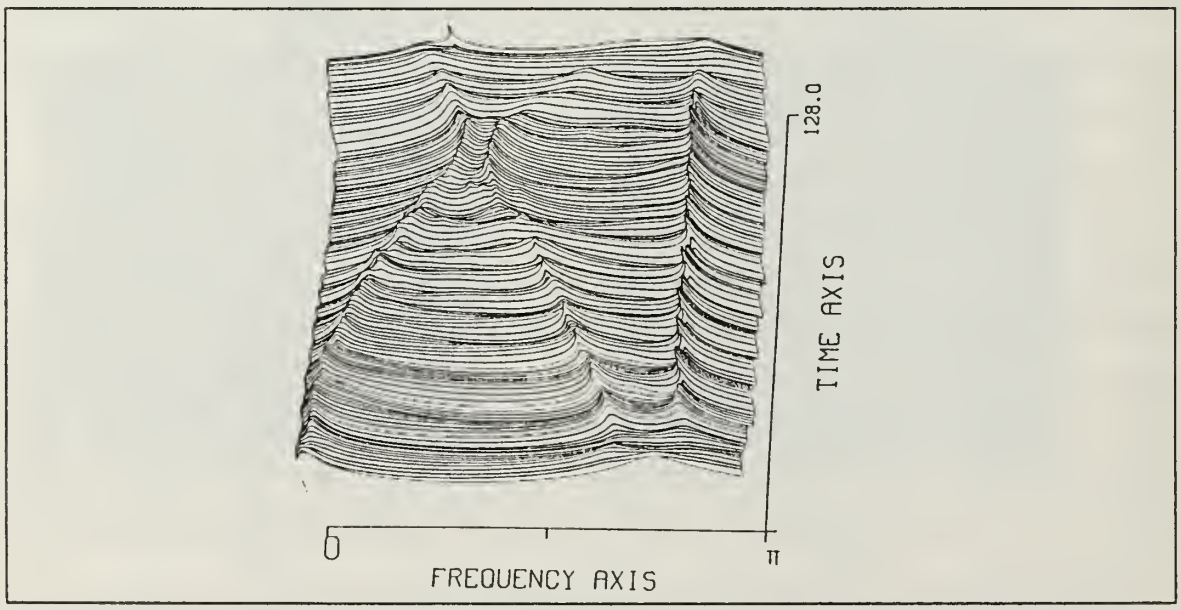

Figure 28. **Three component signal. Parametric IPS. Fourth-order model.**

VI. CONCLUSIONS AND RECOMMENDATIONS

In this thesis, an alternative tool for the spectral analysis of signals with time-varying spectral content is presented (IPS). Having its roots in the definition proposed by Page of "Instantaneous Power Spectrum", IPS has a defining expression very similar to the one defining the Wigner-Ville distribution (WD). Their performance is, however, considerably different. The WD approach, though extensively used in the last decades, suffers from a number of short-comings. The foldover frequency of its discrete frequency is located at $\pi/2$, requiring the use of analytic signals or the use of an interpolation scheme as an alternative to sampling at twice the Nyquist rate. Interference when used with real signals, cross-terms when multi-component signals are present, preference of linear dynamics and loss of resolution at the extremes of the analysis segment are other problems associated with the WD [Ref. 8]. The distribution presented here is shown to have some advantages over the WD. These are: evenness of performance for different dynamics of the signal, direct applicability to real signals sampled at the Nyquist rate, reliability when analyzing multi-component signals, and preservation of spectral resolution at end-points. Also, IPS is shown to behave better in the presence of additive white Gaussian noise (AWGN). As a disadvantage, IPS does not achieve the frequency resolution provided by the WD. Due to its robustness, IPS is especially well fitted to be used as a front-end tool in non-stationary spectral analysis. The usefulness of AR modeling as applied to IPS is investigated. It is found to be a technique very sensitive to the chosen order model, but providing some advantage in defining the location of each spectral component. The use of other parametric techniques should be investigated. In Figure 29, we can see the FSK signal of Figure 20, this time processed with the following expression:

$$D(t, f) = \frac{1}{2}\int_{-\infty}^{\infty} [s(t)s^*(t-\tau) - s^*(t)s(t+\tau)]e^{-j2\pi f\tau}d\tau \,. \qquad (115)$$

That is, Figure 29 is the imaginary part of the Rihaczek distribution of the test signal. As is seen, it shows some natural ability to detect fast transitions in the spectrum, and

seems to be a promising area for future work. Also, linear combinations between IPS and this imaginary part of the Rihaczek distribution should be investigated.

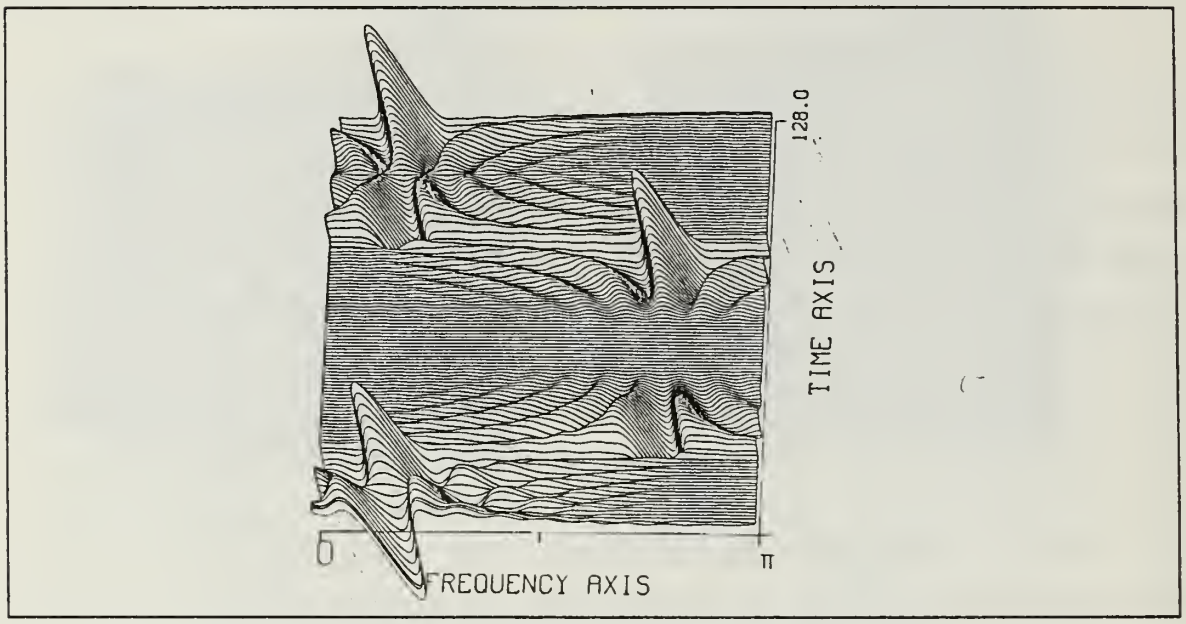

Figure 29. Imaginary part of Rihaczek's Distribution - FSK

Signal synthesis from IPS may also be a promising field of research for speech processing applications.

APPENDIX A. IPS FOR FINITE DURATION DISCRETE SIGNALS

In this appendix, a formal derivation of the expression defining IPS for discrete signals (16) is presented, as an alternative to the direct discretization of (12).

The discrete version of (3) is, assuming that the sequence starts at $n = 0$:

$$S^{-}(n, \theta) = \Delta T \sum_{n=0}^{t} s(n) e^{-j\theta n} \tag{116}$$

Hence,

$$\begin{aligned} | S^{-}(n, \theta) |^2 &= \Delta T^2 \sum_{n=0}^{t} s(n) e^{-j\theta n} \sum_{n=0}^{t} s^{*}(n) e^{j\theta n} \\ &= \Delta T^2 \sum_{k=-t}^{t} c_k^{-} \, e^{-j\theta k} \end{aligned} \tag{117}$$

where

$$c_k^{-} = \sum_{n=k}^{t} s(n) s^{*}(n-k) \qquad k \geq 0 \tag{118}$$

and

$$c_k^{-} = (c_{-k}^{-})^{*} . \tag{119}$$

Similarly

$$S^{+}(n, \theta) = \Delta T \sum_{n=t}^{N-1} s(n) e^{-j\theta n} \tag{120}$$

$$
\begin{aligned}
|\, S^{+}(n,\theta)\,|^2 &= \Delta T^2 \sum_{n=t}^{N-1} s(n) e^{-j\theta n} \sum_{n=t}^{N-1} s^{*}(n) e^{j\theta n} \\
&= \Delta T^2 \sum_{k=-(N-1-t)}^{(N-1-t)} c_k^{+}\, e^{-j\theta k}
\end{aligned}
\tag{121}
$$

where

$$
c_k^{+} = \sum_{n=t+k}^{N-1} s(n) s^{*}(n-k) \qquad k \geq 0 \tag{122}
$$

and

$$
c_k^{+} = (c_{-k}^{+})^{*} . \tag{123}
$$

Now, to get the digital equivalents of (2),(4) we must approximate the derivatives of (117) and (120), which we will do using first order differences:

$$
\begin{aligned}
\rho^{-}(n,\theta) &\approx \Delta T \left[\, |\, S^{-}(n,\theta)\,|^2 - |\, S^{-}(t-1,\theta)\,|^2 \,\right] \\
&= \Delta T \sum_{k=-t}^{t} \varepsilon_k^{-}\, e^{-j\theta k}
\end{aligned}
\tag{124}
$$

where

$$
\varepsilon_k^{-} = s(n) s^{*}(n-k) \qquad k \geq 0 \tag{125}
$$

and

$$
\varepsilon_k^{-} = (\varepsilon_{-k}^{-})^{*} \tag{126}
$$

In the same way,

$$
\begin{aligned}
\rho^{+}(n,\theta) &\approx \Delta T \left[\, |\, S^{+}(n,\theta)\,|^2 + |\, S^{+}(t+1,\theta)\,|^2 \right] \\
&= \Delta T \sum_{k=-(N-1-t)}^{(N-1-t)} \varepsilon_k^{+}\, e^{-j\theta k}
\end{aligned}
\tag{127}
$$

where

$$\varepsilon_k^+ = s^*(n)s(n+k) \quad k \geq 0 \tag{128}$$

and

$$\varepsilon_k^+ = (\varepsilon_{-k}^+)^* . \tag{129}$$

Assuming the signal to be zero outside the known samples, then according to Levin's definition (6):

$$\begin{aligned} IPS(n,\theta) &= \frac{1}{2}[\rho^-(n,\theta) + \rho^+(n,\theta)] \\ &= \frac{\Delta T}{2} \sum_{k=-\infty}^{\infty} [s(n)s^*(n-k) + s^*(n)s(n+k)]e^{-j\theta k} \end{aligned} \tag{130}$$

which is the wanted result.

APPENDIX B. INSTANTANEOUS FREQUENCY AND IPS

The proof of property 6 (55) can be made as follows:

$$\frac{\int_{-\infty}^{\infty} f \cdot IPS(t, f) df}{|s(t)|^2} = \tag{131}$$

$$= \frac{1}{|s(t)|^2} \int_{-\infty}^{\infty} f \frac{1}{2} \int_{-\infty}^{\infty} [s(t)s^*(t-\tau) + s^*(t)s(t+\tau)] e^{-j2\pi f\tau} d\tau df$$

$$= \frac{1}{2|s(t)|^2} \int_{-\infty}^{\infty} [s(t)s^*(t-\tau) + s^*(t)s(t+\tau)] \int_{-\infty}^{\infty} f e^{-j2\pi f\tau} df d\tau$$

$$= \frac{1}{2|s(t)|^2} \int_{-\infty}^{\infty} [s(t)s^*(t-\tau) + s^*(t)s(t+\tau)] \frac{j}{2\pi} \frac{d}{d\tau} [\delta(\tau)] d\tau$$

$$= \frac{1}{2|s(t)|^2} \left(\frac{j}{2\pi} \right) \int_{-\infty}^{\infty} s(t)s^*(t-\tau)\delta'(\tau) d\tau + \tag{132}$$

$$+ \frac{1}{2|s(t)|^2} \left(\frac{j}{2\pi} \right) \int_{-\infty}^{\infty} s^*(t)s(t+\tau)\delta'(\tau) d\tau$$

$$= \frac{j}{4\pi|s(t)|^2} s(t)s^{*\prime}(t) - \frac{j}{4\pi|s(t)|^2} s^*(t)s'(t)$$

$$= \frac{j}{4\pi|s(t)|^2} [s(t)s^{*\prime}(t) - s^*(t)s'(t)]$$

$$= \frac{j}{4\pi|s(t)|^2} [-j2\mathrm{Imag}[s^*(t)s'(t)]] .$$

Therefore

$$\frac{\int_{-\infty}^{\infty} f \cdot IPS(t, f)df}{|s(t)|^2} = \frac{\text{Imag}[s^*(t)s'(t)]}{2\pi |s(t)|^2} \tag{133}$$

For real signals,this *center of mass* is zero, as expected, since the spectrum is conjugate symmetric about DC.

For analytic signals:

$$s(t) = m(t)e^{j\phi(t)} \tag{134}$$

and

$$\begin{aligned}\frac{\int_{-\infty}^{\infty} f \cdot IPS(t, f)df}{|s(t)|^2} &= \frac{\text{Imag}[s^*(t)s'(t)]}{2\pi |s(t)|^2} \\ &= \frac{\text{Imag}\left[m(t)e^{-j\phi(t)}\left[m'(t)e^{j\phi(t)} + j\phi'(t)m(t)e^{j\phi(t)}\right]\right]}{2\pi m^2(t)} \\ &= \frac{\text{Imag}\left[m(t)m'(t) + j\phi'(t)m^2(t)\right]}{2\pi m^2(t)}\end{aligned} \tag{135}$$

and, finally

$$f_i(t) = \frac{1}{2\pi}\frac{d}{dt}[\phi(t)] \tag{136}$$

which is the definition of instantaneous frequency for analytic signals.[7]

[7] This definition of Instantaneous Frequency was introduced by Ville [Ref. 2] in 1952.

Hence, we have that, for analytic signals

$$\frac{\int_{-\infty}^{\infty} f \cdot IPS(t, f) df}{|s(t)|^2} = f_i(t) \tag{137}$$

and our proof is complete.

APPENDIX C. NON-STATIONARY SIGNALS AND THE PRINCIPLE OF UNCERTAINTY

When analyzing signals with time-varying spectral contents, there is a maximum obtainable frequency resolution, determined by the dynamics of the signal. This is in contrast with the stationary case, where the only constraint on the obtainable resolution is the observation time. The presentation and proof of this effect is the goal of this chapter.

A. THE PHYSICAL CONCEPT

Before presenting any mathematical results, we will try to approach the subject with a brief discussion of the involved ideas.

Let us consider our ability to perform spectral estimation on a stationary signal. For that purpose, we will assume that the incoming signal has been segmented into contiguous intervals of Δt seconds. Our final goal is to determine the spectrum occupied by the signal at roughly the moment of analysis, that is, within the last received segment.

If we are given only this last segment, the obtainable frequency resolution is constrained by [Ref. 1]

$$\Delta f \geq \frac{1}{2 \cdot \Delta t} \tag{138}$$

But if now, for some reason, the next to the last segment of data becomes available, we will be able to improve our analysis of the last segment up to a resolution of

$$\Delta f \geq \frac{1}{4 \cdot \Delta t} \tag{139}$$

We can continue the process and, if more segments of data become available, improve our spectral description of the signal at the present time. The rule in this case is:

- The stationarity of the signal allows us to improve the analysis of the present time by using data collected no matter how distant in the past. Hence, if infinite observation time is allowed, infinite spectral resolution can be achieved.

Let us now consider the same scenario, but with a non-stationary incoming signal, which, we will assume, can be considered stationary within the segment. If only the last segment is available, our frequency resolution is again constrained by

$$\Delta f \geq \frac{1}{2 \cdot \Delta t} , \tag{140}$$

and the only way to improve it is to consider more segments. But a qualitative difference appears at this point. Segments of the "distant past" are rendered useless by the dynamics of the signal unless we know or assume its behavior. Considering those segments will only degrade our spectral analysis. The usable data is thus restricted to the most "recent past", which implies an upper bound on the obtainable resolution.

- For a non-stationary signal with unknown dynamics, there is a maximum obtainable frequency resolution, which depends on how distant the unusable "distant past" is. It is an absolute maximum, and depends only on the dynamics of the signal.

Proving this statement is the purpose of this Appendix.

B. MATHEMATICAL FORMULATION

Let us briefly discuss Gabor's result. Gabor [Ref. 1] defined the "effective duration" Δt and the "effective frequency width" Δf of a signal $\psi(t)$ by the following equations

$$\begin{aligned} \Delta t &= \sqrt{\overline{2\pi(t-\bar{t})^2}} \\ \Delta f &= \sqrt{\overline{2\pi(f-\bar{f})^2}} , \end{aligned} \tag{141}$$

where $\overline{[\cdot]}$ stands for the average, and the n^{th} moments are defined, ommiting the argument of $\psi(t)$, as

$$\overline{(t^n)} = \frac{\int_{-\infty}^{\infty} \psi^* t^n \psi \, df}{\int_{-\infty}^{\infty} \psi^* \psi \, dt} \qquad \overline{(f^n)} = \left(\frac{1}{2\pi j} \right)^n \frac{\int_{-\infty}^{\infty} \psi^* \frac{d^n}{dt^n} \psi \, df}{\int_{-\infty}^{\infty} \psi^* \psi \, dt} , \tag{142}$$

resulting in

$$\Delta t \cdot \Delta f \geq \frac{1}{2} . \tag{143}$$

This only states that any signal whose effective duration is Δt (see Figure 30), will have an effective bandwidth Δf (see Figure 31) greater than $\frac{1}{2\Delta t}$; the issue of uncertainty is not addressed in this result.

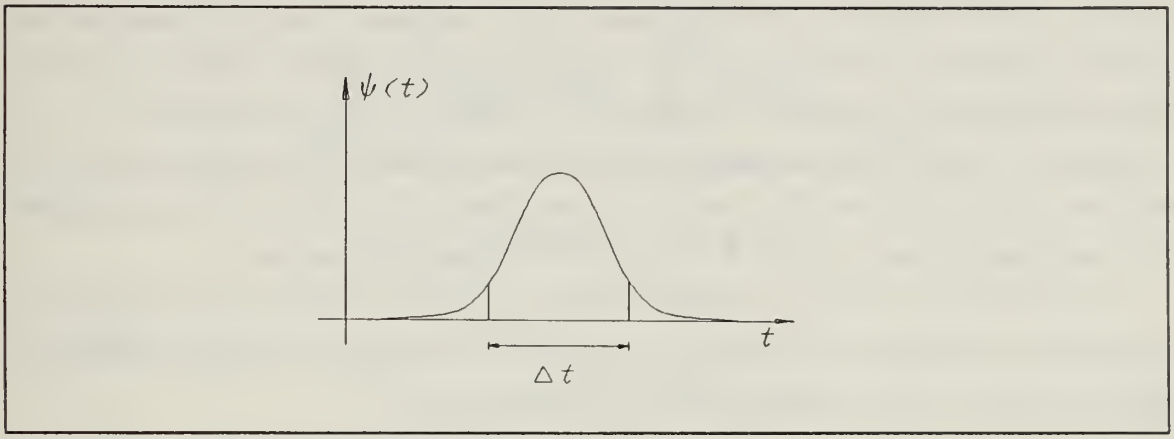

Figure 30. Effective duration of s(t)

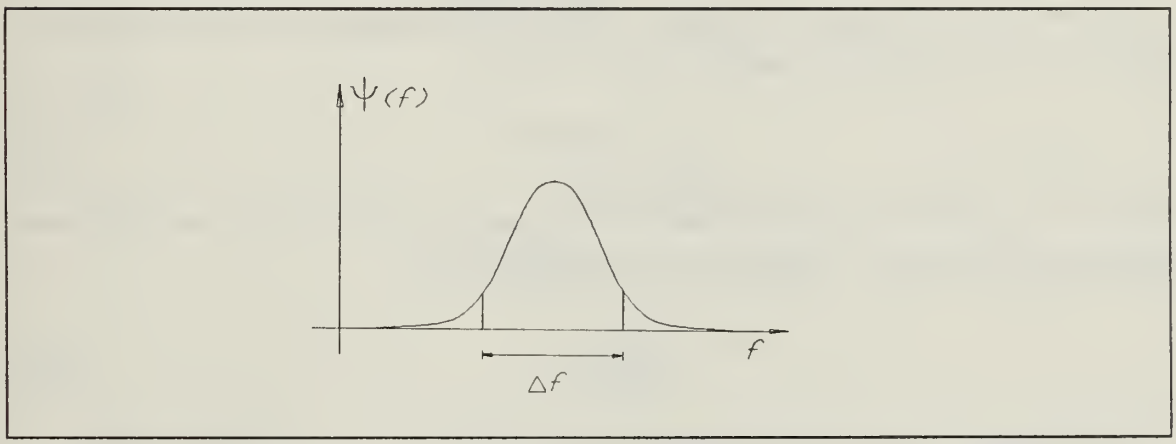

Figure 31. Effective bandwidth of s(t)

In fact, its relevance as an uncertainty principle only comes into play when we realize how classical Spectral Estimation is achieved.

Classical methods are based on the "measure of similarity" between the data and more elementary functions of time which have strong affinities with the physical concept

of frequency. The best example is the Fourier Transform, which conceptually is a bank of correlators, trying to determine the "measure of similarity" between the data and sinusoidal functions, the true representation of our concept of frequency. Other typical examples are in the works of Gabor [Ref. 1] and Priestley [Ref. 22], using elementary functions on the $t-f$ plane, where these functions have what Priestley calls an "oscillatory form" needed to establish the correspondence to our notion of frequency.

Now, if the data is of length T, the elementary functions can have at best the same duration, which implies that their frequency width is greater than $\frac{1}{2T}$. Since the obtainable frequency resolution is at best of the size of the frequency width of the elementary functions, the principle of uncertainty in Spectral Estimation follows.

Gabor's result is only concerned with stationary signals, or at least assumed to be stationary, since Δf is the effective width of the *Fourier Transform* of the signal. However, some implications can also be derived for the non-stationary case.

Let us assume we have an arbitrary stationary signal $\psi(t)$, which we will consider to be analytic to simplify the formulation, with effective duration Δt, effective bandwidth Δf and constant instantaneous frequency. Formally,

$$\frac{1}{2\pi}\frac{d}{dt}\left[\arg[\psi(t)]\right] = constant \tag{144}$$

Let us now force the signal to linearly chirp in frequency, by multiplying it with the phasor $e^{j\pi kt^2}$ and defining the modified signal $\psi_M(t)$ by

$$\psi_M(t) = \psi(t)e^{j\pi kt^2} \tag{145}$$

where k is a positive real number. Due to the exponential, $\psi_M(t)$ is now a non-stationary signal chirping linearly in frequency with a slew rate of

$$\frac{\partial f_i}{\partial t} = k\,. \tag{146}$$

The following results can be established for $\psi_M(t)$:

- *Effective time duration*

  The effective time duration will be

$$\Delta t_M = \sqrt{2\pi\overline{(t_M - \bar{t}_M)^2}} \tag{147}$$

where

$$\bar{t}_M = \frac{\int_{-\infty}^{\infty} \psi_M^* \psi_M \, t \, dt}{\int_{-\infty}^{\infty} \psi_M^* \psi_M dt} = \frac{\int_{-\infty}^{\infty} \psi^* \psi \, t \, dt}{\int_{-\infty}^{\infty} \psi^* \psi dt} = \bar{t} \tag{148}$$

$$\overline{(t_M^2)} = \frac{\int_{-\infty}^{\infty} \psi_M^* \psi_M \, t^2 \, dt}{\int_{-\infty}^{\infty} \psi_M^* \psi_M dt} = \frac{\int_{-\infty}^{\infty} \psi^* \psi \, t^2 \, dt}{\int_{-\infty}^{\infty} \psi^* \psi dt} = \overline{(t^2)} \, . \tag{149}$$

Hence,

$$(\Delta t_M)^2 = 2\pi \left[\overline{(t^2)} - (\bar{t})^2 \right] = (\Delta t)^2 \, . \tag{150}$$

- *Effective bandwidth*

The effective bandwidth will be

$$\Delta f_M = \sqrt{2\pi \overline{(f_M - \bar{f}_M)^2}} = 2\pi \left[\overline{(f_M)^2} - (\bar{f}_M)^2 \right] . \tag{151}$$

where

$$\bar{f}_M = \frac{1}{2\pi j} \frac{\int_{-\infty}^{\infty} \psi_M^* \frac{d}{dt} \psi_M dt}{\int_{-\infty}^{\infty} \psi_M^* \psi_M dt} \, . \tag{152}$$

Using the identity

$$\frac{d\psi_M}{dt} = \frac{d}{dt} \left[\psi(t) e^{j\pi k t^2} \right] = \frac{d\psi}{dt} e^{j\pi k t^2} + j2\pi k t \psi e^{j\pi k t^2} \, , \tag{153}$$

we have that

$$\bar{f}_M = \frac{1}{2\pi j} \frac{\int_{-\infty}^{\infty} \psi_M^* \left[\frac{d\psi}{dt} e^{jk\pi t^2} + j\psi 2\pi k t e^{j\pi k t^2} \right] dt}{\int_{-\infty}^{\infty} \psi^* \psi dt}$$

$$= \frac{1}{2\pi j} \frac{\int_{-\infty}^{\infty} \psi^* \frac{d\psi}{dt} dt}{\int_{-\infty}^{\infty} \psi^* \psi dt} + \frac{\int_{-\infty}^{\infty} \psi^* \psi k t dt}{\int_{-\infty}^{\infty} \psi^* \psi dt} \tag{154}$$

$$= \frac{1}{2\pi j} \frac{\int_{-\infty}^{\infty} \psi^* \frac{d\psi}{dt} dt}{\int_{-\infty}^{\infty} \psi^* \psi dt} + k \frac{\int_{-\infty}^{\infty} \psi^* \psi t dt}{\int_{-\infty}^{\infty} \psi^* \psi dt}$$

$$= \bar{f} + k\bar{t} \, .$$

Hence, all we are missing to completely determine Δf_M is the expression for $\overline{(f_M^2)}$ where [Ref. 1]

$$\overline{(f_M^2)} = \frac{1}{(2\pi)^2} \frac{\int_{-\infty}^{\infty} \frac{d\psi_M^*}{dt} \frac{d\psi_M}{dt} dt}{\int_{-\infty}^{\infty} \psi_M^* \psi_M dt} \, . \tag{155}$$

Noting that

$$\frac{d\psi_M^*}{dt} \frac{d\psi_M}{dt} = \frac{d\psi}{dt} \frac{d\psi^*}{dt} - j2\pi k t \psi^* \frac{d\psi}{dt} + j2\pi k t \psi \frac{d\psi^*}{dt} + (2\pi k)^2 t^2 \psi \psi^* \, , \tag{156}$$

we have

$$\overline{(f_M^2)} = \frac{1}{(2\pi)^2} \frac{\int_{-\infty}^{\infty} \left[\frac{d\psi}{dt}\frac{d\psi^*}{dt} - j2\pi k t\psi^* \frac{d\psi}{dt} + j2\pi k t\psi \frac{d\psi^*}{dt} + (2\pi k)^2 t^2 \psi\psi^* \right] dt}{\int_{-\infty}^{\infty} \psi^*\psi dt}$$

$$= \overline{(f^2)} + k^2 \frac{\int_{-\infty}^{\infty} \psi^* t^2 \psi dt}{\int_{-\infty}^{\infty} \psi^*\psi dt} + \frac{jk}{2\pi} \frac{\int_{-\infty}^{\infty} \psi t \frac{d\psi^*}{dt} dt}{\int_{-\infty}^{\infty} \psi^*\psi dt} - \frac{jk}{2\pi} \frac{\int_{-\infty}^{\infty} \psi^* t \frac{d\psi}{dt} dt}{\int_{-\infty}^{\infty} \psi^*\psi dt} . \tag{157}$$

Considering now the following identities

$$\begin{aligned} \psi \frac{d\psi^*}{dt} &= \frac{\psi\psi^*}{|\psi|} \frac{d}{dt}[\,|\psi|\,] - j\psi\psi^* \frac{d}{dt}[\arg(\psi)] \\ \psi^* \frac{d\psi}{dt} &= \frac{\psi^*\psi}{|\psi|} \frac{d}{dt}[\,|\psi|\,] + j\psi\psi^* \frac{d}{dt}[\arg(\psi)] \end{aligned} \tag{158}$$

we have

$$\overline{(f_M^2)} = \overline{(f^2)} + k^2\overline{(t^2)} + \frac{k}{\pi} \frac{\int_{-\infty}^{\infty} \psi t\psi^* \frac{d}{dt}[\arg(\psi)]dt}{\int_{-\infty}^{\infty} \psi^*\psi dt} , \tag{159}$$

and, using (144) we get

$$\overline{(f_M^2)} = \overline{(f^2)} + k^2\overline{(t^2)} + 2k\bar{t}f_i . \tag{160}$$

Since [Ref. 2]

$$\bar{f} = \frac{1}{2\pi} \frac{\int_{-\infty}^{\infty} \psi f_i \psi^* dt}{\int_{-\infty}^{\infty} \psi^* \psi dt} , \tag{161}$$

we have, by (144) that

$$\bar{f} = f_i \frac{\int_{-\infty}^{\infty} \psi \psi^* dt}{\int_{-\infty}^{\infty} \psi^* \psi dt} = f_i . \tag{162}$$

From where,

$$\overline{(f_M^2)} = \overline{(f^2)} + k^2 \overline{(t^2)} + 2k\bar{t}\bar{f} . \tag{163}$$

Hence, from (151) and (154),

$$\begin{aligned} \Delta f_M{}^2 &= 2\pi \left[\overline{(f^2)} + k^2 \overline{(t^2)} + 2k\bar{t}\bar{f} \right] - 2\pi \left[(\bar{f})^2 + k^2 (\bar{t})^2 + 2k\bar{t}\bar{f} \right] \\ &= 2\pi \left[\overline{(f^2)} - (\bar{f})^2 \right] + k^2 \left[\overline{(t^2)} - (\bar{t})^2 \right] \\ &= (\Delta f)^2 + k^2 (\Delta t)^2 . \end{aligned} \tag{164}$$

Therefore, using (150) we can write the effective time and frequency widths of the modified signal $\psi_M(t)$ in terms of the effective widths of the original stationary signal $\psi(t)$ as

$$\begin{aligned} (\Delta f_M)^2 &= (\Delta f)^2 + k^2 (\Delta t)^2 . \\ (\Delta t_M)^2 &= (\Delta t)^2 . \end{aligned} \tag{165}$$

Using (143) and (165), we get the result

$$
\begin{aligned}
(\Delta f_M \cdot \Delta t_M)^2 &= (\Delta t)^2 \left[(\Delta f)^2 + k^2 (\Delta t)^2 \right] \\
&= (\Delta t \Delta f)^2 + k^2 (\Delta t)^4 \\
&\geq \frac{1}{4} + k^2 (\Delta t)^4 ,
\end{aligned}
\tag{166}
$$

from where

$$
(\Delta f_M)^2 \geq \frac{1}{4(\Delta t)^2} + k^2 (\Delta t)^2 . \tag{167}
$$

Hence, if we minimize the right hand-side of (167), we will find a lower bound on the effective bandwidth of the chirped signal. Proceeding with the minimization, we have

$$
\begin{aligned}
\frac{\partial}{\partial \Delta t} \left[\frac{1}{4(\Delta t)^2} + k^2 (\Delta t)^2 \right] = 0 \;&\Rightarrow \frac{-2}{4(\Delta t)^3} + 2k^2 (\Delta t) = 0 \\
&\Rightarrow k^2 \Delta t = \frac{1}{4(\Delta t)^3} \\
&\Rightarrow (\Delta t)^4 = \frac{1}{4k^2} \\
&\Rightarrow \Delta t = \sqrt{\frac{1}{2k}}
\end{aligned}
$$

Hence

$$
\begin{aligned}
(\Delta f_M)^2 &\geq \frac{k}{2} + \frac{k}{2} \\
\Delta f_M &\geq \sqrt{k}
\end{aligned}
\tag{169}
$$

and we can read the obtained results as stating:

Lemma 1. A linear chirp will always occupy an effective bandwidth greater than $\sqrt{df_i/dt}$, independently of its effective duration.

Lemma 2. A linear chirp will occupy the minimum effective bandwidth of $\sqrt{df_i/dt}$, only if its effective duration is

$$\Delta t = \sqrt{\frac{1}{2\frac{df_i}{dt}}}$$

These results will have obvious implications when classical spectral analysis of the chirped signal is attempted; no matter what the duration of the elementary functions is, the signal will always appear to occupy more than $\sqrt{df_i/dt}$, and this will thus be the best obtainable resolution. This completes our proof.

*Lemma 3.*The maximum obtainable frequency resolution when analyzing signals with unknown frequency dynamics is $\sqrt{df_i/dt}$.

Though the previous discussion was restricted to the case of a linear chirp, the underlying ideas remain valid for laws of variation other than linear; the treated case can be considered as a first order approximation for arbitrary non-stationary signals.

APPENDIX D. PERFORMANCE IN NOISE

As we will see later in this Appendix, an absolute evaluation of the performance of IPS in noise is not possible, because the second moment is data dependent. We will thus, instead, compare the noise performance of IPS with the noise performance of the Wigner-Ville distribution. Let us consider the inverse Fourier transforms of IPS and WD.

$$CI_s(t,\tau) = \frac{1}{2}\left[s(t)s^*(t-\tau) + s^*(t)s(t+\tau)\right]$$
$$\textit{versus} \tag{172}$$
$$CW_s(t,\tau) = s(t+\frac{\tau}{2})s^*(t-\frac{\tau}{2}),$$

Given a signal $z(t)$ that is corrupted by WAGN, where the noise is analytic and bandlimited to the maximum frequency (W) of the signal, that is:

$$v(t) = z(t) + n(t), \tag{173}$$

where

$$S_n(w) = \begin{cases} N_0 & 0 < w < W \\ 0 & \text{otherwise} \end{cases} \tag{174}$$

$$R_n(\tau) = \frac{N_0}{2\pi} \frac{\sin(\frac{W\tau}{2})}{\frac{W\tau}{2}} e^{j\frac{W\tau}{2}} \tag{175}$$

A. MEAN

1. WD

$$\begin{aligned} CW_v(t,\tau) &= v(t+\tfrac{\tau}{2})v^*(t-\tfrac{\tau}{2}) = \left[z(t+\tfrac{\tau}{2}) + n(t+\tfrac{\tau}{2})\right]\cdot\left[z^*(t-\tfrac{\tau}{2}) + n^*(t-\tfrac{\tau}{2})\right] \\ &= z(t+\tfrac{\tau}{2})z^*(t-\tfrac{\tau}{2}) + z(t+\tfrac{\tau}{2})n^*(t-\tfrac{\tau}{2}) \\ &\quad + n(t+\tfrac{\tau}{2})n^*(t-\tfrac{\tau}{2}) + n(t+\tfrac{\tau}{2})z^*(t-\tfrac{\tau}{2}). \end{aligned} \tag{176}$$

$$E\{CW_v(t,\tau)\} = CW_z(t,\tau) + z(t+\frac{\tau}{2})E\left\{n^*(t-\frac{\tau}{2})\right\} + z^*(t-\frac{\tau}{2})E\left\{n(t+\frac{\tau}{2})n^*(t-\frac{\tau}{2})\right\}. \tag{177}$$

Hence,

$$E\{CW_v(t,\tau)\} = CW_z(t,\tau) + R_n(\tau).$$

2. IPS

$$\begin{aligned} CI_v(t,\tau) &= \frac{1}{2}\left[\, v(t)v^*(t-\tau) + v^*(t)v(t+\tau)\,\right] \\ &= \frac{1}{2}\left[z(t)+n(t)\right]\cdot\left[z^*(t-\tau)+n^*(t-\tau)\right] \\ &\quad + \frac{1}{2}\left[z^*(t)+n^*(t)\right]\cdot\left[z(t-\tau)+n(t-\tau)\right]. \end{aligned} \tag{179}$$

$$\begin{aligned} E\{CI_v(t,\tau)\} &= \frac{1}{2}z(t)z^*(t-\tau) + \frac{1}{2}E\left\{n(t)n^*(t-\tau)\right\} \\ &\quad + \frac{1}{2}z^*(t)z(t+\tau) + \frac{1}{2}E\left\{n^*(t)n(t+\tau)\right\} \\ &= CI_z(t,\tau) + \frac{1}{2}R_n(\tau) + \frac{1}{2}R_n(\tau). \end{aligned} \tag{180}$$

Hence,

$$E\{CI_v(t,\tau)\} = CI_z(t,\tau) + R_n(\tau). \tag{181}$$

Therefore, IPS and WD have, as far as their first moment is concerned, identical behavior in the presence of noise.

B. VARIANCE

1. WD

$$\begin{aligned} |\, CW_v(t,\tau)\,|^2 &= v(t+\tfrac{\tau}{2})v^*(t-\tfrac{\tau}{2})v^*(t+\tfrac{\tau}{2})v(t-\tfrac{\tau}{2}) \\ &= [z(t+\tfrac{\tau}{2})+n(t+\tfrac{\tau}{2})][z^*(t-\tfrac{\tau}{2})+n^*(t-\tfrac{\tau}{2})] \\ &\quad\cdot[z^*(t+\tfrac{\tau}{2})+n^*(t+\tfrac{\tau}{2})][z(t-\tfrac{\tau}{2})+n(t-\tfrac{\tau}{2})] \end{aligned}$$

$$
\begin{aligned}
|\,CW_v(t,\tau)\,|^2 = {} & [z(t+\tfrac{\tau}{2})z^*(t-\tfrac{\tau}{2}) + z(t+\tfrac{\tau}{2})n^*(t-\tfrac{\tau}{2}) \\
& + n(t+\tfrac{\tau}{2})z^*(t-\tfrac{\tau}{2}) + n(t+\tfrac{\tau}{2})n^*(t-\tfrac{\tau}{2})] \\
& \cdot[z^*(t+\tfrac{\tau}{2})z(t-\tfrac{\tau}{2}) + z^*(t+\tfrac{\tau}{2})n(t-\tfrac{\tau}{2}) \\
& + n^*(t+\tfrac{\tau}{2})z(t-\tfrac{\tau}{2}) + n^*(t+\tfrac{\tau}{2})n(t-\tfrac{\tau}{2})]\,.
\end{aligned}
\tag{183}
$$

Using now the expectation operator, we have:

$$
\begin{aligned}
E\{|\,CW_v(t,\tau)\,|^2\} = {} & |\,z(t+\tfrac{\tau}{2})\,|^2\,|\,z(t-\tfrac{\tau}{2})\,|^2 \\
& + z(t+\tfrac{\tau}{2})z^*(t-\tfrac{\tau}{2})E\{n^*(t+\tfrac{\tau}{2})\} \\
& + |\,z(t+\tfrac{\tau}{2})\,|^2 E\{|\,n(t-\tfrac{\tau}{2})\,|^2\} \\
& + z(t+\tfrac{\tau}{2})z(t-\tfrac{\tau}{2})E\{n^*(t+\tfrac{\tau}{2})n^*(t-\tfrac{\tau}{2})\} \\
& + z^*(t-\tfrac{\tau}{2})z^*(t+\tfrac{\tau}{2})E\{n(t+\tfrac{\tau}{2})n(t-\tfrac{\tau}{2})\} \\
& + |\,z(t-\tfrac{\tau}{2})\,|^2 E\{|\,n(t+\tfrac{\tau}{2})\,|^2\} \\
& + E\{n(t+\tfrac{\tau}{2})n^*(t-\tfrac{\tau}{2})n^*(t+\tfrac{\tau}{2})n(t-\tfrac{\tau}{2})\} \\
& + z^*(t+\tfrac{\tau}{2})z(t-\tfrac{\tau}{2})E\{n(t+\tfrac{\tau}{2})n^*(t-\tfrac{\tau}{2})\}\,.
\end{aligned}
\tag{184}
$$

And, since[8]

$$
E\{n^*(t+\tfrac{\tau}{2})n^*(\tfrac{t-\tau}{2})\} = E\{n(t+\tfrac{\tau}{2})n(t-\tfrac{\tau}{2})\} = 0\,. \tag{185}
$$

$$
\begin{aligned}
E\{|\,CW_v(t,\tau)\,|^2\} = {} & |\,z(t+\tfrac{\tau}{2})\,|^2\,|\,z(t-\tfrac{\tau}{2})\,|^2 + z(t+\tfrac{\tau}{2})z^*(t-\tfrac{\tau}{2})R_n^*(\tau) \\
& + |\,z(t+\tfrac{\tau}{2})\,|^2\,\frac{N_0W}{2\pi} + z^*(t+\tfrac{\tau}{2})z(t-\tfrac{\tau}{2})R_n(\tau) \\
& + |\,z(t-\tau_2)\,|^2\,\frac{N_0W}{2\pi} + |\,R_n(\tau)\,|^2 + \left(\frac{N_0W}{2\pi}\right)^2,
\end{aligned}
$$

[8] See Appendix F.

where we made use of the fact that, for zero mean Gaussian random variables [Ref. 23],

- $E\{x_1x_2x_3\} = 0$
- $E\{x_1x_2x_3x_4\} = E\{x_1x_2\}\cdot E\{x_3x_4\} + E\{x_1x_3\}\cdot E\{x_2x_4\} + E\{x_1x_4\}\cdot E\{x_2x_3\}$.

Hence,

$$E\left\{ | CW_v(t,\tau) |^2 \right\} = | z(t+\tfrac{\tau}{2})z^*(t-\tfrac{\tau}{2}) |^2 + \frac{N_0}{2\pi}\left[| z(t+\tfrac{\tau}{2}) |^2 + | z(t-\tfrac{\tau}{2}) |^2 \right] + R_n(\tau)z^*(t+\tfrac{\tau}{2})z(t-\tfrac{\tau}{2}) + R_n^*(\tau)z(t+\tfrac{\tau}{2})z^*(t-\tfrac{\tau}{2}) + | R_n(\tau) |^2 + \left(\frac{N_0W}{2\pi}\right)^2 . \tag{187}$$

Now,

$$\begin{aligned} \mathrm{Var}\{CW_v(t,\tau)\} &= E\left\{ | CW_v(t,\tau) |^2 \right\} - E\{CW_v(t,\tau)\}E\{CW_v(t,\tau)\}^* \\ &= E\left\{ | CW_v(t,\tau) |^2 \right\} - [CW_z(t,\tau) + R_n(\tau)]\cdot[CW_z^*(t,\tau) + R_n^*(\tau)] \\ &= E\left\{ | CW_v(t,\tau) |^2 \right\} - | z(t+\tfrac{\tau}{2})z^*(t-\tfrac{\tau}{2}) |^2 - | R_n(\tau) |^2 \\ &\quad - CW_z(t,\tau)R_n^*(\tau) - CW_z^*(t,\tau)R_n(\tau) . \end{aligned} \tag{188}$$

From where, using (187) and (172),

$$\mathrm{Var}\{CW_v(t,\tau)\} = \frac{N_0W}{2\pi}\left[| z(t+\tfrac{\tau}{2}) |^2 + | z(t-\tfrac{\tau}{2}) |^2 \right] + \left(\frac{N_0W}{2\pi}\right)^2 \tag{189}$$

2. IPS

$$\begin{aligned} | CI_v(t,\tau) |^2 &= \frac{1}{4}[v(t)v^*(t-\tau) + v^*(t)v(t+\tau)][v^*(t)v(t-\tau) + v(t)v^*(t+\tau)] \\ &= \frac{1}{4}[v(t)v^*(t)v^*(t-\tau)v(t-\tau)] + \frac{1}{4}[v^*(t)v(t+\tau)v^*(t)v(t-\tau)] \\ &\quad + \frac{1}{4}[v(t)v^*(t-\tau)v(t)v^*(t+\tau)] + \frac{1}{4}[v^*(t)v(t+\tau)v(t)v^*(t+\tau)] . \end{aligned} \tag{190}$$

For simplicity, we will treat each term in (190) separately, and use the fact that the second and third terms are complex conjugates of each other.

- *First term*

$$E\left\{\frac{1}{4}[v(t)v^*(t)v^*(t-\tau)v(t-\tau)]\right\} =$$

$$= \frac{1}{4}E\{[z(t)+n(t)][z^*(t)+n^*(t)][z^*(t-\tau)+n^*(t-\tau)][z(t-\tau)+n(t-\tau)]\}$$

$$= \frac{1}{4}E\{[z(t)z^*(t)+z(t)n^*(t)+z^*(t)n(t)+n(t)n^*(t)]$$

$$\cdot[z^*(t-\tau)z(t-\tau)+z^*(t-\tau)n(t-\tau) \qquad (191)$$

$$+ z(t-\tau)n^*(t-\tau)+n^*(t-\tau)n(t-\tau)]\}$$

$$= \frac{1}{4}\left[z(t)z^*(t)z^*(t-\tau)z(t-\tau)+|z(t)|^2E\{|n(t-\tau)|^2\}\right.$$

$$+ z(t)z^*(t-\tau)E\{n^*(t)n(t-\tau)\}+z^*(t)z(t-\tau)E\{n(t)n^*(t-\tau)\}$$

$$\left.+|z(t-\tau)|^2E\{|n(t)|^2\}+E\{n(t)n^*(t)n(t-\tau)n^*(t-\tau)\}\right].$$

Simplifying,

$$E\left\{\frac{1}{4}[v(t)v^*(t)v^*(t-\tau)v(t-\tau)]\right\} = \frac{1}{4}|z(t)z^*(t-\tau)|^2$$

$$+\frac{1}{4}\frac{N_0W}{2\pi}\left[|z(t)|^2+|z(t-\tau)|^2\right]+\frac{1}{4}z(t)z^*(t-\tau)R_n^*(\tau) \qquad (192)$$

$$+\frac{1}{4}z^*(t)z(t-\tau)R_n(\tau)+\frac{1}{4}\left(\frac{N_0W}{2\pi}\right)^2+\frac{1}{4}|R_n(\tau)|^2.$$

- *Second term*

$$E\left\{\frac{1}{4}[v^*(t)v(t+\tau)v^*(t)v(t-\tau)]\right\} =$$

$$= \frac{1}{4}E\{[z^*(t)+n^*(t)][z(t+\tau)+n(t+\tau)][z^*(t)+n^*(t)][z(t-\tau)+n(t-\tau)]\}$$

$$= \frac{1}{4}E\{[z^*(t)z(t+\tau)+z^*(t)n(t+\tau)+n^*(t)z(t+\tau)+n^*(t)n(t+\tau)]$$

$$\cdot[z^*(t)z(t-\tau)+z^*(t)n(t-\tau)+n^*(t)z(t-\tau)+n^*(t)n(t-\tau)]$$

$$= \frac{1}{4}\left[z^*(t)z^*(t)z(t+\tau)z(t-\tau)+z^*(t)z(t+\tau)E\{n^*(t)n(t-\tau)\}\right.$$

$$+ z^*(t)z(t-\tau)E\{n(t+\tau)n^*(t)\}z^*(t)z(t+\tau)E\{n^*(t)n(t-\tau)\}$$

$$\left.+z^*(t)z(t-\tau)E\{n^*(t)n(t+\tau)\}+E\{n^*(t)n^*(t)n(t+\tau)n(t-\tau)\}\right].$$

$$E\left\{\frac{1}{4}[v^*(t)v(t+\tau)v^*(t)v(t-\tau)]\right\} = \frac{1}{4}z^*(t)z^*(t)z(t+\tau)z(t-\tau)$$

$$+\frac{1}{4}z^*(t)z(t+\tau)R_n^*(\tau)+\frac{1}{4}z^*(t)z(t-\tau)R_n(\tau) \qquad (194)$$

$$+\frac{1}{4}z^*(t)z(t+\tau)R_n^*(\tau)+\frac{1}{4}z^*(t)z(t-\tau)R_n(\tau)+\frac{1}{2}|R_n(\tau)|^2.$$

- *Third term* Since this term is the complex conjugate of the second term, we have:

$$E\left\{\frac{1}{4}[v(t)v^*(t-\tau)v(t)v^*(t+\tau)]\right\} = \frac{1}{4}z(t)z(t)z^*(t+\tau)z^*(t-\tau)$$
$$+\frac{1}{4}z(t)z^*(t+\tau)R_n(\tau)+\frac{1}{4}z(t)z^*(t-\tau)R_n^*(\tau) \qquad (195)$$
$$+\frac{1}{4}z(t)z^*(t+\tau)R_n(\tau)+\frac{1}{4}z(t)z^*(t-\tau)R_n^*(\tau)+\frac{1}{2}|R_n(\tau)|^2.$$

- *Fourth term*

$$E\left\{\frac{1}{4}[v^*(t)v(t+\tau)v(t)v^*(t+\tau)]\right\} =$$
$$=\frac{1}{4}E\{[z^*(t)+n^*(t)][z(t+\tau)+n(t+\tau)][z(t)+n(t)][z^*(t+\tau)+n^*(t+\tau)]\}$$
$$=\frac{1}{4}E\{[z^*(t)z(t+\tau)+z^*(t)n(t+\tau)+n^*(t)z(t+\tau)+n^*(t)n(t+\tau)]$$
$$\cdot[z(t)z^*(t+\tau)+z(t)n^*(t+\tau)+n(t)z^*(t+\tau)+n(t)n^*(t+\tau)]$$
$$=\frac{1}{4}\left[z^*(t)z(t+\tau)z(t)z^*(t+\tau)+z^*(t)z(t+\tau)E\{n(t)n^*(t+\tau)\}\right.$$
$$+|z(t)|^2E\{|n(t+\tau)|^2\}+|z(t+\tau)|^2E\{|n(t)|^2\}$$
$$\left.+z(t)z^*(t+\tau)E\{n^*(t)n(t+\tau)\}+E\{n^*(t)n(t)n(t+\tau)n^*(t+\tau)\}\right].$$

$$E\left\{\frac{1}{4}[v^*(t)v(t+\tau)v(t)v^*(t+\tau)]\right\} = \frac{1}{4}|z^*(t)z(t+\tau)|^2$$
$$+\frac{1}{4}\frac{N_0W}{2\pi}\left[|z(t)|^2+|z(t+\tau)|^2\right]+\frac{1}{4}z^*(t)z(t+\tau)R_n^*(\tau) \qquad (197)$$
$$+\frac{1}{4}z(t)z^*(t+\tau)R_n(\tau)+\frac{1}{4}\left(\frac{N_0W}{2\pi}\right)^2+\frac{1}{4}|R_n(\tau)|^2.$$

Adding the four terms (192), (194), (195) and (197), we thus obtain the expression for the second moment of IPS. Now,

$$\mathrm{Var}\{CI_v(t,\tau)\} = E\{|CI_v(t,\tau)|^2\} - E\{CI_v(t,\tau)\}\cdot E\{CI_v(t,\tau)\}^*, \qquad (198)$$

where

$$E\{CI_v(t,\tau)\}\cdot E\{CI_v(t,\tau)\}^* = [CI_z(t,\tau)+R_n(\tau)]\cdot[CI_z^*(t,\tau)+R_n^*(\tau)]$$
$$= CI_z(t,\tau)CI_z^*(t,\tau)+CI_z(t,\tau)R_n^*(\tau) \qquad (199)$$
$$+CI_z^*(t,\tau)R_n(\tau)+|R_n(\tau)|^2.$$

Substituting in (198), we get that

$$\begin{aligned}\mathrm{Var}\{CI_v(t,\tau)\} &= E\{\,|\,CI_v(t,\tau)\,|^2\} - E\{CI_v(t,\tau)\}\cdot E\{CI_v(t,\tau)\}^* \\ &= \frac{1}{4}\frac{N_0 W}{2\pi}\left[\,|\,z(t)\,|^2 + |\,z(t-\tau)\,|^2 + |\,z(t)\,|^2 + |\,z(t+\tau)\,|^2\,\right] \\ &\quad + \frac{1}{4}\,z(t)z^*(t-\tau)R_n^*(\tau) + \frac{1}{4}\,z^*(t)z(t+\tau)R_n^*(\tau) \\ &\quad + \frac{1}{4}\,z^*(t)z(t-\tau)R_n(\tau) + \frac{1}{4}\,z(t)z^*(t+\tau)R_n(\tau) \\ &\quad + \frac{1}{2}\,|\,R_n(\tau)\,|^2 + \frac{1}{2}\left(\frac{N_0 W}{2\pi}\right)^2 .\end{aligned} \tag{200}$$

We can now compare the variances of $CI_v(t,\tau)$ and $CW_v(t,\tau)$. First of all we realize that, in both cases, the variance is a function of t and τ. If $\tau = 0$, we have:

$$\mathrm{Var}\{CI_v(t,\tau)\} = \frac{N_0 W}{\pi}\,|\,z(t)\,|^2 + \left(\frac{N_0 W}{2\pi}\right)^2 \tag{201}$$

$$\mathrm{Var}\{CW_v(t,\tau)\} = \frac{N_0 W}{\pi}\,|\,z(t)\,|^2 + \left(\frac{N_0 W}{2\pi}\right)^2 \tag{202}$$

That is,

$$\mathrm{Var}\{CI_v(t,\tau)\} = \mathrm{Var}\{CW_v(t,\tau)\} \qquad (\tau = 0)\,. \tag{203}$$

For $\tau \neq 0$, we have from (200) that

$$\begin{aligned}\mathrm{Var}\{CI_v(t,\tau)\} &\le \frac{1}{4}\frac{N_0 W}{2\pi}\left[\,|\,z(t)\,|^2 + |\,z(t-\tau)\,|^2 + |\,z(t)\,|^2 + |\,z(t+\tau)\,|^2\,\right] \\ &\quad + \frac{1}{4}\,|\,R_n(\tau)\,|\left[\,|\,z(t)z^*(t-\tau)\,| + |\,z^*(t)z(t+\tau)\,|\right. \\ &\quad \left. + |\,z^*(t)z(t-\tau)\,| + |\,z(t)z^*(t+\tau)\,|\,\right] \\ &\quad + \frac{1}{2}\,|\,R_n(\tau)\,|^2 + \frac{1}{2}\left(\frac{N_0 W}{2\pi}\right)^2 .\end{aligned} \tag{204}$$

$$\begin{aligned}\mathrm{Var}\{CI_v(t,\tau)\} \le \frac{1}{4}\frac{N_0 W}{2\pi}\Big[& |z(t)|^2 + |z(t-\tau)|^2 + |z(t)|^2 + |z(t+\tau)|^2 \\ & + |z(t)||z(t+\tau)| + |z(t)||z(t-\tau)| + |z(t)||z(t-\tau)| \\ & + |z(t)||z(t+\tau)|\Big] + \left(\frac{N_0 W}{2\pi}\right)^2 .\end{aligned} \tag{205}$$

The time dependency of the expression stops us from a direct comparison with $CW_v(t,\tau)$. However, since the signal is arbitrary, we have no reason to assume any ordering of its magnitude at different points in time. We can thus average over time, and get the following result:

$$\begin{aligned}<\mathrm{Var}\{CI_v(t,\tau)\}>_{av} \le & \frac{N_0 W}{8\pi}\Big[4<|z(t)|^2>_{av} + <|z(t)||z(t+\tau)|>_{av} \\ & + <|z(t)||z(t-\tau)|>_{av} + <|z(t)||z(t-\tau)|>_{av} \\ & + <|z(t)||z(t+\tau)|>_{av}\Big] + \left(\frac{N_0 W}{2\pi}\right)^2 \\ \le & \frac{N_0 W}{\pi}<|z(t)|^2>_{av} + \left(\frac{N_0 W}{2\pi}\right)^2 .\end{aligned} \tag{206}$$

Using (189),

$$<\mathrm{Var}\{CI_v(t,\tau)\}>_{av} \le <\mathrm{Var}\{CW_v(t,\tau)\}>_{av} , \tag{207}$$

and finally, we have

- $\tau = 0$

$$\mathrm{Var}\{CI_v(t,\tau)\} = \mathrm{Var}\{CW_v(t,\tau)\} \tag{208}$$

- $\tau \neq 0$

$$<\mathrm{Var}\{CI_v(t,\tau)\}>_{av} \le <|\mathrm{Var}\{CW_v(t,\tau)\}|>_{av} \tag{209}$$

For the case $\tau \neq 0$, $W \gg 1$, we can make the following approximations, using (189) and (200):

$$<\mathrm{Var}\{CI_v(t,\tau)\}>_{av} \approx \frac{1}{2}\left(\frac{N_0 W}{2\pi}\right)^2 \tag{210}$$

$$<\mathrm{Var}\{CW_v(t,\tau)\}>_{av} \approx \left(\frac{N_0 W}{2\pi}\right)^2 \tag{211}$$

That is, when the bandwidth of the noise approaches infinity, the difference in noise performance between IPS and WD approaches the limiting value of 3 dB.

APPENDIX E. A DIFFERENT DEFINITION OF "INSTANTANEOUS POWER SPECTRUM"

In accordance with the discussion in Section III-C, the following definition of Instantaneous Power Spectrum can be made.

- *Definition* - Instantaneous Power Spectrum at the time of a given sample is the frequency content of the stationary spectrum implied by the existence of that sample.

That is: reading the Fourier transform as a change of basis in an N-dimensional space, the Instantaneous Power Spectrum will be the difference in coordinates (referred to the phasor axis) between the location of the signal in the N-dimensional space and its location in the (N-1)-dimensional space that results from suppressing the dimension corresponding to the sample of interest.

Since in terms of the internal product, the absence of any dimension can be represented by a zero component of any of the vectors along that dimension, this definition leads to a three-step procedure:

1. Compute

$$| X(\omega) |^2 , \tag{212}$$

where

$$X(\omega) = \sum_{n=-\infty}^{\infty} x(n) e^{-j\omega n} . \tag{213}$$

2. Define a new sequence, obtained by zeroing $x(n)$ at the sample of interest, that is:

$$x_z(n) = \begin{cases} x(n) & n \neq r \\ 0 & n = r \end{cases} \tag{214}$$

where r is the time at which the Instantaneous Power Spectrum is to be determined, and obtain

$$| X_z(\omega) |^2 . \tag{215}$$

3. Obtain the Instantaneous Power Spectrum as:

$$\textit{Instantaneous Power Spectrum} = | X(\omega) | - | X_z(\omega) |^2 . \tag{216}$$

The resulting distribution will be (using extended sequences, as in Appendix A)

$$|X(\omega)|^2 = X(\omega)X^*(\omega)$$
$$= \sum_{n=-\infty}^{\infty} x(n)e^{-J\omega n} \cdot \sum_{n=-\infty}^{\infty} x^*(n)e^{J\omega n} \tag{217}$$

and, after some manipulations,

$$|X(\omega)|^2 = \sum_{-\infty}^{\infty} c_k e^{-j\omega k}, \tag{218}$$

where

$$c_k = \sum_{n=k}^{\infty} x(n)x^*(n-k) \qquad k \geq 0 \tag{219}$$

and

$$c_{-k} = c_k^* . \tag{220}$$

Correspondingly,

$$|X_z(\omega)|^2 = \sum_{-\infty}^{\infty} b_k e^{-j\omega k}, \tag{221}$$

where

$$b_k = \sum_{n=k}^{\infty} x_z(n)x_z^*(n-k) \qquad k \geq 0 \tag{222}$$

and

$$b_{-k} = b_k^* . \tag{223}$$

Hence, we have that

$$\begin{aligned} |X(\omega)|^2 - |X_z(\omega)|^2 &= \sum_{k=-\infty}^{\infty} c_k e^{-j\omega k} - \sum_{k=-\infty}^{\infty} b_k e^{-j\omega k} \\ &= \sum_{k=-\infty}^{\infty} \Delta_k e^{-j\omega k} - |x(r)|^2 , \end{aligned} \tag{224}$$

where

$$\Delta_k = [x(r)x^*(r-k) + x(r+k)x^*(r)] \qquad k \geq 0 \tag{225}$$

and

$$\Delta_{-k} = \Delta_k^* . \tag{226}$$

that is, this definition leads almost exactly (up to a constant, for fixed time) to IPS. What is important to realize is that this definition has no concept of *past* or *future*, and that all points are equally treated, no matter what point they occupy in the sequence. This result seems to put an end to our hope of finding assymetries in the IPS concept.

As a final note, a more formal proof of the relation between this distribution and IPS can be made as follows: Define

$$x_z(n) = \begin{cases} x(n) & n \neq r \\ 0 & n = r \end{cases} \tag{227}$$

$$d(n) = \begin{cases} 0 & n \neq r \\ x(n) & n = r \end{cases} \tag{228}$$

Hence,

$$x(n) = x_z(n) + d(n) . \tag{229}$$

Let

$$\begin{aligned} X(\omega) &= F\{x(n)\} \\ D(\omega) &= F\{d(n)\} \\ X_z(\omega) &= F\{x_z(n)\} . \end{aligned} \tag{230}$$

Then,

$$X(\omega) = X_z(\omega) + D(\omega) \tag{231}$$

and

$$\begin{aligned} |X(\omega)|^2 - |X_z(\omega)|^2 &= (X_z(\omega) + D(\omega))(X_z^*(\omega) + D^*(\omega)) - X_z(\omega)X_z^*(\omega) \\ &= X_z(\omega)D^*(\omega) + X_z^*(\omega)D(\omega) + D(\omega)D^*(\omega)\,. \end{aligned} \tag{232}$$

But we know that $D(\omega) = x(r)e^{-j\omega r}$. Therefore,

$$\begin{aligned} |X(\omega)|^2 - |X_z(\omega)|^2 &= 2\mathrm{Re}\{X_z(\omega)x^*(r)e^{j\omega r}\} + D(\omega)x^*(r)e^{j\omega r} \\ &= 2\mathrm{Re}\{[X_z(\omega) + D(\omega)]\,x^*(r)e^{j\omega r}\} - |x(r)|^2 \\ &= 2\mathrm{Re}\{X(\omega)x^*(r)e^{j\omega r}\} - |x(r)|^2 \\ &= 2\cdot\Delta t\cdot IPS - |x(r)|^2\,. \end{aligned} \tag{233}$$

APPENDIX F. ON THE SECOND MOMENT OF ANALYTIC SIGNALS

The purpose of this appendix is to proof the following theorem:

Theorem: For an arbitrary *analytic* random signal $z(t)$, defined as

$$z(t) = x(t) + j\hat{x}(t)\,, \tag{234}$$

where $\hat{x}(t)$ is the Hilbert transform of $x(t)$, the following identity is satisfied:

$$E\{z(n)z(s)\} = 0 \tag{235}$$

Proof:

$$\begin{aligned} E\{z(n)z(s)\} &= E\{\,[x(n) + j\hat{x}(n)]\cdot[x(s) + j\hat{x}(s)]\,\} \\ &= E\{x(n)x(s)\} + jE\{\hat{x}(n)x(s)\} + jE\{x(n)\hat{x}(s)\} - E\{\hat{x}(n)\hat{x}(s)\}\,. \end{aligned} \tag{236}$$

But, from the properties of the Hilbert transform, we have that

$$\begin{aligned} R_{x\hat{x}}(\tau) &= -\,R_{\hat{x}x}(\tau) \\ R_{\hat{x}\hat{x}}(\tau) &= R_{xx}(\tau) \end{aligned} \tag{237}$$

Hence,

$$\begin{aligned} E\{z(n)z(s)\} &= R_{xx}(n-s) + jR\hat{x}x(n-s) + jRx\hat{x}(n-s) - R\hat{x}\hat{x}(n-s) \\ &= 0\,. \end{aligned} \tag{238}$$

Our proof is thus complete.

LIST OF REFERENCES

1. D. Gabor, "Theory of Communication," *Journal of the Institution of Electrical Engineers*, Vol. 93, pp. 429-457, November 1946.

2. J. Ville, "Theorie et Applications de la Notion de Signal Analytique," *Cables et Transmission*, Vol. 2.A, N. 1, pp. 61-74, 1948.

3. M. J. Levin, "Instantaneous Spectra and Ambiguity Functions," *IEEE Trans. Information Theory*, Vol. IT-10, pp. 95-97, January 1964.

4. A. W. Rihaczek, "Signal Energy Distribution in Time and Frequency," *IEEE Trans. Information Theory*, Vol. IT-14, N. 3, pp. 369-374, May 1968.

5. C. H. Page, "Instantaneous Power Spectra," *Journal of Applied Physics*, Vol. 23, pp. 103-206, January 1952.

6. T. A. C. M. Claasen and W. F. G. Mecklenbraeuker, "The Wigner Distribution-A Tool for Time-Frequency Analysis, PART I: Continuous Time Signals," *Philips Journal of Res.*, Vol. 35, pp. 217-250, 1980.

7. T. A. C. M. Claasen and W. F. G. Mecklenbraeuker, "The Wigner Distribution-A Tool for Time-Frequency Analysis, PART II: Discrete Time Signals," *Philips Journal of Res.*, Vol. 35, pp. 276-300, 1980.

8. B. Bouashash, "Notes on the Use of the Wigner Distribution for Time-Frequency Signal Analysis," *IEEE Trans. ASSP*, Vol. 36, N. 9, pp. 1518-1521, September 1988.

9. G. F. Boudreaux-Bartels and Thomas W. Parks, "Time-varying Filtering and Signal Estimation Using Wigner Distribution Synthesis Techniques," *IEEE Trans. ASSP*, Vol. 34, N. 3, pp. 442-451, June 1986.

10. F. Peyrin and R. Prost, "A Unified Definition for the Discrete-Time, Discrete Frequency, and Discrete Time Frequency Wigner Distributions," *IEEE Trans. ASSP*, Vol. 34, N. 4, pp. 858-866, August 1986.

11. O. D. Grace, "Instantaneous Power Spectra," *J. Acoust. Soc. Amer.*, Vol. 69, N. 1, pp. 191-197, January 1981.

12. M. H. Ackroyd, "Instantaneous and Time-Varying Spectra-An Introduction," *The Radio and Electronic Engineer*, Vol. 39, N. 3, pp. 145-152, March 1970.

13. L. Cohen, "Generalized Phase Space Distribution Functions," *J. Math. Phys.*, Vol. 7, pp. 781-786, May 1966.

14. T. A. C. M. Claasen and W. F. G. Mecklenbraeuker, "The Wigner Distribution-A Tool for Time-Frequency Analysis, PART III: Relations With Other Time-Frequency Signal Transformations," *Philips Journal of Res.*, Vol. 35, pp. 372-389, 1980.

15. H. Margeneau and R. N. Hill, "Correlation Between Measurements In Quantum Theory," *Progress of Theoretical Physics*, Vol. 26, N. 5, pp. 722-738, November 1961.

16. A. J. E. M. Janssen, "Positivity Properties of Phase-Plane Distribution Functions," *J. Math. Phys.*, Vol. 25, N. 7, pp. 2240-2252, July 1984.

17. J. E. Moyal, "Quantum Mechanics as a Statistical Theory," *Proc. Cambridge Philos. Soc.*, Vol. 45, pp. 99-123, 1949.

18. R. M. Fano, "Short-time Autocorrelation Functions and Power Spectra, " *J. Acoust. Soc. Amer.*, Vol. 22, N. 5, pp. 546-550, September 1950.

19. M. R. Schroder and B. S. Atal, "Generalized Short-Time Power Spectra and Autocorrelation Functions," *J. Acoust. Soc. Amer.*, Vol. 34, N. 11, pp. 1679-1683, November 1962.

20. P. A. Ramamoorthy, V. K. Iyer, and Y. Ploysongsang, "Autoregressive Modeling of the Wigner Spectrum," *Intern. Conf. on Acc. Speech and Signal Proc.*, Dallas, 1987.

21. Steven M. Kay, *Modern Spectral Estimation. Theory and Application* , pp. 217-252, Prentice-Hall, 1988.

22. M. B. Priestley, *Spectral Analysis and Time Series*, Vol. 2, Academic Press Inc, 1981.

23. Whalen, *Detection of Signals in Noise*, pp. 96-98, Academic Press Inc., 1971.

INITIAL DISTRIBUTION LIST

		No. Copies
1.	Defense Technical Information Center Cameron Station Alexandria, VA 22304-6145	2
2.	Library, Code 0142 Naval Postgraduate School Monterey, CA 93943-5002	2
3.	Professor Ralph D. Hippenstiel, Code 62Hi Department of Electrical and Computer Engineering Naval Postgraduate School Monterey, CA 93943-5004	3
4.	Professor Roberto Cristi, Code 62Cx Department of Electrical and Computer Engineering Naval Postgraduate School Monterey, CA 93943-5004	1
5.	Chairman, Code 62 Department of Electrical and Computer Engineering Naval Postgraduate School Monterey, CA 93943-5000	1
6.	Professor Charles W. Therrien, Code 62Ti Department of Electrical and Computer Engineering Naval Postgraduate School Monterey, CA 93943-5004	1
7.	Professor Murali Tummala, Code 62Tu Department of Electrical and Computer Engineering Naval Postgraduate School Monterey, CA 93943-5004	1
8.	Naval Ocean Systems Center Attn : Dr. C. E. Persons, Code 732 San Diego, CA 92152	1
9.	Lcdr. Luiz A. Lopes de Souza, Brazilian Navy Instituto de Pesquisas da Marinha 4706 Wisconsin Ave. Washington, DC 20016	1

10. Lt. Armando M. P. Jesus Sequeira — 1
Direcção do Serviço de Instrução e Treino
Edifício da Administração Central de Marinha
Praça do Comércio
1100 Lisboa
Portugal

11. Direcção do Serviço de Instrução e Treino — 1
Edifício da Administração Central de Marinha
Praça do Comércio
1100 Lisboa
Portugal

12. Lt. Paulo M. D. Mónica de Oliveira — 2
Direcção do Serviço de Instrução e Treino
Edifício da Administração Central de Marinha
Praça do Comércio
1100 Lisboa
Portugal

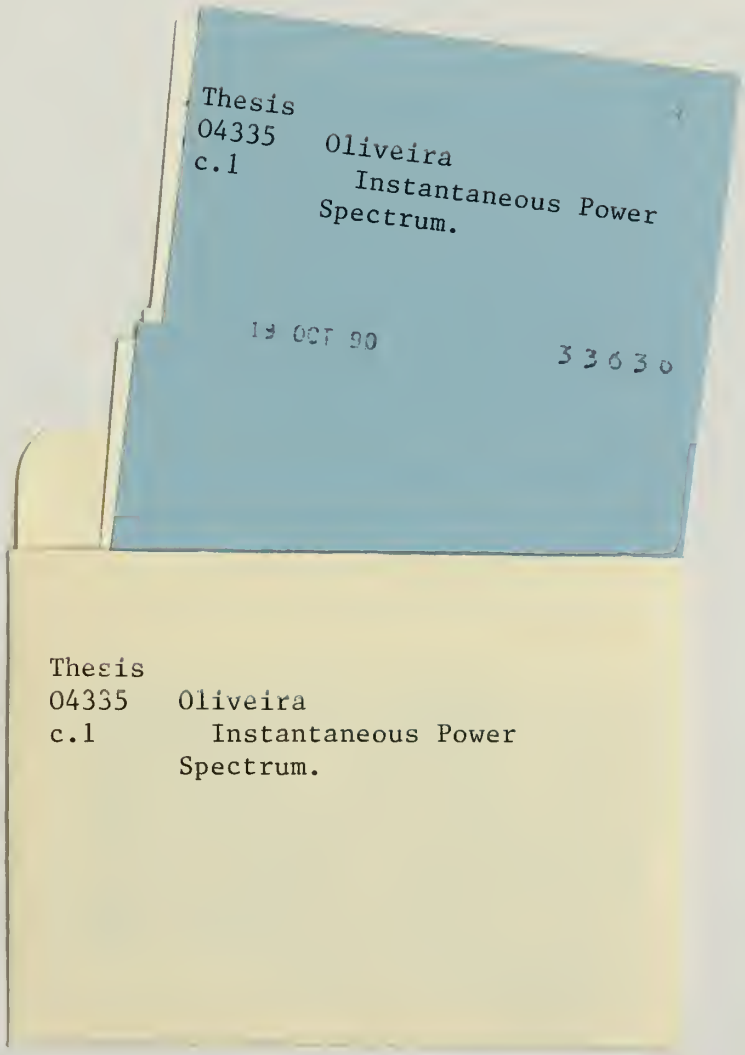
Thesis
04335
c.1
Oliveira
Instantaneous Power
Spectrum.
19 OCT 90
33630
Thesis
04335
c.1
Oliveira
Instantaneous Power
Spectrum.